

Application of Advanced Reservoir Characterization, Simulation, and Production
Optimization Strategies to Maximize Recovery in Slope and Basin Clastic Reservoirs,
West Texas (Delaware Basin)

Final Report

By

Shirley P. Dutton and William A. Flanders

August 2001

Work Performed Under Contract No. DE-FC22-95BC14936

Prepared for
U.S. Department of Energy
Assistant Secretary for Fossil Energy

Daniel J. Ferguson, Project Manager
National Petroleum Technology Office
Williams Center, Tower One
One West Third St., Suite 1400
Tulsa, OK 74103

Prepared by
Bureau of Economic Geology
The University of Texas at Austin
Austin, TX 78713-8924

CONTENTS

ABSTRACT	1
EXECUTIVE SUMMARY	2
INTRODUCTION	5
Geologic Setting.....	10
Delaware Sandstone Oil Play	12
OUTCROP CHARACTERIZATION OF BELL CANYON SANDSTONE RESERVOIR ANALOGS.....	14
Depositional Model.....	16
RESERVOIR CHARACTERIZATION OF FORD GERALDINE UNIT	21
Geologic Characterization	21
Reservoir Quality	27
Petrophysics of the Ramsey Sandstone	29
Porosity Transforms	31
Calculation of Water Saturation.....	32
<i>True Formation Resistivity</i>	32
<i>Archie Parameters m and n</i>	33
Net-Pay Cutoffs.....	34
Application.....	35
Geophysical Interpretation of the Ramsey Sandstone	35
Synthetic Seismograms and Wavelet Extraction	36
Structure and Coherency Maps	40
Conclusions.....	42
Development History and Simulation	43
Field Development History.....	43

Simulation of Tertiary Recovery.....	43
RESERVOIR CHARACTERIZATION OF FORD WEST FIELD.....	46
RESERVOIR CHARACTERIZATION OF EAST FORD UNIT	51
Geologic Characterization	51
Mapping of Ramsey Sandstone Genetic Units	54
<i>Upper Ford Siltstone</i>	56
<i>Ramsey 1 Sandstone</i>	56
<i>SH1 Siltstone</i>	59
<i>Ramsey 2 Sandstone</i>	59
<i>Lower Trap Siltstone</i>	62
Ramsey Sandstone Facies.....	62
<i>Channel Facies</i>	65
<i>Levee Facies</i>	72
<i>Lobe and Overbank-Splay Facies</i>	72
<i>Laminated Siltstone Facies</i>	73
<i>Lutite Facies</i>	74
Sandstone Diagenesis	74
Petrophysical Characterization	79
Porosity Transforms	81
Volume of Clay	81
Calculation of Water Saturation.....	83
<i>Formation-Water Resistivity</i>	83
<i>Archie Parameters m and n</i>	85
Net-Pay Cutoffs.....	85
Saturation Distribution	85

Transferability of Log-Interpretation Methods	88
Reservoir Description.....	89
Porosity Distribution	90
Permeability Distribution.....	93
Structure.....	96
Net Pay	96
Natural Water Influx.....	100
Geologic Heterogeneity in East Ford Unit	100
Siltstones.....	100
Net:Gross Sandstone	101
Diagenetic Heterogeneity	105
<i>Gas Effect in EFU 41R Well</i>	105
<i>Correlation of Calcite-Cemented Layers</i>	107
<i>Chlorite Cement</i>	113
EAST FORD FIELD PRIMARY DEVELOPMENT HISTORY	114
Primary Development	115
Secondary Recovery.....	122
Volumetrics.....	122
CO ₂ FLOOD OF EAST FORD UNIT	125
Results	125
Influence of Geologic Heterogeneity on East Ford Production.....	135
North Part of East Ford Unit.....	135
Middle Part of East Ford Unit.....	139
South Part of East Fort Unit.....	139
TECHNOLOGY TRANSFER ACTIVITIES	140

Presentations	141
Publications.....	142
Workshops	143
CONCLUSIONS	143
ACKNOWLEDGMENTS.....	145
REFERENCES	146
APPENDIX 1: LIST OF PRESENTATIONS PRODUCED BY BEG CLASS 3 PROJECT	157
APPENDIX 2: LIST OF PUBLICATIONS PRODUCED BY BEG CLASS 3 PROJECT	161
APPENDIX 3: CONTENT OF SHORT COURSES PRODUCED BY BEG CLASS 3 PROJECT	167

Figures

1. Map showing location of the Delaware Basin and paleogeographic setting during the Late Permian	6
2. Stratigraphic nomenclature of the Delaware Mountain Group in the Delaware Basin subsurface and outcrop areas and time-equivalent formations on the surrounding shelves.....	7
3. Detailed location map of the East Ford and Ford Geraldine units, Ford West field, and other, nearby Bell, Cherry, and Brushy Canyon reservoirs.....	9
4. Location of the 182 largest fields producing from the Bell, Cherry, and Brushy Canyon Formations in the Delaware Basin, Texas and New Mexico	11
5. Map showing location of outcrop study area and exposure of Bell Canyon Formation	15
6. Depositional model proposed for the Bell Canyon sandstone, showing deposition in submarine channels with levees, overbank splays, and attached lobes, photograph of channel-levee deposits, Facies 5 sandstone showing deformed bedding contemporaneous with deposition, climbing	

dunes in Facies 6 sandstone, and thin-bedded sandstones and siltstones, Facies 4	17
7. Diagram illustrating depositional facies model for one high-order cycle in the Bell Canyon Formation exposed at Willow Mountain, Culberson County, Texas	18
8. Strike-oriented cross sections from Willow Mountain outcrop	20
9. Typical log from the Ford Geraldine Unit No. 108.....	23
10. Photos of Ramsey sandstone cores from the Ford Geraldine unit	24
11. Isopach map of the Ramsey 1 sandstone, the main reservoir interval at Geraldine Ford field	25
12. Isopach map of the Ramsey 2 sandstone	26
13. Flow chart of petrophysical analysis and normalized relative permeability curves used to select an S_w cutoff for net pay at 60 percent	30
14. Synthetic seismogram generated for the FGU-128 well to correlate the seismic reflection character with the formation tops interpreted from well logs	38
15. Representative seismic line showing the top of the Castile, Lamar, Ramsey, and Manzanita intervals.....	39
16. Residual map of the Lamar peak showing localized structural high and lows.....	41
17. Plots of total oil production in the Ford Geraldine unit and volumes of water and CO ₂ injected.....	44
18. Location map of Ford West field, which produces from the upper Cherry Canyon Formation and lowermost Bell Canyon Formation, Delaware Mountain Group	47
19. Typical log, Ford West field from the Exxon Texaco Fee C No. 1	48
20. Northwest-southeast strike cross section A–A' of the upper Cherry Canyon and lower Bell Canyon interval in Ford West field	49
21. Status of wells in the East Ford unit, Reeves County, Texas	52
22. Typical log from East Ford Unit No. 24.....	53

23.	North-south dip cross section A–A' of the length of the East Ford unit	55
24.	Isopach map of the Ramsey 1 sandstone, which is thickest along a north-south, elongate trend on the east side of the East Ford unit	58
25.	Isopach map of the SH1 laminated siltstone, which was deposited during a break in Ramsey sandstone deposition.....	60
26.	Isopach map of the Ramsey 2 sandstone	61
27.	Description of core from East Ford Unit No. 41R	63
28.	Photograph of core from the EFU 41R well, from a depth of 2,754 to 2,764 ft.....	66
29.	Northwest-southeast strike cross section B–B' of the central part of the East Ford unit	68
30.	West-east strike cross section C–C' of the south tip of the East Ford unit.....	69
31.	Isopach map of the Ramsey 1 sandstone in the East Ford unit, with interpreted facies distribution shown	70
32.	Isopach map of the Ramsey 2 sandstone in the East Ford unit, with interpreted facies distribution shown	71
33.	Plot of porosity versus permeability from core-analysis data from the EFU 41R well.....	76
34.	Plot showing that calcite-cement volume is the main control on permeability in Ramsey sandstones from the EFU 41R well	77
35.	Plot of permeability versus depth across a calcite-cemented layer in the EFU-41R well	78
36.	Distribution of geophysical log suites available in the East Ford unit.....	80
37.	Cross plot of core porosity versus core permeability with porosity–permeability transform for the Ramsey sandstone in the East Ford unit, Reeves County, Texas	82
38.	Cross plot of interval transit time versus core porosity with porosity transform for the Ramsey sandstone in the East Ford unit.....	82
39.	Isosalinity map with formation-water resistivities at 75°F for the East Ford unit.....	84

40.	Map of water saturation of the Ramsey sandstone in the East Ford unit	87
41.	Distribution of porosity in Ramsey 1 and 2 sandstones and SH1 siltstones in the East Ford unit from core analyses	91
42.	Map of average porosity of the Ramsey sandstone in the East Ford unit	92
43.	Distribution of permeability in Ramsey 1 and 2 sandstones and SH1 siltstones in the East Ford unit, based on core analyses	94
44.	Cumulative distribution function of core-analysis permeability for Ramsey 1 and 2 sandstones in 11 wells in the East Ford unit.....	95
45.	Structure contoured on the top of the Lamar limestone dipping to the east in the East Ford unit	97
46.	Map of net pay of the Ramsey sandstone in the East Ford unit.....	98
47.	Map of hydrocarbon pore-feet ($S_o \times \emptyset \times H$) of the Ramsey sandstone in the East Ford unit.	99
48.	Isopach map of percentage of net:gross sandstone in the Ramsey 1 interval.....	103
49.	Isopach map of percentage of net:gross sandstone in the Ramsey 2 interval.....	104
50.	Gamma-ray, neutron, and density logs from the EFU 41R well.....	106
51.	West-east cross section D–D' of south end of the East Ford unit.....	108
52.	Map of percentage of the Ramsey 1 sandstone that is cemented by calcite	110
53.	Map of percentage of the Ramsey 2 sandstone that is cemented by calcite	111
54.	Interpretive model of possible calcite-cement distribution in turbidite sandstones in the East Ford unit.....	112
55.	Map of primary oil production from the Ramsey sandstone in the East Ford unit.....	116
56.	Map of normalized production in the East Ford unit in barrels/acre	117
57.	Map of the percentage of water (water cut) produced during initial- potential tests.....	118
58.	Map of oil produced during initial-potential tests in wells of the East Ford unit.....	120

59.	Map of primary oil production from the Ramsey sandstone in East Ford field.....	121
60.	Outline of the producing area of the East Ford unit and individual leases.....	123
61.	Outline of the CO ₂ flood area within the East Ford unit, superimposed on a streamline-pattern model of the flood	126
62.	Bottom-hole pressure in the East Ford unit in July 1995 and January 1999	128
63.	Plot of monthly oil production from the East Ford unit since the field was discovered in 1960.....	130
64.	Plot of oil production, water:oil ratio, and gas:oil ratio in the East Ford unit since 1990	132
65.	Plot of gas and water injection in the East Ford unit since 1995	133
66.	Outlines of the three areas of better interwell communication within the East Ford unit	136
67.	Plots of oil production from the EFU 1 and EFU 4 wells	137

Tables

1.	Mean porosity and permeability of upper Bell Canyon sandstones and siltstones in Ford Geraldine unit and range of values	28
2.	Design parameters for 3-D seismic acquisition	37
3.	Summary of core-analysis data from upper Bell Canyon sandstones and siltstones, East Ford unit.....	57
4.	Volume of original oil in place in the East Ford Unit	124
5.	Volume of original oil in place in the CO ₂ flood area within the East Ford Unit.....	127
6.	Injection and production data from East Ford CO ₂ flood	131

ABSTRACT

The objective of this Class III project was to demonstrate that reservoir characterization and enhanced oil recovery (EOR) by CO₂ flood can increase production from slope and basin clastic reservoirs in sandstones of the Delaware Mountain Group in the Delaware Basin of West Texas and New Mexico. Phase 1 of the project, reservoir characterization, focused on Geraldine Ford and East Ford fields, which are Delaware Mountain Group fields that produce from the upper Bell Canyon Formation (Ramsey sandstone). The demonstration phase of the project was a CO₂ flood conducted in East Ford field, which is operated by Orla Petco, Inc., as the East Ford unit.

Reservoir characterization utilized outcrop characterization, high-resolution sequence stratigraphy, subsurface field studies, and 3-D seismic data. Ramsey sandstones are interpreted as having been deposited in a channel-levee system that terminated in broad lobes; overbank splays filled topographically low interchannel areas. Porosity and permeability of the reservoir sandstones are controlled by calcite cement that can be concentrated in layers ranging from 2 to 16 inches in thickness.

CO₂ injection in the East Ford unit began in July 1995. As a result of the CO₂ flood, production from the East Ford unit has increased from 30 bbl/d at the end of primary production to more than 185 bbl/d in 2001. The unit has produced 180,097 bbl of oil from the start of tertiary recovery through May 2001, and essentially all production can be attributed to the enhanced oil recovery project. Oil recovery has been improved by the CO₂ flood, but not as much as had been expected. Geologic heterogeneities caused by both depositional and diagenetic processes are apparently influencing reservoir displacement operations. Results of the reservoir characterization can guide modifications to the existing pattern of injectors and producers.

EXECUTIVE SUMMARY

This volume summarizes work done by the Bureau of Economic Geology, The University of Texas at Austin, as part of the U.S. Department of Energy (DOE) Oil Recovery Field Demonstration Program, Class III. The goal of the program, and this project, is to increase oil production from domestic slope and basin clastic reservoirs in the near term to prevent their premature abandonment and the resulting permanent loss of resources to the United States. Specifically this project demonstrated that enhanced oil recovery (EOR) by CO₂ flood can increase production from slope and basin clastic reservoirs of the Delaware Mountain Group in West Texas and New Mexico. Furthermore, the project demonstrated that reservoir characterization, using outcrop characterization, subsurface field studies, and other techniques, provides essential information for designing efficient production strategies.

Slope and basin clastic reservoirs in sandstones of the Delaware Mountain Group in the Delaware Basin of West Texas and New Mexico contained more than 1.8 billion barrels (Bbbl) of oil at discovery. Recovery efficiencies of these reservoirs have averaged less than 20 percent since production began in the 1920's, and, therefore, a substantial amount of the original oil in place remains unproduced. Many of these mature fields are nearing the end of primary or secondary production and are in danger of abandonment unless effective, economic methods of EOR can be implemented.

Project objectives were divided into two main phases. The original objectives of the reservoir-characterization phase of the project were (1) to gain a detailed understanding of the architecture and heterogeneity of two representative fields of the Delaware Mountain Group, Geraldine Ford and Ford West, which produce from the Bell Canyon and Cherry Canyon Formations, respectively; (2) to choose a demonstration area in one of the fields; and (3) to simulate a CO₂ flood in the demonstration area. After completion

of the study of Geraldine Ford and Ford West fields, the original industry partner, Conoco, Inc., decided not to continue.

A new industry partner, Orla Petco, Inc., joined the project, and the reservoir-characterization phase was expanded to include the East Ford unit, which it operates. The East Ford unit, immediately adjacent to the Ford Geraldine unit, produces from the same reservoir, the Ramsey sandstone. This additional reservoir characterization demonstrated that the geologic model and log-interpretation methods developed during the study of the Ford Geraldine unit could be successfully transferred to another field in the Delaware sandstone play.

The East Ford unit underwent primary recovery through June 1995. As a result of serious producibility problems—particularly high water production without a water drive—primary recovery efficiency at the East Ford unit was less than 15 percent. Unless methodologies and technologies to overcome these producibility problems could be applied, much of the remaining oil in the East Ford unit would not be recovered.

The Phase 2 demonstration for the project was the CO₂ flood being conducted in the East Ford unit. Orla Petco began the CO₂ flood in the Ramsey sandstone in July 1995, and the response phase was reached in December 1997. As a result of the CO₂ flood, production from the East Ford unit has increased from 30 bbl/d at the end of primary production to more than 185 bbl/d in 2001. The unit has produced 180,097 bbl of oil from the start of tertiary recovery through May 2001, and essentially all production can be attributed to the EOR project.

Oil recovery has been improved by the CO₂ flood of the East Ford unit, but not as much as had been expected. Analysis of the results of the flood suggests that geologic heterogeneities affect reservoir displacement operations. CO₂ injector wells in splay sandstones apparently have poor communication with wells in channel sandstones, perhaps because communication is restricted through levee deposits. The field also appears to be divided into three areas of better interwell communication; communication

between wells in different areas is restricted. The areas may result from facies changes, subtle structural or bathymetric controls on deposition, or variations in sediment-transport direction.

Modification of the existing east-west alignment of injectors and producers may overcome the problem of apparently restricted communication between splay sandstones and channel sandstones at the north end of the field. Pressure response in the central area of the field has been slow, suggesting that communication is restricted between the producing wells in this area and the injector wells that are located in the north and south areas of the field. Adding an injector well in the central area may overcome this problem. The south area of the field is responding well to the existing north-south line of injectors. Recovery might be improved in this area by bringing on additional producers, which could be accomplished by overcoming mechanical problems with some of the shut-in wells.

Through technology transfer, the knowledge gained in the study of the East Ford and Ford Geraldine units can be applied to increasing production from the more than 350 other Delaware Mountain Group reservoirs in West Texas and New Mexico, which together contain more than 1.5 Bbbl of remaining oil. The technology and methodology used in this project have been transferred to Delaware Basin operators through inexpensive workshops and through technical presentations and publications at the local level. Presentations at national technical meetings have made technologies and results available to all domestic operators.

INTRODUCTION

This report summarizes the results of research conducted for the DOE Class III project “Application of Advanced Reservoir Characterization, Simulation, and Production Optimization Strategies to Maximize Recovery in Slope and Basin Clastic Reservoirs, West Texas (Delaware Basin).” The objective of the project was to demonstrate that reservoir characterization and enhanced oil recovery (EOR) by CO₂ flood can increase production from clastic reservoirs in basinal sandstones of the Delaware Mountain Group in West Texas and New Mexico. Because current production from Delaware Mountain Group reservoirs averages less than 20 percent of the 1.8 billion barrels (Bbbl) of original oil in place (OOIP), a clear opportunity for improving recovery exists. The goal is to increase production and prevent premature abandonment of reservoirs in mature fields in the Delaware Basin of West Texas and New Mexico.

Project objectives were divided into two main phases. The original objectives of the reservoir-characterization phase of the project were (1) to gain a detailed understanding of the architecture and heterogeneity of two representative fields of the Delaware Mountain Group, Geraldine Ford and Ford West (fig. 1), which produce from the Bell Canyon and Cherry Canyon Formations (fig. 2), respectively; (2) to choose a demonstration area in one of the fields; and (3) to simulate a CO₂ flood in the demonstration area (Dutton and others, 1996, 1997a, b, 1998). After completion of the study of Geraldine Ford and Ford West fields, the original industry partner, Conoco, Inc., decided not to continue.

When a new industry partner, Orla Petco, Inc., joined the project, the reservoir-characterization phase was expanded to include the East Ford unit, which lies immediately adjacent to the Ford Geraldine unit and produces from a branch of the same

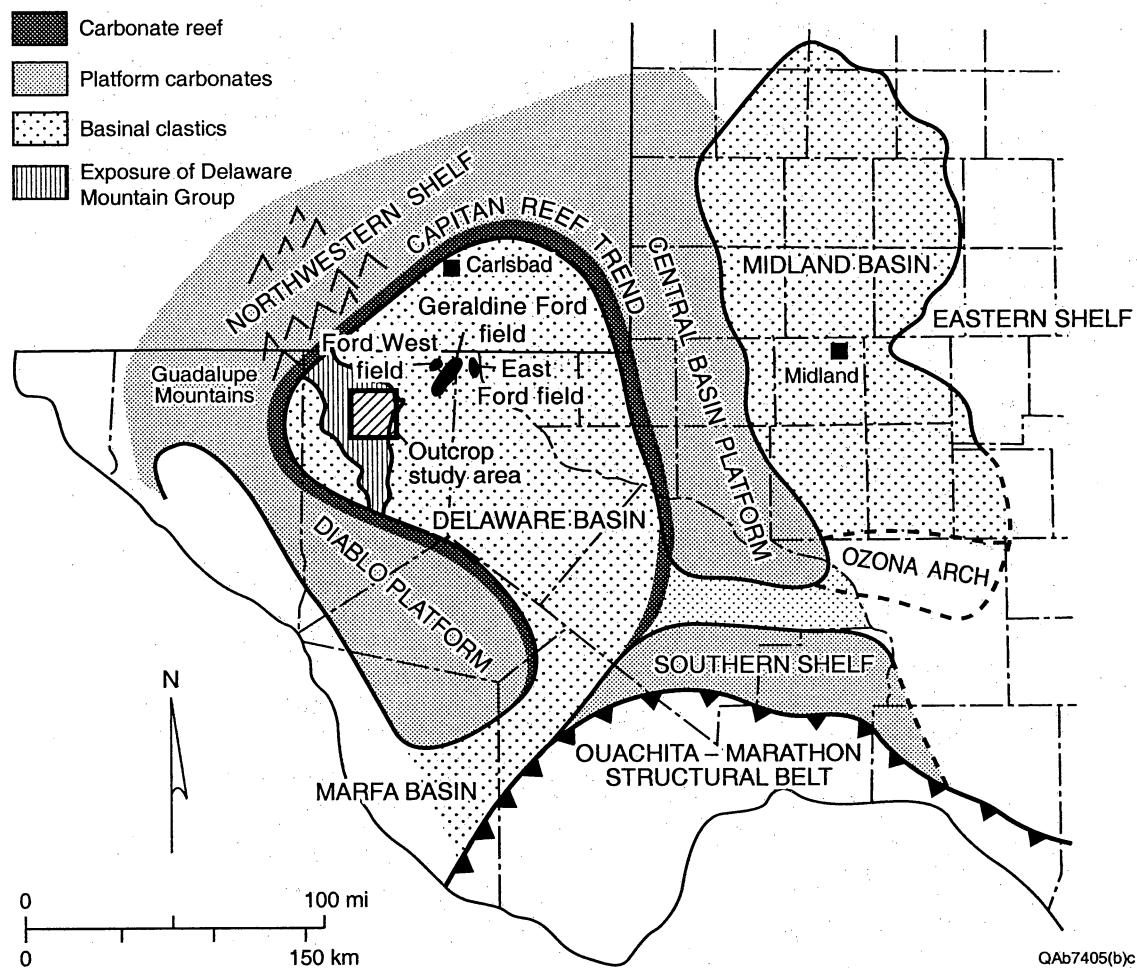
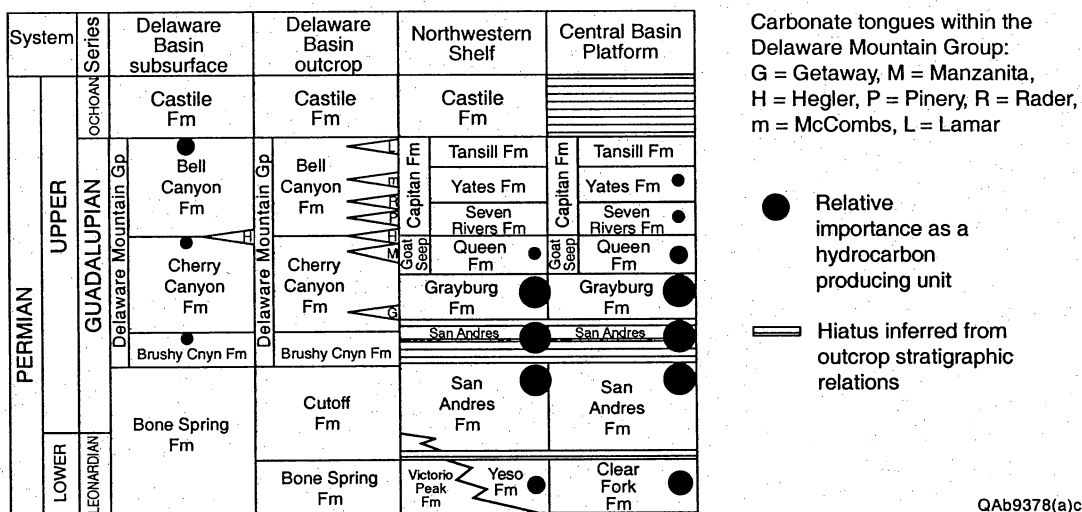


Figure 1. Map showing location of the Delaware Basin and paleogeographic setting during the Late Permian. Present-day exposures of the Delaware Mountain Group and locations of the outcrop study area, Geraldine Ford, Ford West, and East Ford fields are superimposed onto the paleogeographic map. Modified from Silver and Todd (1969).



QAb9378(a)c

Figure 2. Stratigraphic nomenclature of the Delaware Mountain Group in the Delaware Basin subsurface and outcrop areas and time-equivalent formations on the surrounding shelves. Modified from Galloway and others (1983), Ross and Ross (1987), Kerans and Fitchen (1995).

Ramsey sandstone channel (fig. 3). Reservoir characterization focused on the Ramsey sandstone, the youngest sandstone in the Delaware Mountain Group and the main producing interval in the East Ford unit.

This additional reservoir characterization provided an excellent opportunity to test the transferability of the geologic model and log-interpretation methods developed during reservoir characterization of the Ford Geraldine unit to another field in the Delaware sandstone play. Reservoir characterization of the East Ford unit built upon the earlier, integrated reservoir-characterization study of the Ford Geraldine unit (Dutton and others, 1999a). Both units produce from the most prolific horizon in the Bell Canyon Formation, and the reservoir-characterization studies of these units provide insights that are applicable to other slope and basin clastic fields in the Delaware Basin. The technologies used for reservoir characterization of the East Ford unit included (1) subsurface log, core, and petrophysical study; (2) high-resolution sequence stratigraphy; (3) mapping of nearby outcrop reservoir analogs; and (4) analysis of production history.

The Phase 2 demonstration for the project was a CO₂ flood being conducted in the East Ford unit. Orla Petco, the operator of the East Ford unit, began the CO₂ flood in the Ramsey sandstone in July 1995. Orla Petco has made available to the project all the injection and production data generated since the flood was initiated, providing an excellent opportunity to evaluate the success of the flood and compare the results with the reservoir characterization. The CO₂ flood at East Ford field reached the response phase in December 1997, so evaluation of the flood results could begin as soon as Phase 2 started in July 1999. Assessment of the effectiveness of the CO₂ flood to improve recovery in a mature Ramsey sandstone field was the focus of Phase 2.

In Phase 2 the knowledge gained during reservoir characterization was applied to increasing recovery from the CO₂ flood in the East Ford unit. Comparisons were made between production from the unit during the CO₂ flood and the geologic model developed during Phase 1. This comparison provided an important opportunity to test the

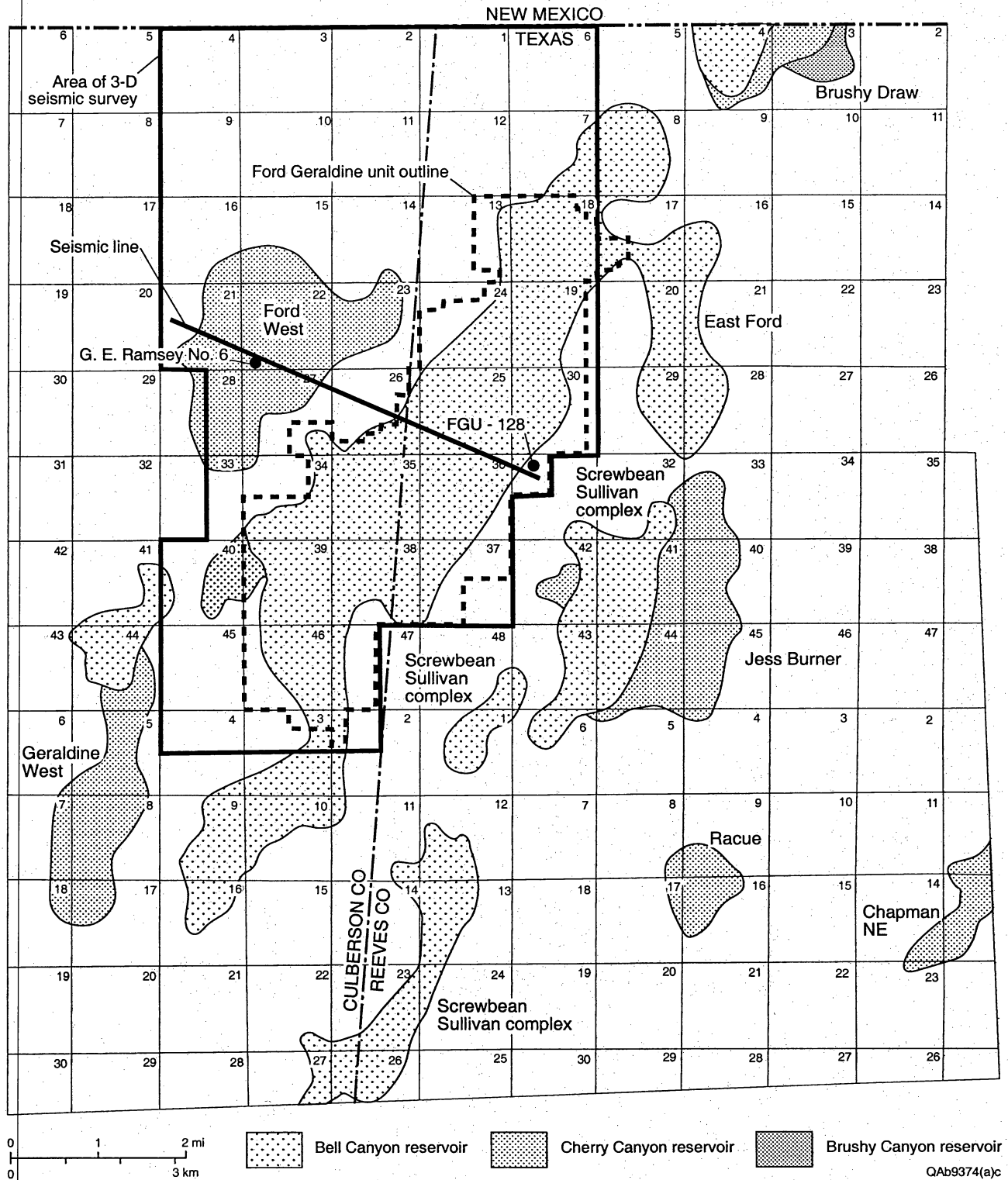


Figure 3. Detailed location map of the East Ford and Ford Geraldine units, Ford West field, and other, nearby Bell, Cherry, and Brushy Canyon reservoirs. Also shown are the outline of the area in which the 3-D seismic survey was acquired, the location of wells having synthetic seismograms (Conoco G. E. Ramsey No. 6 and FGU-128), and the location of the seismic line shown in figure 15.

accuracy of reservoir-characterization studies as tools in resource preservation of mature fields. In addition, the results of the CO₂ flood were used to refine and improve the geologic model of the East Ford unit.

Through technology transfer, the knowledge gained in the study of the East Ford and Ford Geraldine units can be applied to increasing production from the more than 350 other Delaware Mountain Group reservoirs in West Texas and New Mexico (fig. 4), which together contain more than 1.5 Bbbl of remaining oil.

Geologic Setting

Upper Permian (Guadalupian) Delaware Mountain Group strata (fig. 2) compose a 3,500-ft-thick succession of slope and basin deposits in the Delaware Basin that are important contributors to Permian Basin petroleum production. The Delaware Basin, the western subbasin of the Permian Basin, is located in West Texas and southeastern New Mexico (fig. 1). The Delaware Basin was semirestricted, with its south end partly open to the seaway and its north end surrounded by an extensive carbonate shelf and reef complex. Shelf to basin floor correlations of time-equivalent strata indicate that water depths were between 1,000 and 2,000 ft during deposition of the Bell Canyon Formation (Kerans and others, 1992).

Basinal limestones and organic-rich siltstones divide the Delaware Mountain Group into cyclic successions of sandstone and siltstone at several scales (Jacka and others, 1968; Meissner, 1972; Jacka, 1979; Gardner, 1992, 1997a, b). At the largest scale, thick limestones or organic-rich siltstones that are basinwide in extent divide the Delaware Mountain Group into three clastic wedges. These wedges, which are each 1,000 to 1,500 ft thick, are approximated by the Brushy Canyon, Cherry Canyon, and Bell Canyon Formations (fig. 2). The Bell Canyon Formation contains five limestone tongues that extend basinward from the shelf margin and divide the Bell Canyon into four sandstone

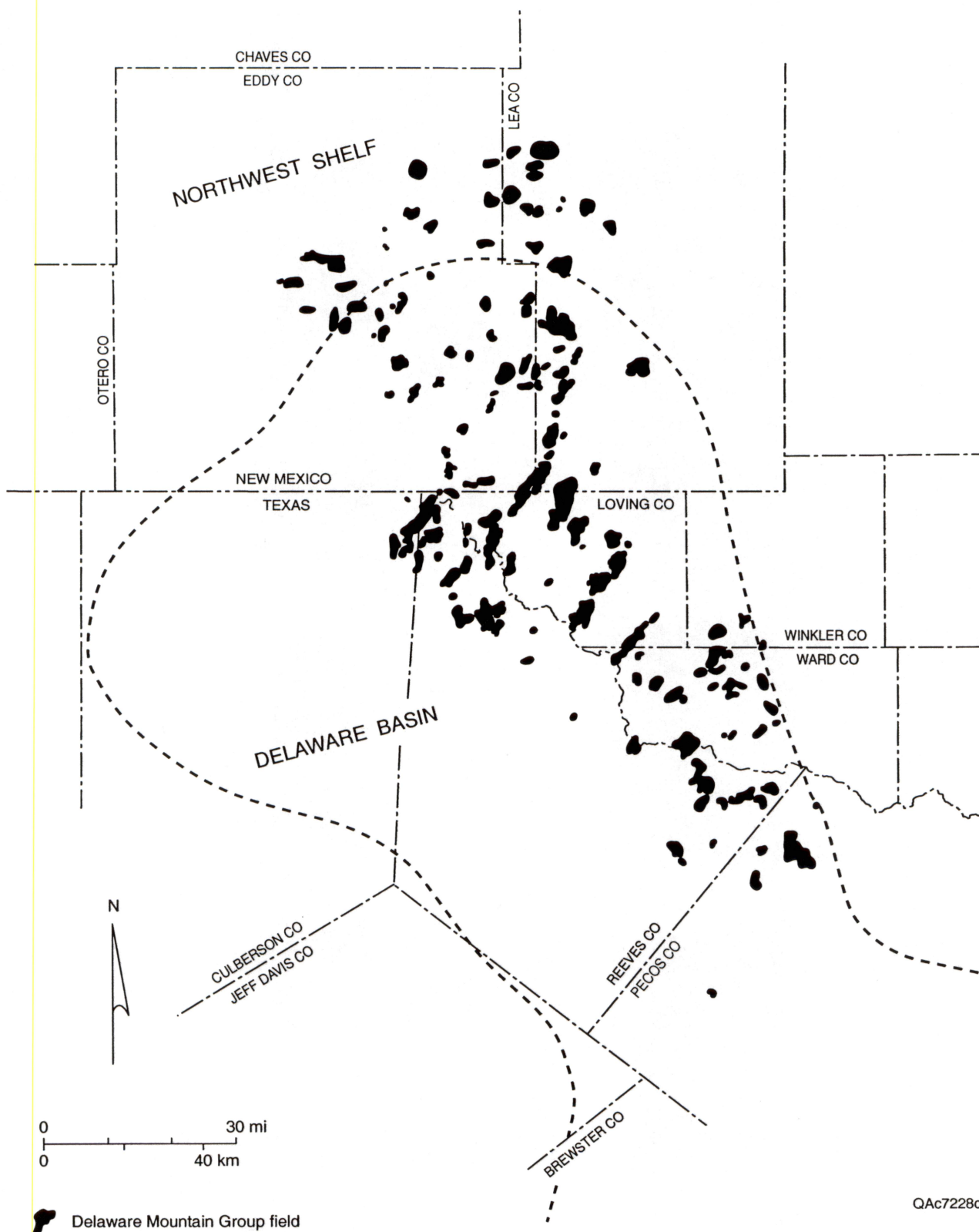


Figure 4. Location of the 182 largest fields (cumulative field production >100,000 bbl) producing from the Bell, Cherry, and Brushy Canyon Formations in the Delaware Basin, Texas and New Mexico. Field outlines and locations are approximate and are based on information from Grant and Foster (1989), Kusters and others (1989), Basham (1996), Lewis and others (1996), and the Railroad Commission of Texas.

bodies or intermediate cycles. The intermediate-order sandstone bodies are further subdivided by thin, organic-rich siltstones into 20- to 100-ft thick units referred to as high-order cycles (Gardner, 1992, 1997a, b).

The Bell Canyon Formation is composed of sandstones, siltstones, and minor amounts of carbonate. Detrital clay-size material is almost completely absent. Sandstones and siltstones of the Bell Canyon Formation thin near the margins of the basin where they interfinger with and onlap adjacent carbonate slope deposits of the Capitan Formation (fig. 2). The Bell Canyon Formation is overlain by gypsum deposits of the Castile Formation.

The cyclic interbedding of sandstones with organic-rich siltstones and limestones in the Delaware Mountain Group has been interpreted to record frequent changes in relative sea level (Meissner, 1972; Fischer and Sarnthein, 1988; Gardner, 1992, 1997a, b). During highstands in relative sea level, sands were trapped behind a broad, flooded shelf and prevented from entering the basin. Thin, widespread, organic-rich siltstones accumulated on the basin floor by the slow settling of marine algal material and airborne silt. Associated limestones were deposited by sediment gravity flows that originated by the slumping of carbonate debris along the flanks of a rapidly aggrading carbonate platform. During subsequent lowstands in relative sea level, the carbonate shelf was exposed and sandstones bypassed to the basin floor. Textural characteristics of the sands, such as the absence of detrital clay-size material and the lack of channels on the shelf, suggest that wind was an important agent in transporting the sands to the shelf margin (Fischer and Sarnthein, 1988). Paleocurrent indicators show that the sands entered the basin from the Northwestern Shelf and Central Basin Platform (Williamson, 1978) (fig. 1).

Delaware Sandstone Oil Play

Fields in the Delaware play produce oil and gas from slope and basin sandstone deposits that form long, linear trends. Structural contours on limestone beds capping the

reservoir sandstones indicate monoclinal dip to the east and northeast, almost directly opposite original depositional dip, because Late Cretaceous movement associated with the Laramide orogeny tilted the Delaware Basin eastward (Hills, 1984). Production from Geraldine Ford, East Ford, and other upper Bell Canyon fields in the Delaware Basin occurs from the distal (southwest) ends of east-dipping, northeast-oriented linear trends of thick Ramsey sandstone deposits. Most hydrocarbons in these fields are trapped by structurally updip facies changes from higher permeability reservoir sandstones to low-permeability siltstones.

The Delaware play is now mature and has a drilling history of progressively deeper pool discoveries in the Bell Canyon, Cherry Canyon, and Brushy Canyon Formations. Approximately 379 reservoirs have been discovered in sandstones of the Delaware Mountain Group in West Texas and southeast New Mexico (Dutton and others, 2000a). In the 1920's, reservoirs were discovered in the Ramsey sandstone, the youngest sandstone of the Bell Canyon Formation. Geraldine Ford field (figs. 1, 3) was discovered in 1956, and East Ford field was discovered in 1960. By 1998, 79 large fields (having cumulative productions of >100,000 bbl) had been discovered in the Bell Canyon Formation (Dutton and others, 2000a). The 63 large Bell Canyon fields in Texas had produced 178 MMbbl of oil through 1998, and the 16 large Bell Canyon fields in New Mexico had produced 30.7 MMbbl.

In 1952, deeper reservoirs were discovered in the Cherry Canyon Formation (fig. 2). By 1998, 62 large Cherry Canyon fields had been developed (Dutton and others, 2000a). The 36 large Cherry Canyon fields in Texas had produced 48.3 MMbbl of oil through 1998, and the 26 large Cherry Canyon fields in New Mexico had produced 26.7 MMbbl. More recently, deeper pool discoveries have been made in the Brushy Canyon Formation (DeMis and Cole, 1996). A total of 41 large Brushy Canyon fields had been discovered through 1998 (Dutton and others, 2000a). The 3 large Brushy Canyon fields in Texas had

produced 0.5 MMbbl of oil through 1998, and the 38 large Bell Canyon fields in New Mexico had produced 44.8 MMbbl (Dutton and others, 2000a).

Delaware Mountain Group fields in Texas and New Mexico contained more than 1.8 Bbbl of OOIP (M. Holtz, BEG, personal communication, 1994). These fields had produced more than 340 MMbbl of oil through December, 1998, but 1.5 Bbbl remains.

OUTCROP CHARACTERIZATION OF BELL CANYON SANDSTONE RESERVOIR ANALOGS

Interpretation of processes that deposited the sandstones of the Delaware Mountain Group has long been controversial, and this controversy is of practical importance because different depositional models predict different sandstone distribution, geometry, and continuity. Applying the correct depositional model is critical to effective reservoir development, but subsurface data commonly do not provide the interwell-scale information needed to differentiate between competing depositional models. Thus, a key component of the reservoir characterization was to investigate well-exposed outcrop analogs of the Ramsey sandstone reservoirs.

Outcrops of the Bell Canyon Formation are present within 24 mi of the East Ford and Ford Geraldine units (figs. 1, 5). We studied these outcrops to better interpret the depositional processes that formed the reservoirs and to determine the dimensions and characteristics of reservoir sandstone bodies in well-exposed sections. The geologic model developed by this outcrop study provides insight into the production performance of the East Ford unit and other Delaware Mountain Group reservoirs.

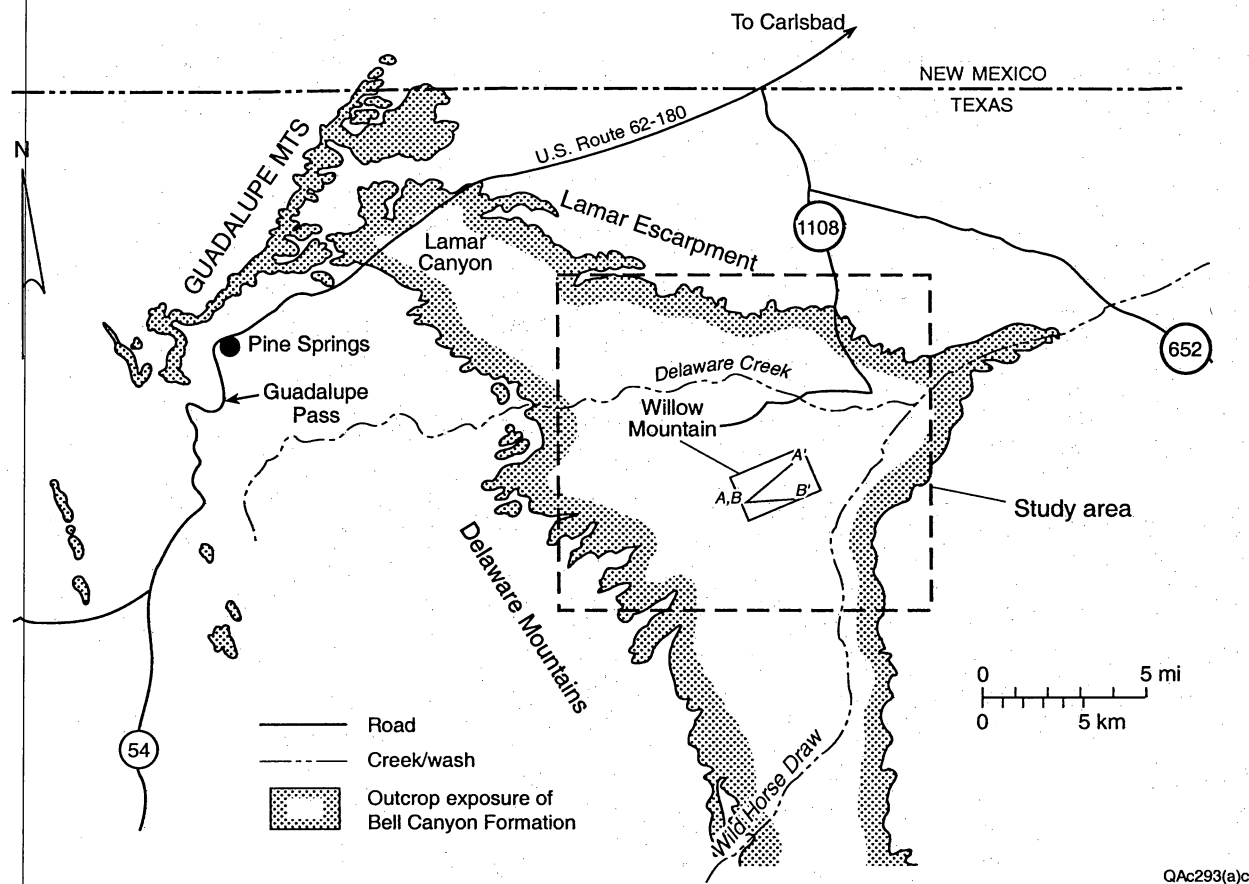


Figure 5. Map showing location of outcrop study area and exposure of Bell Canyon Formation From Barton and Dutton (1999). Cross sections A–A' and B–B' are shown in figure 8.

The outcrop study focused on a stratigraphic unit in the Bell Canyon Formation that is analogous to, but older than, the Ramsey Sandstone. The interval is the uppermost high-order cycle below the McCombs Limestone (fig. 2). The scale and position of this stratigraphic unit are analogous to that of the Ramsey interval, which is the uppermost high-order cycle below the Lamar Limestone (fig. 2).

Depositional Model

Bell Canyon sandstones are interpreted as having been deposited by sandy high- and low-density turbidity currents that carried a narrow range of sediment size, mostly very fine sand to coarse silt. Six facies were identified in outcrop: facies 1 is a massive, organic-rich siltstone; facies 2 is an organic-rich, laminated siltstone; facies 3 is a laminated siltstone; facies 4 is composed of thin-bedded sandstones and siltstones that are graded or display partial Bouma sequences (Bouma, 1962); facies 5 is a structureless sandstone; and facies 6 is a large-scale, cross-laminated sandstone (Barton and Dutton, 1999).

Stratigraphic relationships mapped in outcrop indicate that the sandstones were deposited in a basin-floor setting by a system of leveed channels having attached lobes and overbank splays (figs. 6a, 6b, 7) (Barton, 1997; Barton and Dutton, 1999; Dutton and others, 1999a). Individual channel-levee and lobe complexes stack in a compensatory fashion and are separated by laterally continuous, laminated siltstones. These siltstones are interpreted to have been deposited by the settling of marine organic matter and airborne silt during periods when coarser particles were prevented from entering the basin.

Lobe deposits, which are broadly lenticular sandstone bodies, are as much as 25 ft thick and 2 mi wide. They are composed of massive sandstones having dewatering features such as dish and flame structures (fig. 6c). Lobe sandstones were deposited by

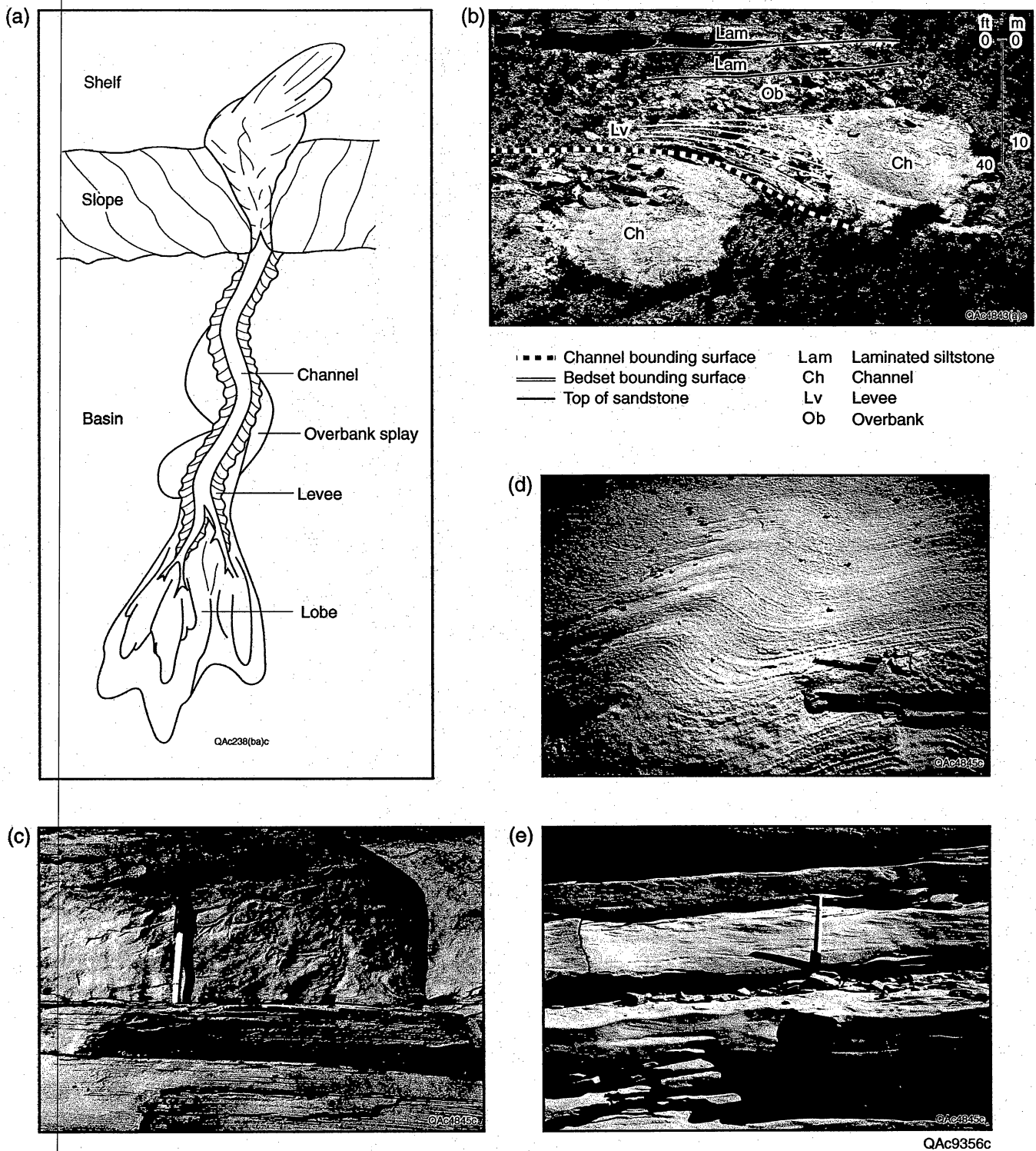
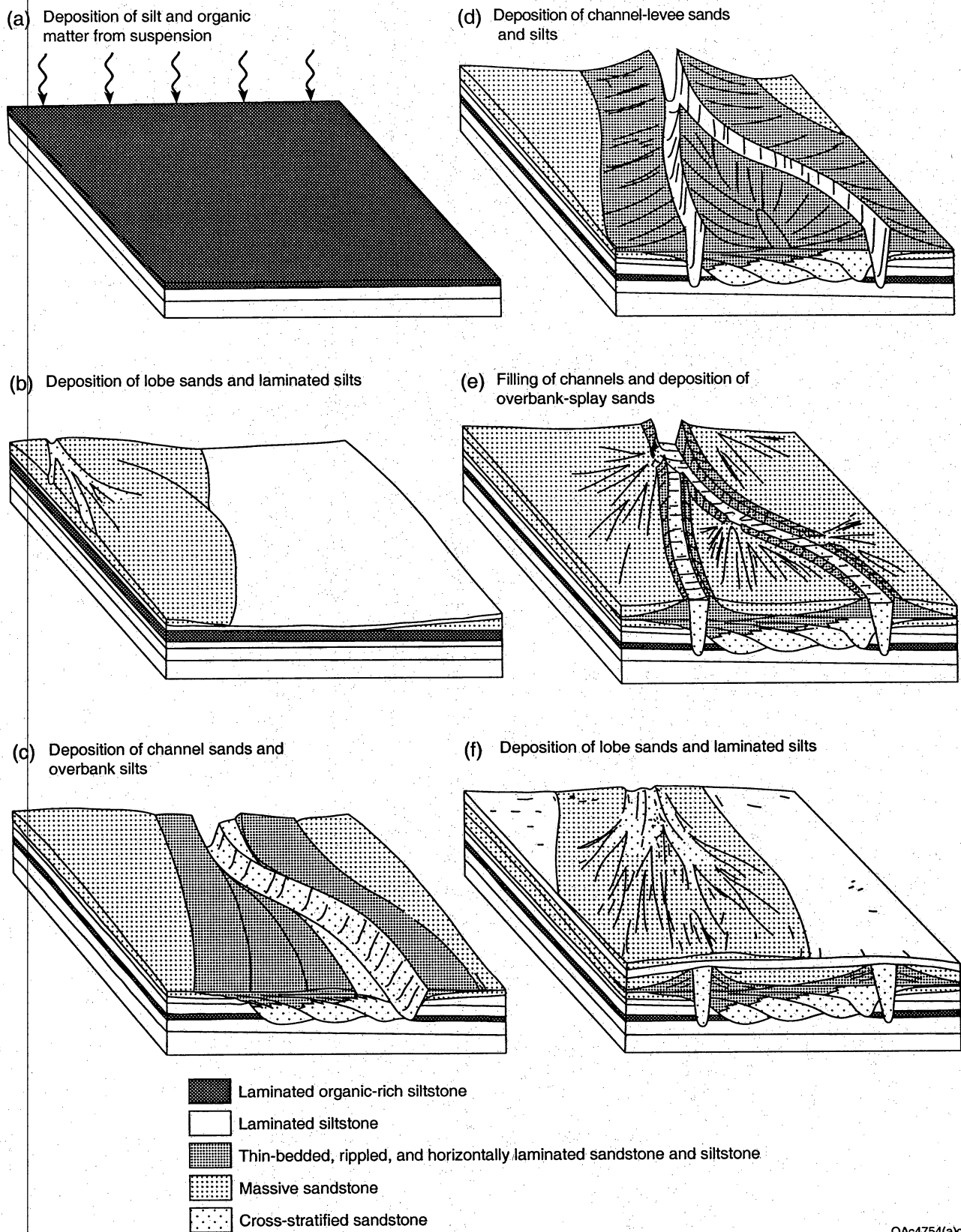


Figure 6. (a) Depositional model proposed for the Bell Canyon sandstone, showing deposition in submarine channels with levees, overbank splays, and attached lobes. The model was developed from outcrop study of a high-order cycle in the upper Bell Canyon Formation. After Barton (1997); modified from Galloway and Hobday (1996). (b) Photograph of channel-levee deposits; the two channels are vertically stacked in an offset fashion. (c) Facies 5 sandstone showing deformed bedding contemporaneous with deposition. (d) Climbing dunes in Facies 6 sandstone. (e) Thin-bedded sandstones and siltstones, Facies 4. All photos from Barton and Dutton (1999).



QA4754(a)c

Figure 7. Diagram illustrating depositional facies model for one high-order cycle in the Bell Canyon Formation exposed at Willow Mountain, Culberson County, Texas. From Barton and Dutton (1999).

unconfined flow at the mouths of channels. In a prograding system, lobe facies would have been deposited first and then overlain and partly eroded by the channel-levee-overbank system (fig. 7). Lobe sandstones are commonly interbedded with sheets of laminated siltstone.

Channels are largely filled with massive and cross-stratified sandstone (fig. 6d). Channels mapped in outcrop range from 10 to 60 ft in thickness; most are 20 to 40 ft thick. Channel widths are 300 to 3,000 ft, giving aspect ratios of 10 to 100. In updip areas, channel positions remained relatively fixed. As a result, individual channels are highly amalgamated and form a body that has dimensions larger than those of any single channel (fig. 8a) (Barton and Dutton, 1999). Downdip the spacing of the channels expands (fig. 8b). The expansion reflects migration of the channel laterally during the initial stages of channelization and channel avulsion or bifurcation, or both, during later stages (Barton and Dutton, 1999).

Flanking the channels on both sides, wedges composed of thinly bedded sandstone and siltstone (fig. 6e) are interpreted to be levees. The width of levee deposits mapped in outcrop varies (fig. 8). Many levee deposits are about 500 ft wide, but some are as wide as 0.5 mi (Barton, 1997). The levees thin away rapidly from the channel, decreasing in thickness from 20 to 3 ft over the distance of a few hundred feet to 0.5 mi (Barton and Dutton, 1999). Sandstone-bed thickness and sandstone content (net:gross) decrease in a similar fashion. Near the channel margin, sandstone beds in the levees are several feet thick, whereas several hundred feet away they are several inches to a foot thick. Sandstone content decreases from about 70 percent near the channel margin to less than 10 percent where the levees pinch out.

Massive sandstones that display a broad, tabular to irregular geometry onlap the levee deposits (figs. 7, 8). Convolute bedding and dewatering structures such as dish and pillar structures are common in these beds. The massive sandstones are 3 to 25 ft thick and as much as 3,000 ft wide (Barton, 1997). These massive sandstones are interpreted as

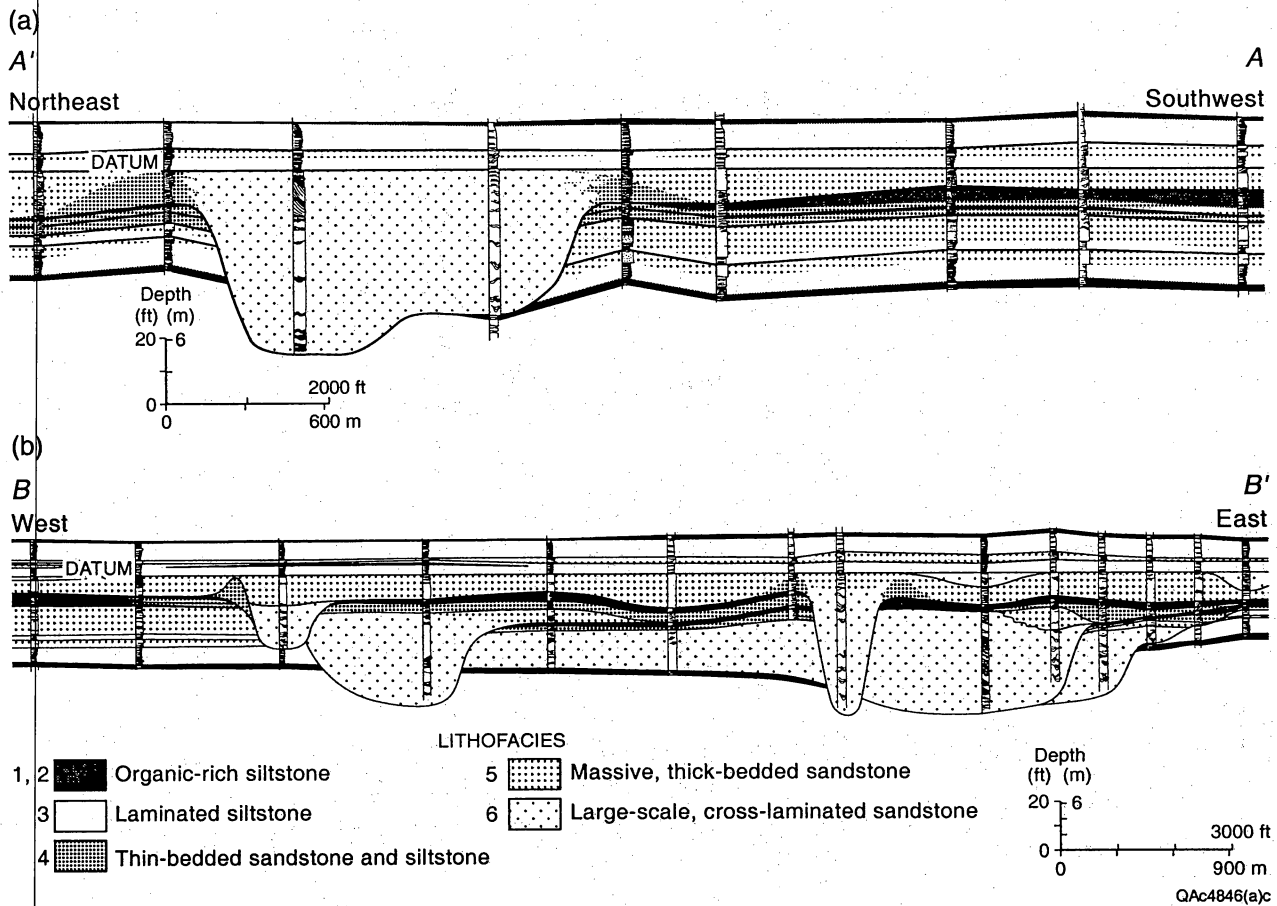


Figure 8. Strike-oriented cross sections from Willow Mountain outcrop. See figure 5 for locations. (a) Northeast-southwest cross section A'-A showing distribution of facies and traces of key surfaces within a single high-order cycle, Bell Canyon Formation. A 60-ft-thick channel incises deeply into the underlying sheet sandstones and laminated siltstones. (b) West-east cross section B-B' showing channels amalgamated to form a composite body. From Barton and Dutton (1999).

overbank splays that filled topographically low interchannel areas (fig. 7); the somewhat irregular geometry of the overbank splays is related to the underlying topography. Stratigraphic relationships suggest that the splays formed during the final stages of channel filling (Barton and Dutton, 1999). Volumetrically they contain much of the sandstone in the system (fig. 8). It is difficult to distinguish overbank-splay deposits from lobe deposits by lithofacies alone; the location, shape, and stratigraphic position of massive sandstones are needed to differentiate these depositional elements.

Interpretation of the subsurface reservoirs at the Ford Geraldine and East Ford units was guided by the depositional model developed from this study of well-exposed outcrop analogs in the Bell Canyon Formation. The depositional model is widely applicable to other reservoirs that produce from Delaware Mountain Group sandstones. The results of the outcrop study can be transferred by operators to their own fields and guide reservoir characterization. A benefit of this study, therefore, was the development of a depositional model that can be applied throughout the play at no cost to operators.

RESERVOIR CHARACTERIZATION OF FORD GERALDINE UNIT

Geologic Characterization

Geraldine Ford field, operated as the Ford Geraldine unit, produces at 2,600 ft from a stratigraphic trap in the upper part of the Bell Canyon Formation of the Delaware Mountain Group (fig. 2). The 99 MMbbl of OOIP (Pittaway and Rosato, 1991) makes it the largest Delaware Mountain Group field in the basin.

The depositional model developed from outcrop study of Bell Canyon sandstones (Barton and Dutton, 1999) was used to interpret the processes that deposited the Ramsey sandstone at the Ford Geraldine unit and to map the geometry and dimensions of the architectural elements within it (Dutton and Barton, 1999; Dutton and others, 1999a). The

Ramsey reservoir interval at the Ford Geraldine unit is composed of a 0- to 60-ft-thick sandstone bounded by the Ford and Trap laminated siltstones (fig. 9). In the north part of the Ford Geraldine unit, the Ramsey is divided into two sandstones (Ramsey 1 and Ramsey 2) separated by a 1- to 3-ft-thick laminated siltstone (SH1) (Ruggiero, 1985). In the south part of Ford Geraldine unit, only the Ramsey 1 sandstone is present.

The Ford Geraldine unit has an excellent subsurface database for reservoir characterization. Geophysical logs from 305 of the 340 wells in the unit and 3,615 ft of Ramsey sandstone core from 70 wells were available (Dutton and others, 1999a). These data were supplemented by descriptions of 681 ft of core from 13 additional wells by Ruggiero (1985). Previous studies of Geraldine Ford field and other nearby Bell Canyon fields by Payne (1973, 1976), Williamson (1978, 1979), Berg (1979), Ruggiero (1985, 1993), and Gardner (1992, 1997a, b) provided the foundation for this study.

The facies observed in cores from the Ramsey interval of the Ford Geraldine unit are similar to those that were identified in the upper Bell Canyon outcrop (Barton and Dutton, 1999; Dutton and others, 1999a). The six facies are (1) organic-rich siltstone (lutite); (2) laminated siltstone (laminite); (3) rippled sandstone and siltstone (fig. 10a); (4) massive and contorted sandstones with abundant dewatering features (fig. 10b, c, d); (5) cross-stratified sandstone (fig. 10e), and (6) massive sandstone (fig. 10f).

The Ramsey 1 sandstone occurs throughout the Ford Geraldine unit (fig. 11). It pinches out at the northwest and southeast margins of the field and reaches a maximum thickness of >35 ft along a curving northeast-southwest trend. At the southwest end of the field, the single trend of thick sandstone splits into several smaller trends (fig. 11). The SH1 siltstone represents a break in sandstone deposition within the Ramsey interval, when laminated siltstone was deposited. The younger sandstone in the Ramsey cycle, called the Ramsey 2 (Ruggiero, 1985), is thinner than the Ramsey 1, having a maximum thickness of 14 to 18 ft along a sinuous, bifurcating, northeast-southwest trend (fig. 12).

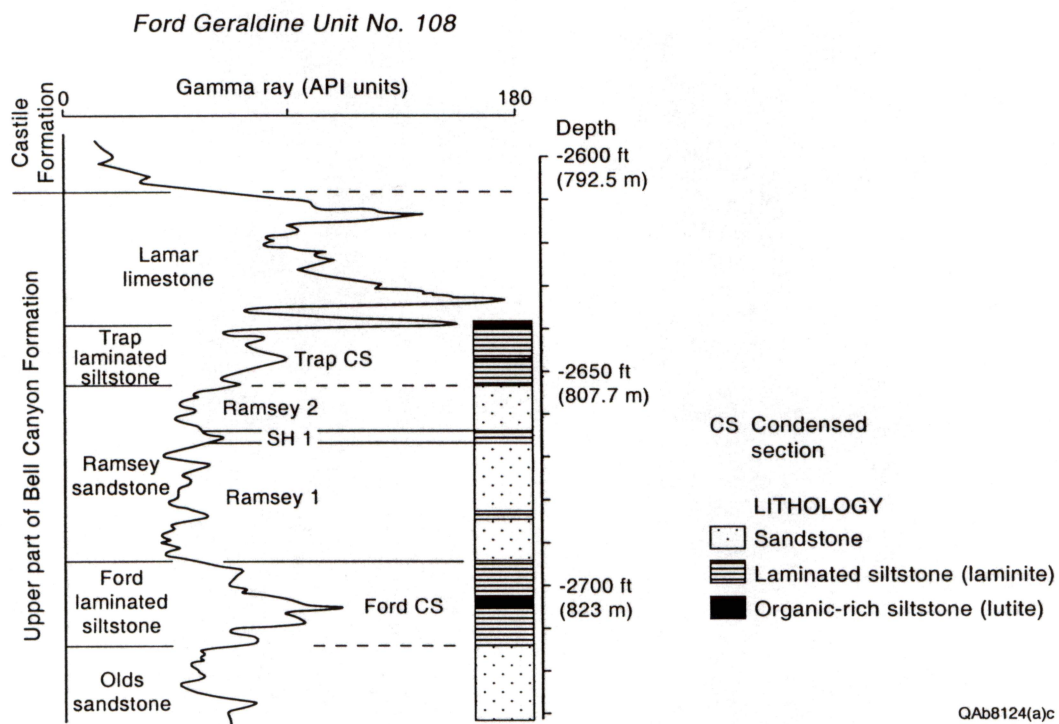


Figure 9. Typical log from the Ford Geraldine Unit No. 108. Modified from Ruggiero (1985).

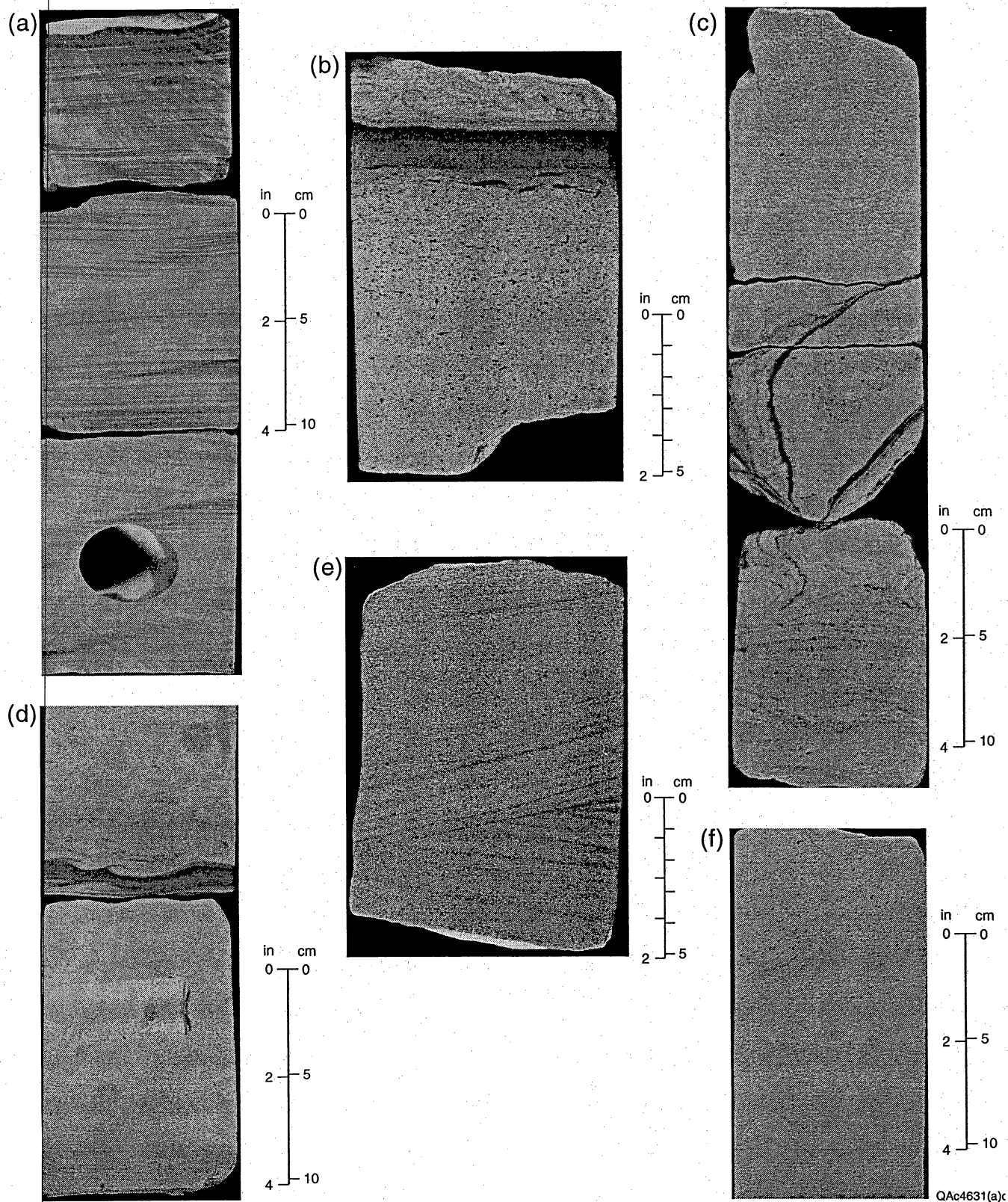


Figure 10. Photos of Ramsey sandstone cores from the Ford Geraldine unit. (a) Rippled sandstone. (b) Graded sandstone with floating clasts and overlying lutite. (c) Sandstone with convoluted beds interpreted as loading and dewatering features. (d) Sandstone with flame structure. (e) Cross-laminated sandstone. (f) Massive sandstone. From Dutton and Barton (1999).

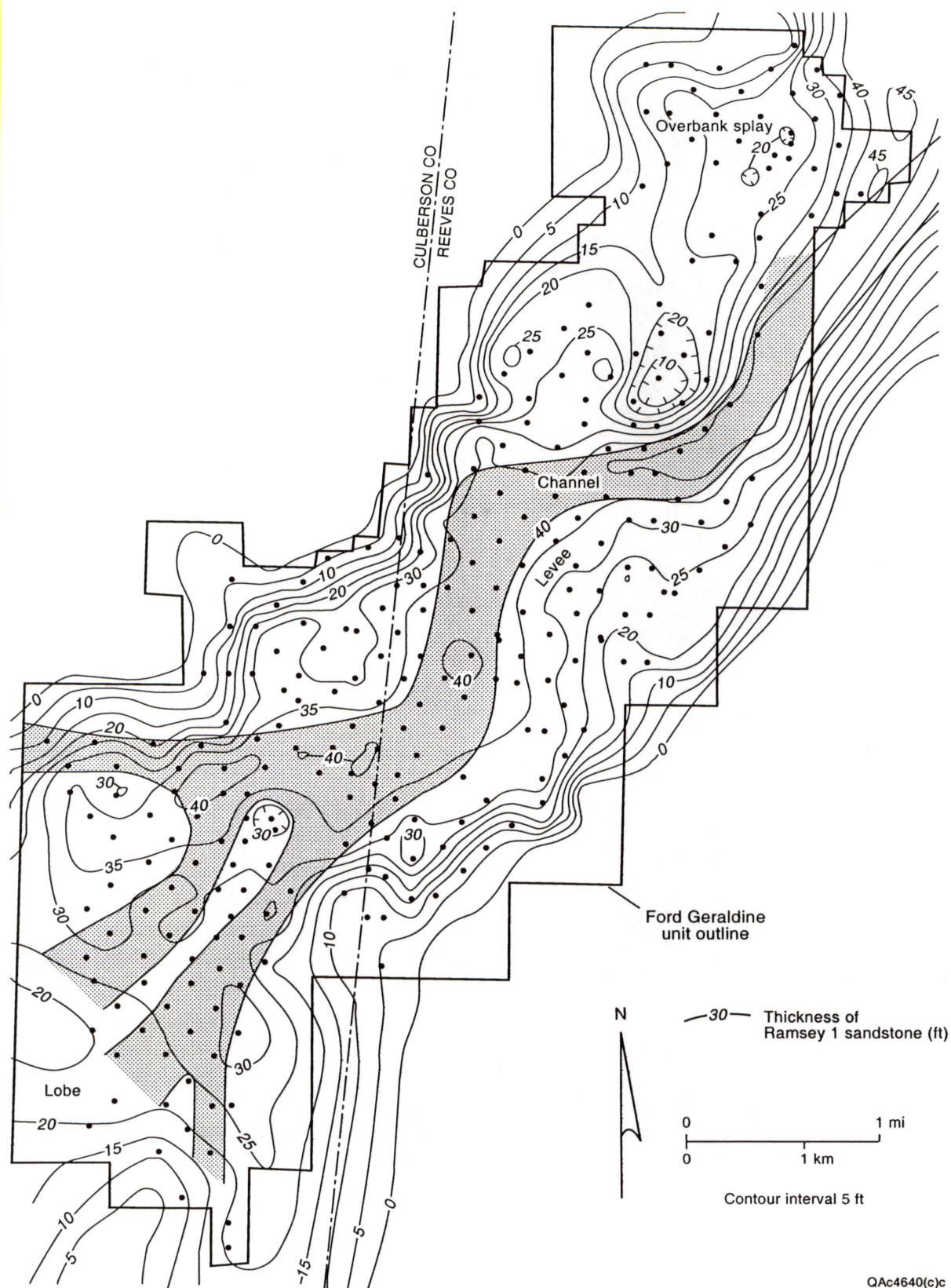


Figure 11. Isopach map of the Ramsey 1 sandstone, the main reservoir interval at Geraldine Ford field. It is interpreted as a channel-levee system that progrades over an elongate lobe. At the southwest end of the field, the channel (shaded) apparently breaks up into many smaller branches with attached lobes. The channel was identified from core descriptions and the sandstone thickness.

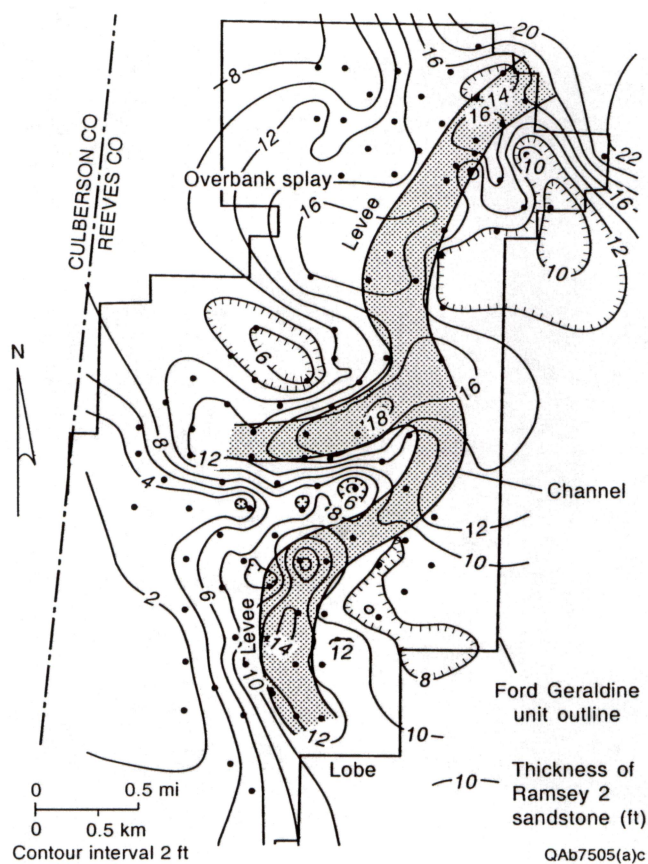


Figure 12. Isopach map of the Ramsey 2 sandstone. This sandstone is also interpreted as a channel-levee system that prograded over lobe deposits, but it did not prograde as far into the basin as did the Ramsey 1 sandstone. Many of the thickest areas of Ramsey 2 sandstone correspond to thin Ramsey 1, suggesting that Ramsey 2 sandstones were deposited in the adjacent topographic depressions created by deposition of the preceding Ramsey 1 beds. Note that the map covers only the north part of the Ford Geraldine unit.

The Ramsey 2 sandstone did not prograde as far into the basin in the Ford Geraldine area as did the Ramsey 1 sandstone.

On the basis of core descriptions, subsurface mapping, and the depositional model developed from outcrop, the 0- to 60-ft-thick Ramsey sandstone interval in the Ford Geraldine unit is interpreted to consist of sheetlike lobe deposits overlain and incised by channel and levee deposits. Because of the narrow range of grain sizes in Ramsey sandstones and the absence of detrital clay, log patterns are generally not diagnostic of facies. Comparison of sedimentary structures viewed in core with facies identified in outcrop was key to interpreting the reservoir facies. Lobe and overbank splay deposits consist of massive and convoluted sandstones with load and dewatering structures, which suggest that the sandstones were deposited rapidly from high-density turbidity currents. Channel facies, which are approximately 1,200 ft wide and 15 to 35 ft thick (figs. 11, 12), overlie and locally incise the lobe deposits. They consist of massive and crossbedded sandstones interpreted to have been deposited from high-density turbidity currents. Channel margins, characterized by rippled and convoluted sandstones interbedded with siltstones, are interpreted as channel levees formed by overbanking of low-density turbidity currents. The levees are onlapped by massive sandstones interpreted as overbank splays.

Reservoir Quality

Average porosity in the Ramsey interval (Ramsey 1 and 2 sandstones and SH1 siltstone) is 22.0 percent, as determined by 4,900 core analyses. Standard deviation is 4.1 percent. Geometric mean permeability of the Ramsey interval is 16.2 md, with a standard deviation of 6.3 md. Arithmetic average permeability is 38.4 md. The Ramsey 1 sandstone is somewhat more porous and permeable than is the Ramsey 2 sandstone (table 1).

Table 1. Mean porosity and permeability of upper Bell Canyon sandstones and siltstones in Ford Geraldine unit and range of values.

	Mean porosity (range)(percent)	Geometric mean permeability (range) (md)
Trap siltstone	12.7 (4.3–21.7)	0.4 (0.01–45)
Ramsey 2 sandstone	20.5 (10.2–25.3)	17 (2–230)
SH1 siltstone	18.0 (3.8–26.8)	0.2 (0.1–26)
Ramsey 1 sandstone	21.8 (2.9–29.2)	19 (0.01–400)
Ford siltstone	16.9 (1.1–20.3)	2 (1–33)

Ramsey sandstones at Geraldine Ford field are arkoses having an average framework-grain composition of $Q_{63}F_{32}R_5$. Ramsey sandstones in the Ford Geraldine unit have a very narrow range of grain sizes. The average grain size in sandstone samples is 0.092 mm (3.44 phi), and the range is 0.085 to 0.107 mm (3.6 to 3.2 phi). The proportion of silt-sized grains in the sandstones ranges from 4 to 20 percent.

Cements constitute between 4 and 30 percent of the sandstone volume in Ramsey sandstones, with calcite and chlorite being the most abundant. Calcite cement has an average volume of 7 percent and ranges from 1 to 29 percent. Chlorite (average = 3 percent) forms rims around detrital grains, extending into pores and pore throats.

There is a statistically significant relationship between volume of cement and both porosity and permeability (Dutton and others, 1999a). Calcite is the most important component of total cement, and it has the greatest impact on reservoir quality. In samples with more than 10 percent calcite cement, geometric mean permeability is 1.3 md and average porosity is 14.4 percent. Sandstones having less than 10 percent calcite cement have geometric mean permeability of 46 md and average porosity of 23.1 percent. When only the poorly calcite cemented samples (containing <10 percent calcite) are analyzed, grain size and chlorite cement volume show a significant correlation with permeability. Thus, the main control on porosity and permeability in the Ramsey sandstones is authigenic calcite, and to a lesser extent chlorite and grain size also influence reservoir quality.

Petrophysics of the Ramsey Sandstone

Petrophysical characterization of the Ford Geraldine unit was accomplished by integrating core and log data and quantifying petrophysical properties from wireline logs (fig. 13a) (Asquith and others, 1997; Dutton and others, 1999b). The first step in the petrophysical analysis was to construct cross plots of neutron porosity and interval transit

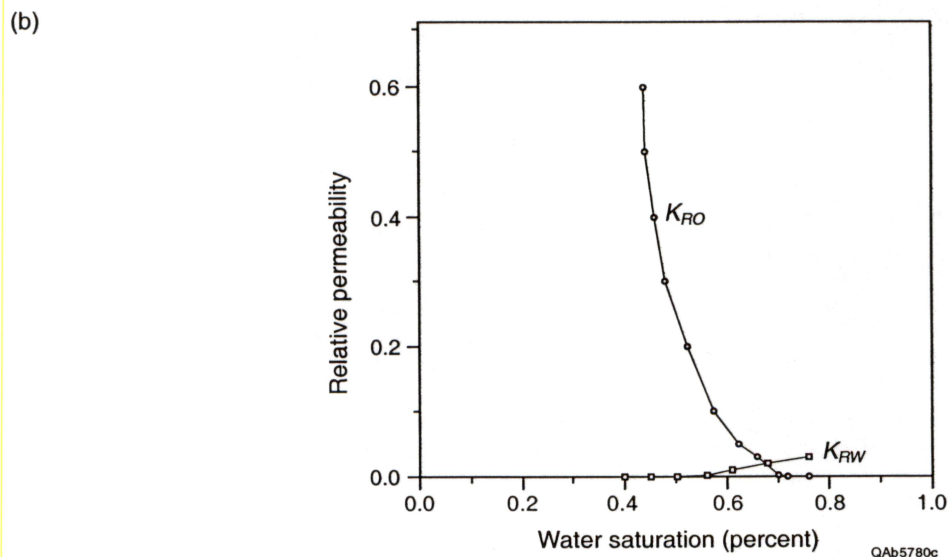
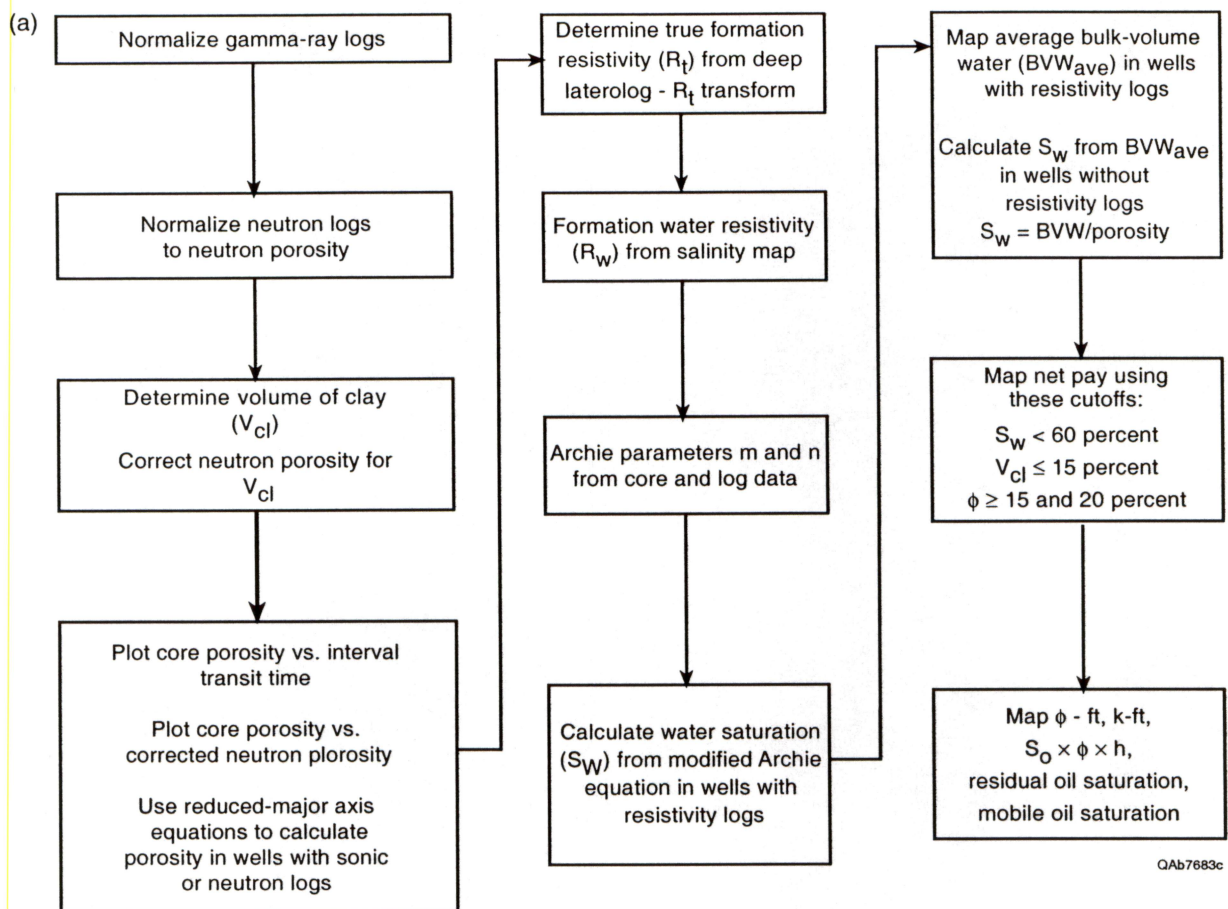


Figure 13. (a) Flow chart of petrophysical analysis. (b) Normalized relative permeability curves were used to select an S_w cutoff for net pay at 60 percent (from Asquith and others, 1997). Normalized curves were derived from five curves measured in the FGU 156 well. The method of normalization was based on the work of Schneider (1987). K_{ro} is the relative permeability to oil, and K_{rw} is the relative permeability to water.

time (ITT) versus core porosity in order to determine log-to-core porosity transforms. Core porosity was plotted versus core permeability to derive a porosity–permeability transform equation. Additional tasks included (1) mapping formation water resistivity (R_w) across the unit, (2) determining the Archie Parameters m (cementation exponent) and n (saturation exponent), and (3) developing a transform for converting resistivity measured by the deep laterolog (LLD) to true formation resistivity (R_t) when a log measuring flushed-zone resistivity (R_{xo}) is unavailable (fig. 13) (Asquith and others, 1997).

This approach combines traditional log-analysis techniques with new methods that were developed for this study to compensate for missing data. The approach is presented in detail in Asquith and others (1997) and is summarized later.

Porosity Transforms

Because the old gamma-ray and neutron logs were run by many different companies at different scales and sensitivities, the gamma-ray logs were normalized to API units and the neutron logs to porosity units. The procedure for normalization was similar to that outlined by Barrett (1995). High and low gamma-ray and neutron values were selected for each well, however, so that the normalizing transforms each had different slopes and intercepts.

Because the Ramsey sandstone contains authigenic clays and interbedded organic-rich siltstone, it was necessary to correct for the volume of clay and silt in the calculation of neutron porosity. The clay correction was obtained from gamma-ray responses in clean sandstones versus response in organic-rich siltstones, the closest lithology to shale available in the section. Gamma-ray cutoffs for organic-rich siltstone and clean sandstone were determined at 90 and 40 API units, respectively, by plotting gamma-ray response

versus interval transit times (Asquith and others, 1997). The volume of clay (V_{cl}) was then calculated by the following equations:

$$IGR = (GR - 40)/(90 - 40)$$

$$V_{cl} = 0.33[2^{(2 \times IGR)} - 1.0] \text{ (Atlas Wireline, 1985)}$$

where IGR = gamma-ray index and GR = gamma-ray value from log. The V_{cl} was used to correct the normalized neutron porosity by multiplying by $(1.0 - V_{cl})$ (Asquith and others, 1997).

Interval transit time (ITT) logs and normalized and clay-corrected neutron logs were then correlated to core porosity by reduced major axis regression (Asquith and others, 1997). The resulting equations for porosity are as follows:

$$\text{Porosity (percent)} = (0.59 \times \text{ITT}) - 31.5$$

$$\text{Porosity (percent)} = (1.11 \times \text{clay-corrected neutron porosity}) + 0.67$$

Calculation of Water Saturation

Resistivity logs are electric logs that are used to determine hydrocarbon-versus-water-bearing zones (Asquith and Gibson, 1982). Resistivity logs can be used to calculate water saturation in a formation if several parameters are known, including (1) formation water resistivity (R_w), (2) true formation resistivity (R_t), (3) Archie's cementation exponent (m), and (4) Archie's saturation exponent (n) (Archie, 1942). R_w values were calculated across the Ford Geraldine unit from a map of prewaterflood salinity (Ruggiero, 1985; Asquith and others, 1997). The R_w values at 75°F ranged from 0.11 to 0.18 ohm-m, with the highest values to the southwest.

True Formation Resistivity

Calculating accurate water saturations in the Ford Geraldine unit was difficult because a deep laterolog (LLD) was commonly run without an accompanying log to

measure either flushed-zone resistivities (Microlaterolog, MLL, or Microspherically Focused Log, MSFL) or invaded-zone resistivities (Shallow Laterolog). These additional logs make it possible to correct the resistivities of the partially invaded zone measured by the LLD to the true formation resistivity (R_t) needed for calculation of accurate saturations. Without applying this transform, water saturations in wells with only LLD logs would be overestimated. To overcome this problem, a linear regression transform was developed between R_t (as calculated in 12 Ford Geraldine unit wells having both shallow-resistivity measurement tools run as well as the LLD) and the LLD curve response (Asquith and others, 1997):

$$R_t = 1.3002 \times \text{LLD} + 0.3397$$

Archie Parameters m and n

Special core analyses from a well in the Ford Geraldine unit (FGU-156) included four measurements of the cementation exponent, m . The average of the measured m values was 1.88. To verify the measured values, we used log data to back-calculate m from ITT porosity and flushed-zone resistivity log values (Asquith and others, 1997). This method gave a value for m of 1.83, which was used in the modified Archie equation for the Ford Geraldine unit.

Special core analyses also measured saturation exponent (n), but the values were low (average = 1.32) and probably not accurate. For this reason, a new technique was developed (Asquith and others, 1997) to calculate the value of n using core porosity and water-saturation values from relative permeability curves by the following equation:

$$n = \text{LOG} (F \times R_w / R_t) / \text{LOG} (S_w)$$

where:

n = saturation exponent

$F = 1/\phi^{1.83}$ (ϕ is porosity)

R_w = formation water resistivity at formation temperature (0.092 ohm-m)

R_t = true formation resistivity ($R_t = 1.67 \times \text{LLD} - 0.67 \times \text{MLL}$)

S_w = water saturation from relative permeability curves

The value of n that was calculated using this method, 1.90, is more realistic than the core-measured average value of 1.32 (Asquith and others, 1997). Therefore, for the Bell Canyon sandstones in the Ford Geraldine area, water saturations should be calculated by the following modified Archie equation:

$$S_w = [(1/\phi^{1.83}) \times (R_w / R_t)]^{1/1.90}$$

Net-Pay Cutoffs

Cutoffs to define net pay for the Ramsey sandstone in the Ford Geraldine unit were established for V_{cl} , ϕ , and S_w on the basis of core and log data and published information. Accurate values for V_{cl} are difficult to determine for the Delaware sandstone because of the absence of adjacent shales. Therefore, we selected a V_{cl} cutoff on the basis of the work of Dewan (1984), which suggests a V_{cl} cutoff of 15 percent for reservoirs with dispersed authigenic clay. This cutoff was used because of the common occurrence of authigenic clay in the Delaware sandstones (Williamson, 1978; Thomerson, 1992; Walling, 1992; Asquith and others, 1995; Green and others, 1996).

A plot of core porosity versus core permeability for the Ramsey sandstone in the Ford Geraldine unit resulted in the selection of the following ϕ cutoffs:

$\phi \leq 15$ percent for a permeability of 1.0 md

$\phi \leq 20$ percent for a permeability of 5.0 md

Normalization of five relative-permeability curves (fig. 13b) led to the selection of an S_w cutoff for net pay at 60 percent, a value at which the relative permeability to oil is about eight times that of permeability to water (Asquith and others, 1997; Dutton and others, 1999a).

Application

The approach to petrophysical analysis that was developed in the Ford Geraldine unit can be used in other fields in the Delaware sandstone play. Core-analysis and log data from the field being studied should be used to the greatest extent possible, but where they do not exist, the Ford Geraldine values provide a reasonable substitute. For example, if core-analysis data are available, they should be used to develop core-porosity to log-porosity transforms specific to that field, but in a field having no core analyses, the transforms developed in the Ford Geraldine unit can be used instead. Similarly, if a field has both Laterologs (LLD) and accompanying Microlaterologs, Microspherically Focused Logs, or Shallow Laterologs, an R_t –LLD transform specific to that field should be developed, but if these logs are not available, the Ford Geraldine equation can be used instead. Unless special core-analyses have determined m and n in a field, the values determined for these parameters in the Ford Geraldine unit are the best data available, and water saturations should be calculated by the following modified Archie equation:

$$S_w = [(1/\phi^{1.83}) \times (R_w/R_t)]^{1/1.90}.$$

When applying this method of petrophysical analysis to another field, it is important to compare the results with other field information, such as production data. In fields with poor, incomplete data, there is probably no unique solution to log interpretation that will always be successful. Instead, a variety of techniques must be tried and their validity tested using all available information about the field.

Geophysical Interpretation of the Ramsey Sandstone

To supplement the interpretation of the Ford Geraldine unit, we evaluated the Ramsey sandstone using 3-D reflection seismic data from a 36-mi² area (Dutton and others, 1999a) (fig. 3). These data were acquired over the Geraldine Ford complex (fig. 3), which includes Bell Canyon and Cherry Canyon producing fields, in order for us

to determine whether large-scale heterogeneities in the Delaware Mountain Group could be imaged using 3-D seismic data. The 3-D seismic survey was designed to image the Delaware Mountain Group. The acquisition parameters are summarized in table 2.

Synthetic Seismograms and Wavelet Extraction

Synthetic seismograms were generated using the FGU-128 well (fig. 14) and the Conoco G. E. Ramsey No. 6 well to correlate the seismic reflection character with the formation tops interpreted from well logs. Both wells penetrated the Ramsey interval, with the FGU 128 having 37 ft of Ramsey sandstone present and the Conoco G. E. Ramsey No. 6 having the Ramsey sandstone absent. The location of these two wells is shown in figure 3. The FGU-128 well is located on the east side of the field, and the synthetic seismogram shows in detail the picks associated with the Ramsey sandstone (fig. 14). This synthetic seismogram shows that the base of the Castile Formation salt and the top of the Lamar Limestone produce a peak response that will be referred to as the Lamar peak. The trough below the Lamar peak was also picked to help us characterize the Ramsey reservoir. This trough, which will be referred to as the Ramsey trough, is related to the base of the Ramsey and the top of the Ford siltstone (fig. 14). A representative seismic line (fig. 15) shows the seismic response of the Castile, Lamar, Ramsey, and Manzanita intervals. The Manzanita Limestone in the Cherry Canyon Formation underlies the main Cherry Canyon reservoir interval in Ford West field (fig. 14).

The FGU-128 well has 37 ft of Ramsey sandstone in an area of the field associated with 21-percent average porosity; the well has a cumulative production of approximately 50,000 bbl of oil. The dominant frequency of the seismic data is 50 to 60 Hz. According to a wavelet derived from the seismic data, the Ramsey sandstone in this well is less than one-quarter of a wavelength thick (Dutton and others, 1997a). This wavelet was derived

Table 2. Design parameters for 3-D seismic acquisition.

Area	36 mi ²
Bin size	110 × 110 ft
Spread	8 lines × 96 channels/line (768 channels live)
Receiver line spacing	1,100 ft
Receiver flags	220 ft
Receiver arrays	24 geophones/linear array
Array dimension	220-ft inline, 100-ft crossline
Source line spacing	880 ft
Source flags	220 ft
Source arrays	4 vibs × 8 sweeps (5 vibs actually used)
Sweep	8–60 Hz/12 sec long
Sample rate	2 millisecs
Listen time	4 secs

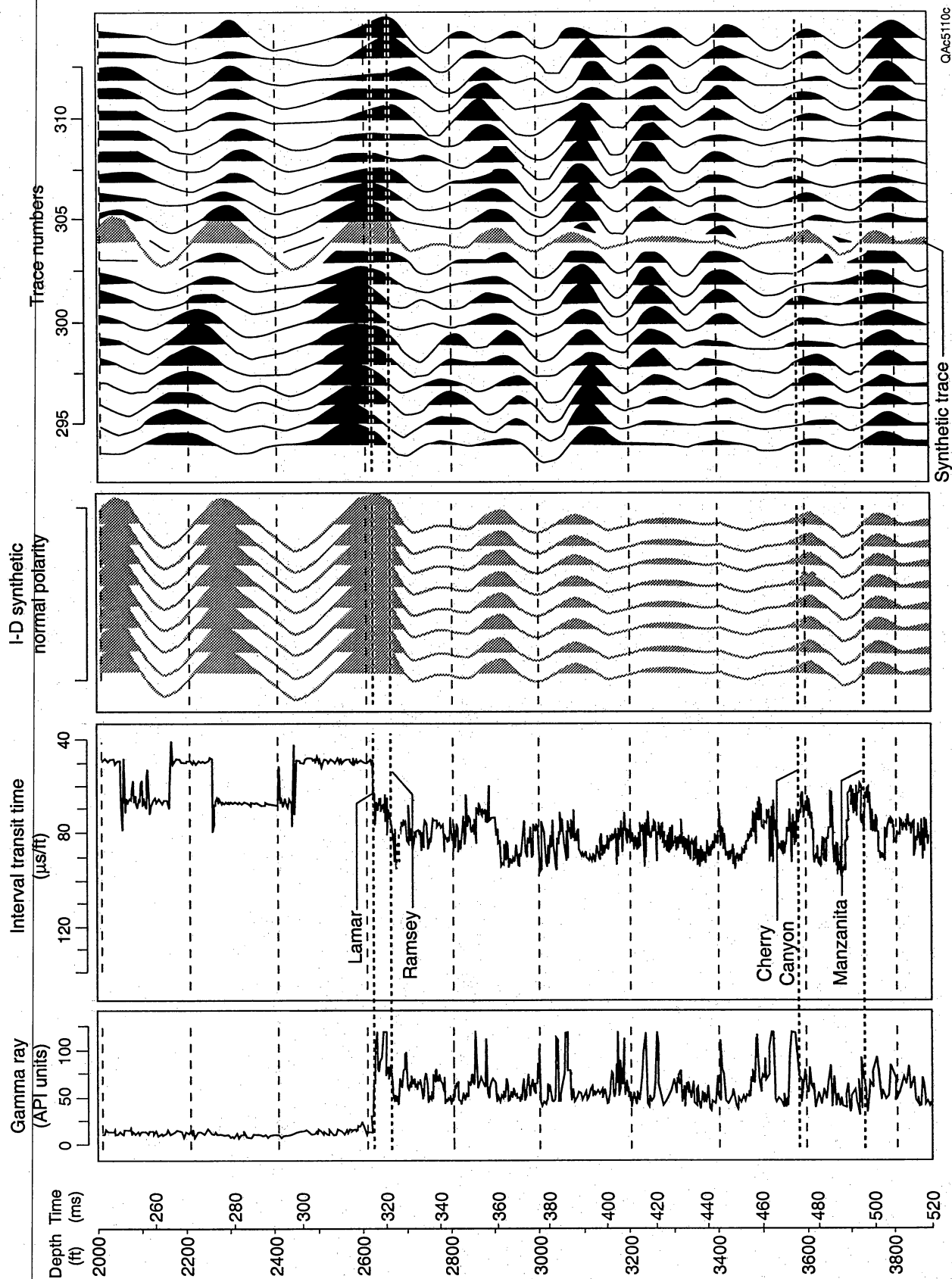


Figure 14. Synthetic seismogram generated for the FGU-128 well to correlate the seismic reflection character with the formation tops interpreted from well logs; well location is shown in figure 3. The horizon tops and their associated seismic response are shown.

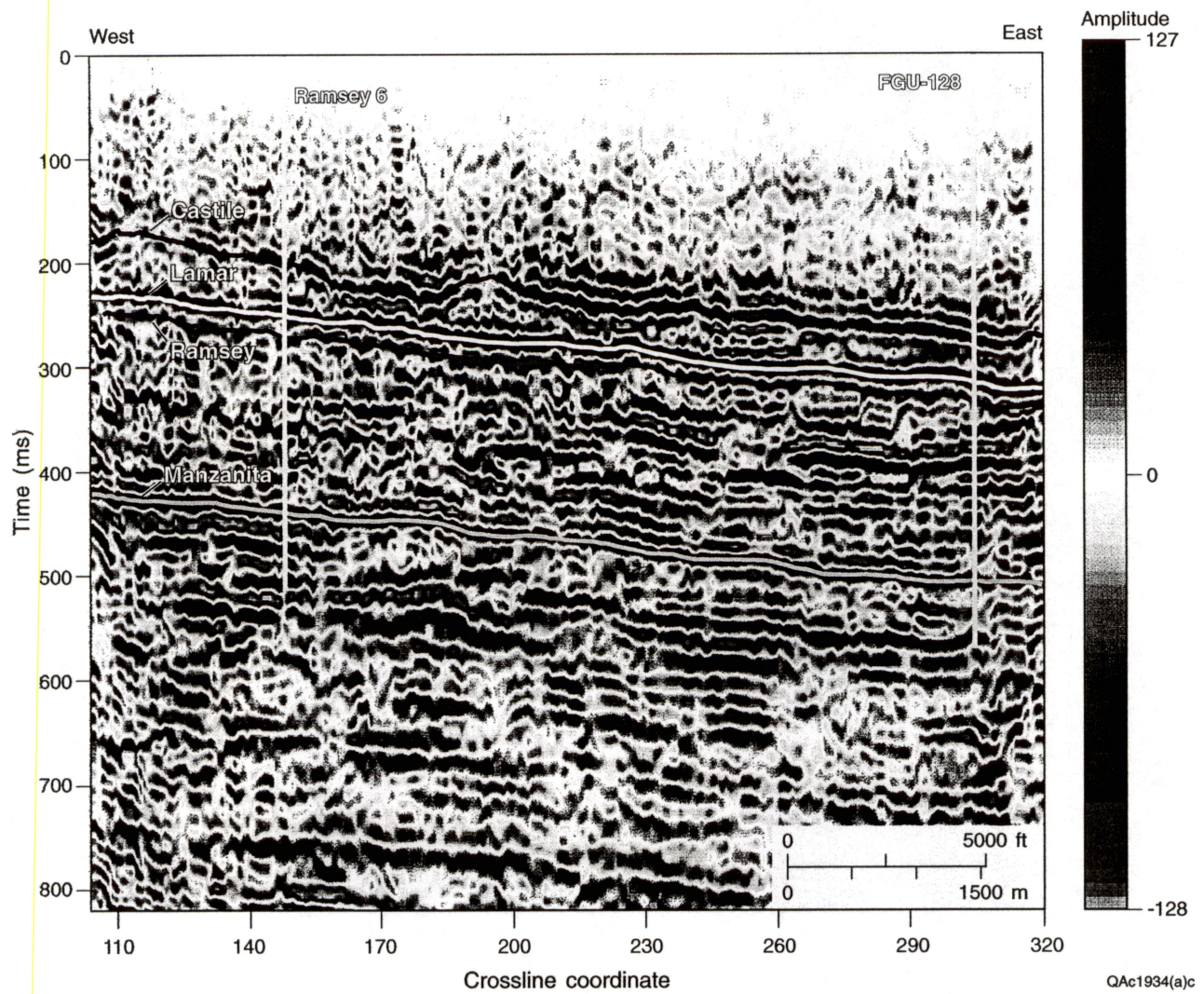


Figure 15. Representative seismic line showing the top of the Castile, Lamar, Ramsey, and Manzanita intervals. Location of seismic line shown in figure 3.

from the data set between 250 and 1,500 ms and was used to derive the seismograms. The wavelet has moderated side-lobe energy but is quite low frequency for imaging the Delaware Mountain Group. Ormsby (8-14-50-60 Hz) or Ricker (28 HZ) theoretical wavelets approximate the derived wavelet. The maximum thickness of the Ramsey sandstone in the field is 61 ft, which would be approximately one-quarter of a wavelength thick. The Ramsey sandstone is always below the tuning thickness of this seismic data and would therefore be considered a thin bed. As a result, amplitude is not a measure of thickness alone because other factors such as velocity and thickness of the Lamar limestone and composition of the Ford siltstone affect the seismic interval that is being used to characterize the Ramsey.

Structure and Coherency Maps

A structure map of the top of the Lamar Limestone was made by depth converting the Lamar time horizon using an average velocity gradient calculated between the seismic datum and the Lamar. All wells were used in the calculation of the structure map. The structure on the top of the Lamar shows a gentle northeast dip into the deeper part of the Delaware Basin. A residual map of the Lamar peak (fig. 16) was generated by filtering the Lamar peak horizon with a 60×60 filter then subtracting the resulting smoothed horizon from the original horizon. The residual map shows localized structural highs and lows. The residual accentuates the subtle high ridge in the structure map that is related to differential compaction over the main Ramsey 1 channel. Another residual high is present at the north end of the unit, where the Ramsey 1 and Ramsey 2 channels stack.

We processed the seismic volume by using the coherency-cube algorithm (Bahorich and Farmer, 1995) in an attempt to identify discontinuities such as channels, compartmentalization, or faulting in the Delaware Mountain Group. The coherency-cube algorithm calculates localized waveform similarity in both inline and crossline directions,

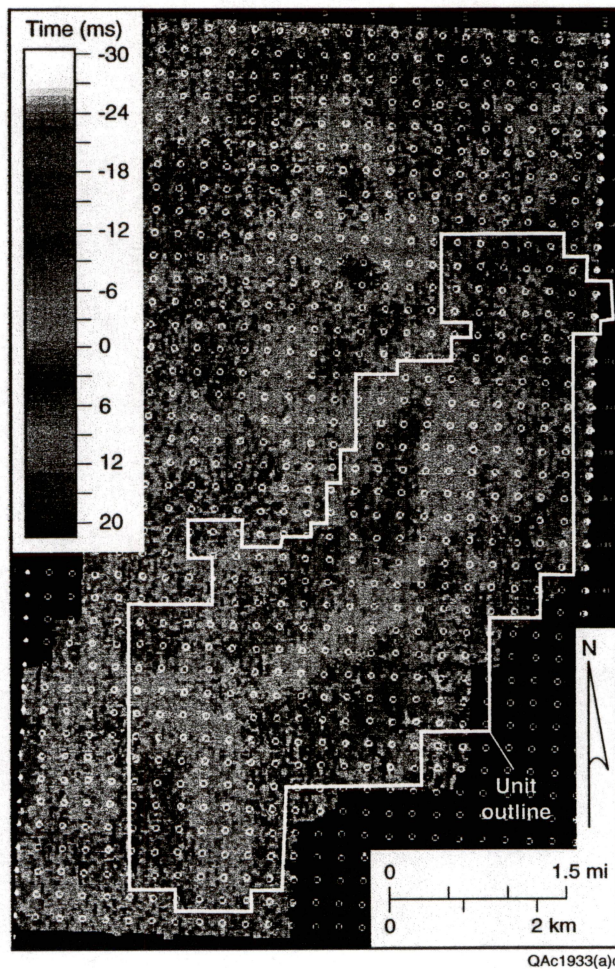


Figure 16. Residual map of the Lamar peak showing localized structural high and lows. The residual accentuates the subtle high ridge in the structure map that is related to differential compaction over the main Ramsey 1 channel.

thus giving estimates of 3-D seismic coherence. Faults and stratigraphic boundaries generate regions of seismic traces having a different seismic character than the corresponding regions of neighboring traces, resulting in a discontinuity in local trace-to-trace coherence (Bahorich and Farmer, 1995). We derived coherency cubes using 3-, 5-, and 7-trace windows and determined that the 5-trace window was best for imaging the upper Delaware section. A coherence extraction on the Lamar shows a crude outline of the productive wells in the Ford Geraldine unit but does not have the resolution to determine compartmentalization and did not indicate faulting in the Ramsey sandstone.

Conclusions

Accurate seismic characterization of the Ramsey sandstone is difficult because Ramsey sandstone thickness is always one-quarter of a wavelength or less of the seismic data within the target interval, putting the Ramsey sandstone into the thin-bed category. As a result, amplitude is not a measure of thickness alone because other factors such as velocity and thickness of the Lamar limestone and composition of the Ford siltstone affect the seismic interval that is being used to characterize the Ramsey. The coherency-cube data, although effective in delineating the field outline, failed to detect reservoir compartmentalization. Residual mapping of the Lamar assisted in the visualizing of thick sandstones associated with the Ramsey 1 sandstone near the center of the field. Slight ridges can be seen in the structure map, but the residual maps make these ridges more obvious.

Development History and Simulation

Field Development History

Primary recovery in Geraldine Ford field began in 1956 and continued until June 1969 (fig. 17). A total of 301 wells were drilled for primary production. Primary cumulative production was 13.2 MMbbl, or 13.3 percent of the 99 MMbbl OOIP.

The Ford Geraldine unit was formed in November 1968, and a pilot waterflood project started in June 1969 (Pittaway and Rosato, 1991). The waterflood was expanded throughout the south part of the unit in stages between 1972 and 1980, but the north part of the unit received only a short, low-volume waterflood. An additional 6.8 MMbbl of oil was produced after unitization (fig. 17), but only 3.5 MMbbl was attributed to the waterflood, significantly less than predicted from reservoir simulation. By the end of secondary development, recovery efficiency had increased to only 20 percent.

Tertiary recovery by CO₂ injection began in March 1981 in the entire unit except for the north end, but CO₂ supply was erratic until December 1985. Production response occurred in 1986 after higher and constant CO₂ injection began in December 1985 (fig. 17) (Pittaway and Rosato, 1991). Cumulative tertiary production through 1998 was 5.8 MMbbl. Estimated ultimate tertiary recovery is 9.0 percent (K. R. Pittaway, written communication, 1997).

Simulation of Tertiary Recovery

To estimate the effectiveness of tertiary recovery, flow simulation was performed for a CO₂ flood (Malik, 1998). One-quarter of a five-spot injection pattern in the north part of the Ford Geraldine unit, an area that was not part of the CO₂ flood, was selected for the simulation. The simulation used layered permeabilities having a $6 \times 5 \times 6$ grid.

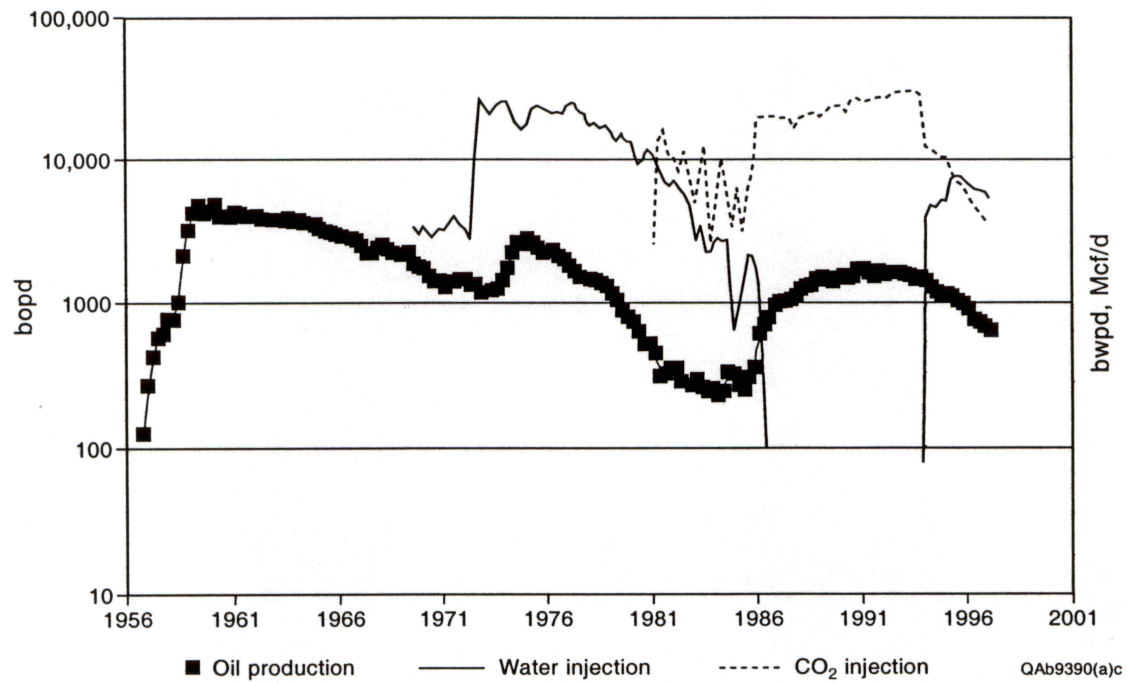


Figure 17. Plots of total oil production in the Ford Geraldine unit and volumes of water and CO₂ injected.

The block size was 150 ft in the areal (x and y) directions and 5.33 ft in the vertical (z) direction. The Ramsey 1 and 2 sandstones are both present in the simulation area, and average total sandstone thickness in the area is 32 ft. A permeability cutoff of 5 md was used to exclude the nonproducing zones. Maximum permeability was limited to 200 md. The rock compressibility factor used was $7.499 \times 10^{-6}/\text{psi}$, and the water compressibility was $3.15 \times 10^{-6}/\text{psi}$.

We performed the flow simulation using UTCOMP, an isothermal, three-dimensional, compositional simulator for miscible gas flooding (Chang, 1990). The solution scheme is analogous to IMPES (Implicit Pressure, Explicit Saturations) (Chang, 1990). For this work, the Peng-Robinson equation of state (EOS) is used for flash calculations, phase identification, and fluid property calculations (Peng and Robinson, 1976). Three-phase simulation for a CO₂ flood was performed. Postwaterflood oil saturations were estimated to be 35 to 39 percent; an average oil saturation of 37 percent was used for the simulation. No attempt was made to match primary and waterflood response with the preliminary model. An exponential relative permeability model for water, oil, and gas flow was fitted to the measured relative permeability data.

Five hydrocarbon components were used in the simulation. Reservoir hydrocarbons were characterized as four pseudocomponents (Khan, 1992), and their properties were calculated from the PVT (pressure, volume, temperature) data. The fifth component is CO₂. Injection pressure is limited to 2,000 psia, and production wells have a flowing bottomhole pressure of 700 psia.

The simulation estimates breakthrough oil recovery of 10 percent (Malik, 1998). Unlike a waterflood, the simulation indicates that CO₂ injection results in a gradual increase in recovery even after breakthrough. Oil-production rates increase until breakthrough. At the time of breakthrough, the oil rate sharply rises to its peak value and gradually declines thereafter. Water:oil ratio (WOR) gradually decreases with progress of

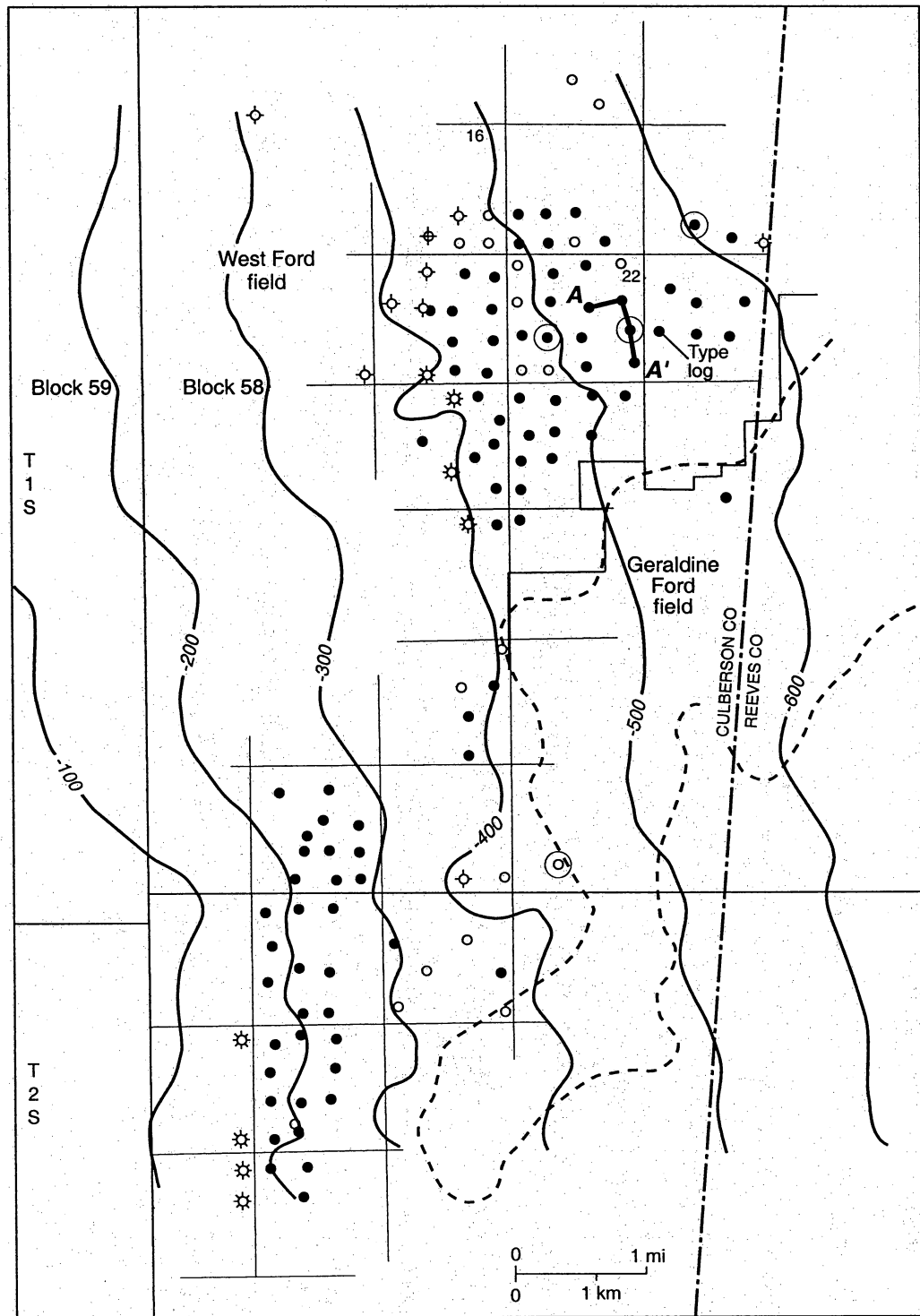
the flood and remains low even after breakthrough, but gas:oil ratio (GOR) continues to increase after breakthrough.

The simulation indicates that 10 percent of remaining oil in place (ROIP) in the demonstration area could be recoverable through CO₂ flood. The south part of the Ford Geraldine unit has already undergone CO₂ flood for tertiary recovery. Current data indicate that about 8 percent of OOIP in the CO₂ area has been recovered by this CO₂ flood, and ultimate recovery is expected to be 9 percent of OOIP in the CO₂ area (K. Pittaway, written communication, 1997). The results of the simulation appeared to be slightly optimistic, but the model was not refined further because the industry partner decided not to continue in the project. Twofreds Field East Side, which has also been CO₂ flooded, recovered 16 percent of the OOIP, or 19 percent of the ROIP, from tertiary CO₂ operators.

RESERVOIR CHARACTERIZATION OF FORD WEST FIELD

The second field that was studied during the initial reservoir-characterization phase of this project was Ford West (4100) field in Culberson County (figs. 3, 18). Ford West field is still in primary production from deeper (3,400-ft) slope and basin clastic reservoirs. This field, located 2 mi west of Geraldine Ford field, produces from a similar style trap in the upper part of the Cherry Canyon and basal Bell Canyon Formations (fig. 19). The field produces from two principal reservoir zones (figs. 19, 20), the lower B2 sandstone reservoir in the uppermost part of the Cherry Canyon Formation and the overlying B1 sandstone in the lower part of the Bell Canyon Formation.

Three cores through the B2 sandstone (fig. 18) and 16 logs formed the Ford West data base for the project. Because of the limited number of cores and logs available and because the outcrop analogs were from the upper Bell Canyon Formation and, hence,



QAb8123c

- Oil-producing well
- Oil, temporarily shut-in
- ✱ Gas-producing well
- ◇ Dry hole
- ⊙ Cored well
- Contour interval 100 ft
- Datum: sea level

Figure 18. Location map of Ford West field, which produces from the upper Cherry Canyon Formation and lowermost Bell Canyon Formation, Delaware Mountain Group. Modified from Linn (1985). Type log shown in figure 19, and cross section A–A' shown in figure 20.

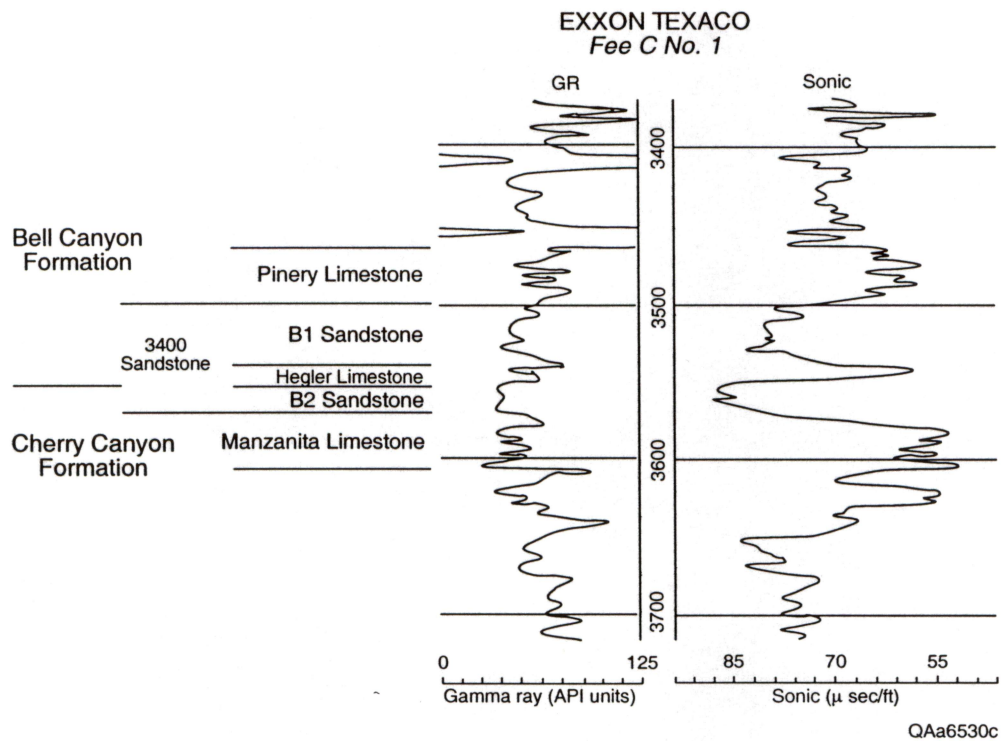


Figure 19. Typical log, Ford West field from the Exxon Texaco Fee C No. 1. From Linn (1985). Well location shown in figure 18.

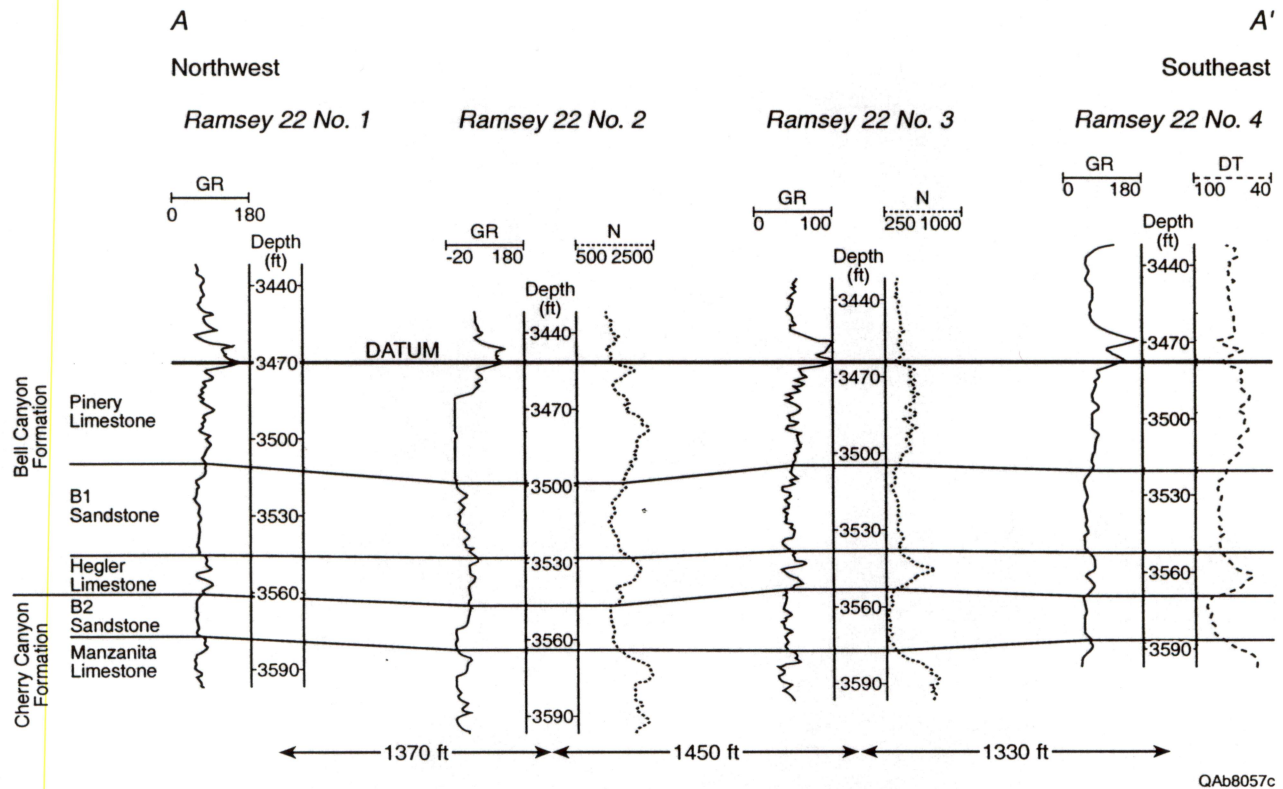


Figure 20. Northwest-southeast strike cross section A-A' of the upper Cherry Canyon and lower Bell Canyon interval in Ford West field. Location of cross section shown in figure 18.

more applicable to Geraldine Ford field, reservoir characterization of Ford West field was not as extensive as that of Geraldine Ford field.

The sandstones in Ford West field have a very narrow range of grain sizes. The average grain size in B2 sandstone samples is 0.093 mm (Linn, 1985). B1 sandstones are slightly finer grained, averaging 0.088 mm (Linn, 1985). Both are very well sorted.

Sandstones in Ford West field were interpreted as turbidite deposits (Linn, 1985), and the channel-levee and lobe depositional model developed for the Ramsey sandstone may apply to the Ford West reservoirs as well. A northeast-southwest trend of thick B2 sandstone in the southeast part of section 22 is interpreted as a channel. Thinner sandstones along the margins of the channel may be levee and splay facies. Core-analysis data from 33 B2 sandstone samples from two wells show an average porosity of 22.6 percent and geometric mean permeability of 19.5 md. The B1 sandstone is thickest at the northwest margin of the study area, possibly where a channel cuts the study area and thins to the southeast.

Regional mapping of the distribution of the B1 and B2 sandstones shows that the younger B1 sandstone progrades farther basinward with respect to the older B2 sandstone (Linn, 1985). Kerans and others (1992) interpreted this to have been a time of relative fall of sea level, which would be consistent with basinward stepping of the B1 sandstone.

On the basis of the initial reservoir-characterization phase of this project, the north end of Ford Geraldine unit was chosen as the proposed demonstration area. This area was selected over Ford West field because of (1) the greater number of available data from Ford Geraldine unit, including cores, logs, and core-analysis data; (2) a larger volume of oil in place in the Ford Geraldine unit than in Ford West field; and (3) the greater applicability of outcrop information to the upper Bell Canyon reservoir interval in the Ford Geraldine unit than to the lower Bell Canyon/upper Cherry Canyon reservoir in Ford West field.

RESERVOIR CHARACTERIZATION OF EAST FORD UNIT

After reservoir characterization and simulation of a CO₂ flood of the north part of the Ford Geraldine unit were completed, the original industry partner decided not to continue in the project. A new industry partner, Orla Petco, Inc., participated in the remainder of the project, and the focus shifted to the East Ford unit in Reeves County, Texas (fig. 21). The reservoir-characterization phase of the project was expanded to include the East Ford unit. This additional reservoir characterization provided an excellent opportunity to test the transferability of the geologic model and log-interpretation methods developed during reservoir characterization of the Ford Geraldine unit to another field in the Delaware sandstone play.

Reservoir characterization of the East Ford unit built upon the earlier, integrated reservoir-characterization study of the Ford Geraldine unit (Dutton and others, 1996, 1997a, b, 1998, 1999a). Like the Ford Geraldine unit, the East Ford unit produces from the Ramsey sandstone (fig. 22), the most prolific horizon in the Bell Canyon Formation. The technologies used for reservoir characterization of the East Ford unit included (1) subsurface log, core, and petrophysical study; (2) high-resolution sequence stratigraphy; (3) mapping done previously of nearby outcrop reservoir analogs; and (4) analysis of production history.

Geologic Characterization

Investigation of Bell Canyon sandstones in outcrop (Barton, 1997; Barton and Dutton, 1999) and subsurface characterization of the Ford Geraldine unit (Dutton and others, 1999a) formed the basis for the depositional model developed for the East Ford unit. Ramsey sandstones at East Ford are interpreted as having been deposited by turbidity currents. Like the sandstones in outcrop and at the Ford Geraldine unit, Ramsey sandstones that form the reservoir at the East Ford unit are interpreted as having been

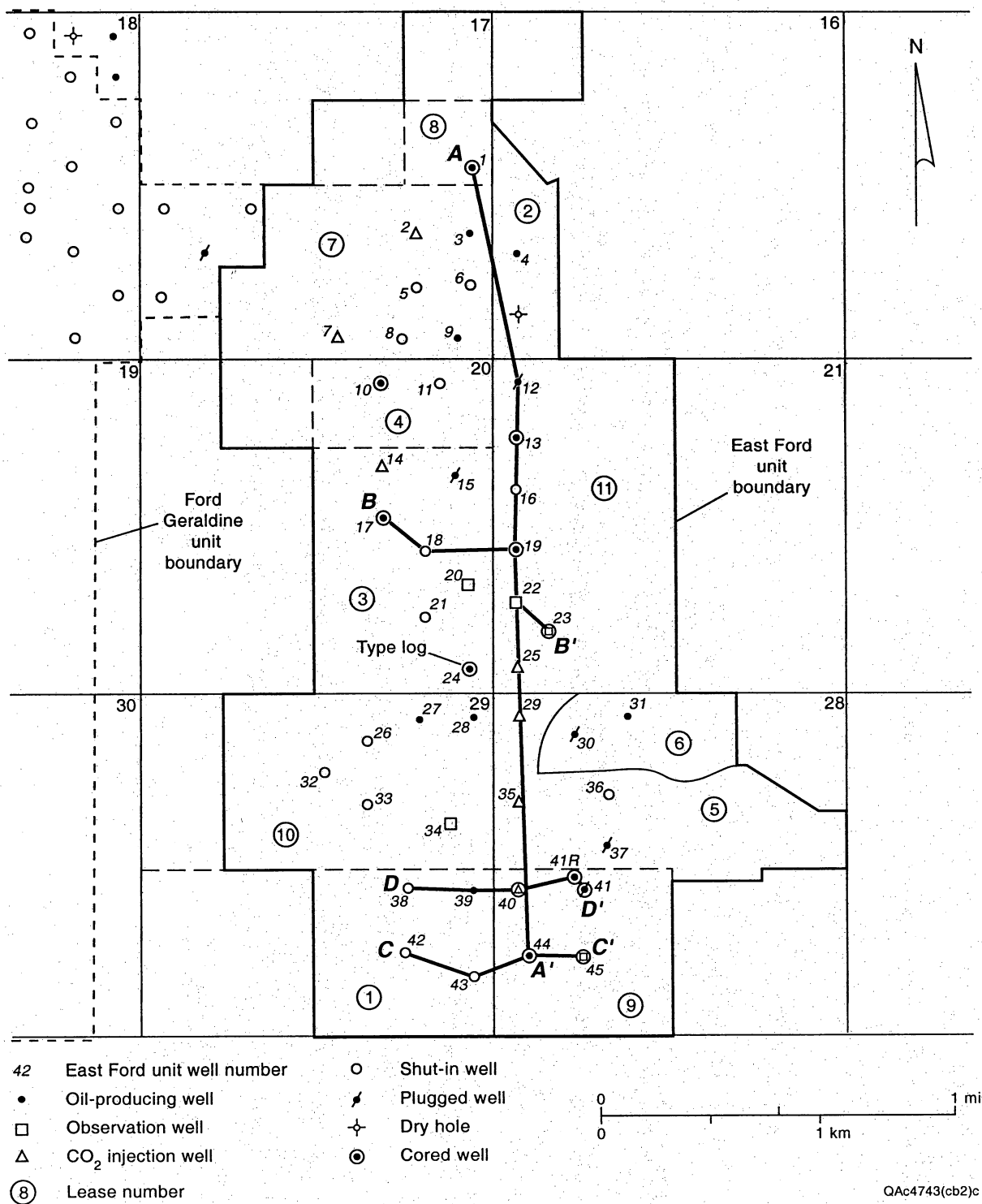


Figure 21. Status of wells in the East Ford unit, Reeves County, Texas. Type log shown in figure 22. Cross sections A–A', B–B', C–C', and D–D' shown in figures 23, 29, 30, and 51, respectively.

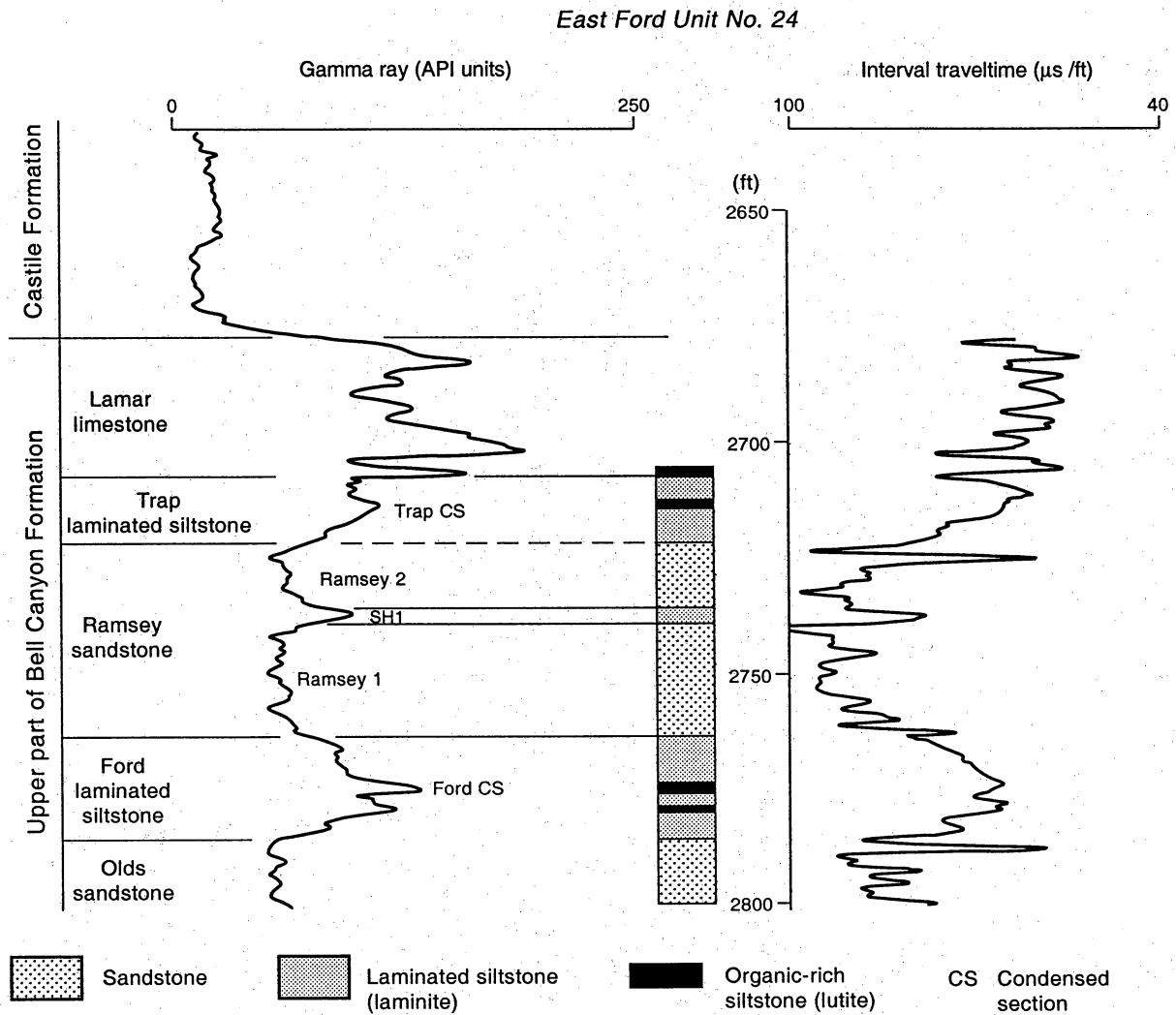


Figure 22. Typical log from East Ford Unit No. 24. Well location shown in figure 21.

deposited by a system of leveed channels having attached lobes and overbank splays (fig. 6a). Individual channel-levee and lobe complexes stack in a compensatory fashion and are separated by laterally continuous, laminated siltstones. These siltstones are interpreted to have been deposited by the settling of marine organic matter and airborne silt during periods when coarser particles were prevented from entering the basin.

Three major rock types are present in the East Ford unit—very fine grained sandstone, laminated siltstone (laminite), and organic-rich siltstone (lutite) (Ruggiero, 1985; Dutton and others, 1997a). The sandstone facies (a silty, very fine grained, well-sorted arkose) forms the reservoir. The laminite facies consists of parallel-laminated siltstone alternating with laminae (0.2 to 2 mm thick) of organics and silt. The laminated siltstone forms the seal of the stratigraphic trap. Lutite (a dark, fissile, organic-rich siltstone) also contributes to the seal.

Mapping of Ramsey Sandstone Genetic Units

The Ramsey sandstone in the East Ford unit is a 0- to 45-ft-thick sandstone that is bounded by the Ford and Trap laminated siltstones. Lutites in the underlying Ford siltstone and the overlying Trap siltstone (figs. 22, 23) are interpreted to be condensed sections that mark the top and base of a genetic unit, equivalent to a high-order cycle (Gardner, 1992; Kerans and others, 1992). In the East Ford unit, the Ramsey is divided into two sandstones (Ramsey 1 and Ramsey 2) separated by a 1- to 3-ft-thick laminated siltstone (SH1). The Ramsey high-order cycle is thus subdivided into five units, from oldest to youngest: (1) upper Ford siltstone, from the Ford condensed section to the top of the Ford siltstone; (2) Ramsey 1 sandstone; (3) SH1 siltstone; (4) Ramsey 2 sandstone; and (5) lower Trap siltstone, from the base of the Trap siltstone to the Trap condensed section (figs. 22, 23).

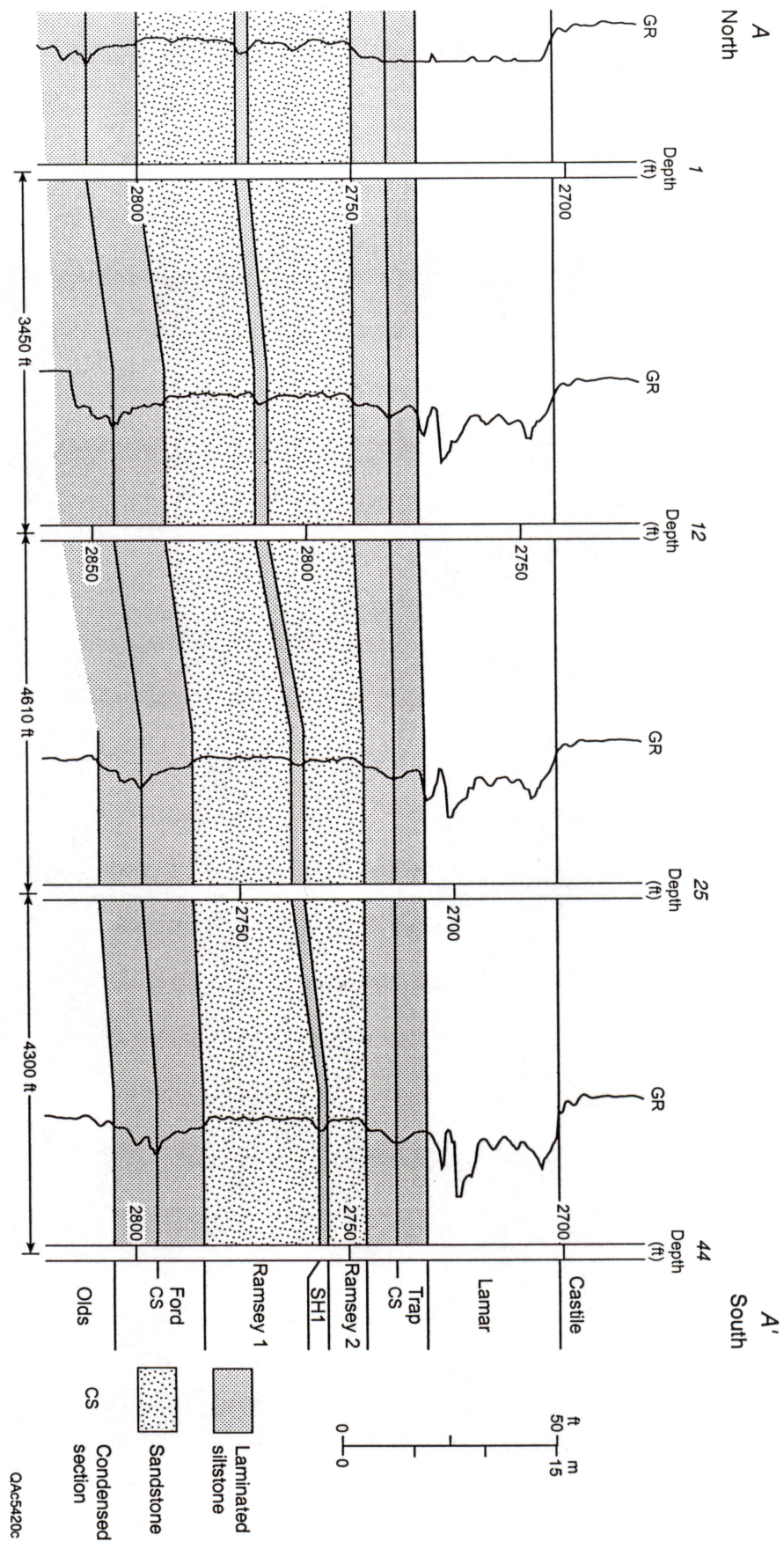


Figure 23. North-south dip cross section A-A' of the length of the East Ford unit. Location of cross section shown in figure 21.

We correlated key stratigraphic horizons using digitized logs from the 45 wells in the East Ford unit. A seven-layer, three-dimensional, deterministic geologic model was constructed by means of stratigraphic-interpretation computer software.

Upper Ford Siltstone

The upper Ford thins from the northwest side of East Ford field (15 to 16 ft) to the southeast (11 to 12 ft) (Dutton and others, 1999c). The upper Ford is interpreted as being composed of organic-rich siltstone laminae interbedded on a millimeter scale with organic-poor siltstone laminae. The average grain size of the silt coarsens upward from the Ford condensed section to the top of the Ford, and the percentage of sand, amount of burrowing, and thickness of organic-poor laminae all increase toward the sandstone. Gamma-ray response decreases over this interval (fig. 22), probably because much of the radioactivity is contained in organic matter within the organic-rich layers.

Porosity in the Ford siltstone in the East Ford unit ranges from 7.5 to 22.4 percent and averages 15.9 percent (table 3). Permeability ranges from 0.1 to 5 md and averages 1 md. Average water saturation measured in cores is 65 percent.

Ramsey 1 Sandstone

The Ramsey 1 sandstone is thickest on the east side of the East Ford unit (fig. 24). It pinches out along the west and south margins of the unit and reaches a maximum thickness of more than 25 ft along an elongate, north-south trend. The Ramsey 1 sandstone has at least two branches, one of which forms the reservoir at the Ford Geraldine unit and the other in the East Ford unit. The two branches divide north of the East Ford unit.

In most wells the gamma-ray response in the Ramsey 1 sandstone is distinctly lower than in the underlying Ford siltstone; in some wells the gamma response continues to

Table 3. Summary of core-analysis data from upper Bell Canyon sandstones and siltstones, East Ford unit.

	Average porosity (range)(percent)	Average permeability (range) (md)	Dykstra-Parsons coefficient (V)	Water saturation (percent)	No. samples
Trap siltstone	14.7 (2.9-18.8)	1 (0.01-8)		67	23
Ramsey 2 sandstone	21.4 (6.5-30.6)	34 (0.1-249)	0.57	48	133
SH1 siltstone	18.2 (17.2-20.7)	4 (0.3-14)		54	19
Ramsey 1 sandstone	22.5 (6.5-27.0)	46 (0.02-183)	0.44	46	182
Ford siltstone	15.9 (7.5-22.4)	1 (0.1-5)		65	31

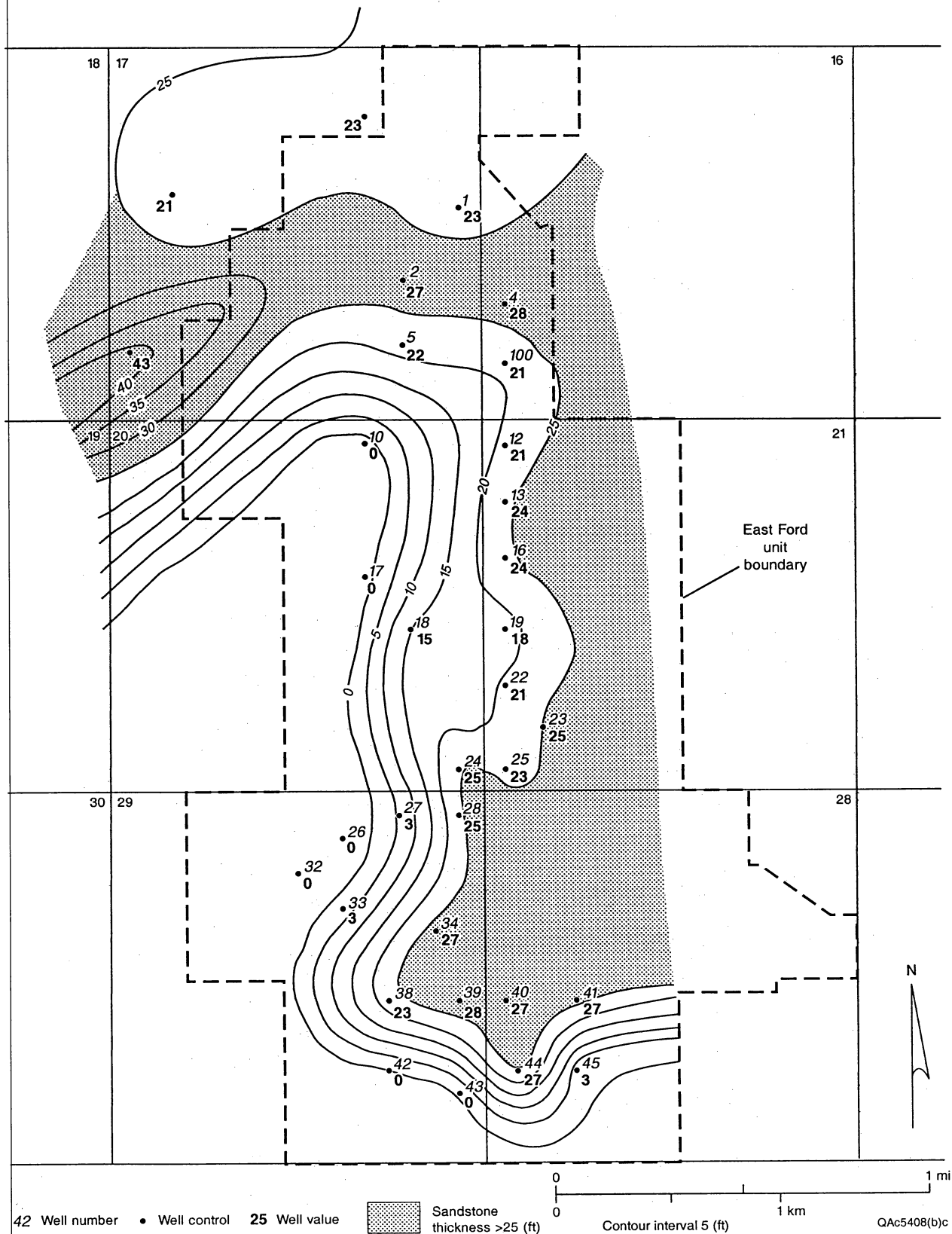


Figure 24. Isopach map of the Ramsey 1 sandstone, which is thickest along a north-south, elongate trend on the east side of the East Ford unit. Interpreted facies distribution shown.

decrease upward in the lower Ramsey 1 interval. Porosity in the Ramsey 1 sandstone ranges from 6.5 to 27.0 percent and averages 22.5 percent (table 3). Permeability ranges from 0.02 to 183 md and averages 46 md. Average water saturation measured in cores is 46 percent.

SH1 Siltstone

The SH1 siltstone represents a break in sandstone deposition within the Ramsey interval, when laminated siltstone was deposited. The SH1 siltstone forms a broad sheet that is 2 to 3 ft thick across the East Ford unit (fig. 25). The SH1 siltstone is composed of laminated siltstone similar to that of the Ford. Porosity in the SH1 siltstone in the East Ford unit ranges from 17.2 to 20.7 percent and averages 18.2 percent (table 3). Permeability ranges from 0.3 to 14 md and averages 4 md. Average water saturation measured in SH1 siltstone cores is 54 percent.

Ramsey 2 Sandstone

The younger sandstone in the Ramsey cycle, the Ramsey 2, is thickest along a north-south trend that is shifted to the west, as compared with the underlying Ramsey 1 sandstone (fig. 26). The offset of the Ramsey 2 sandstone trend suggests that the younger sandstones were deposited in the adjacent topographic depression created by deposition of the preceding Ramsey 1 sandstone. The Ramsey 2 sandstone is thinner than the Ramsey 1, having a maximum thickness of 24 ft at the north end of the unit and 10 ft at the south end.

Porosity in the Ramsey 2 sandstone in the East Ford unit ranges from 6.5 to 30.6 percent and averages 21.4 percent (table 3). Permeability ranges from 0.1 to 249 md and averages 34 md. Average water saturation measured in Ramsey 2 sandstone cores is 48 percent.

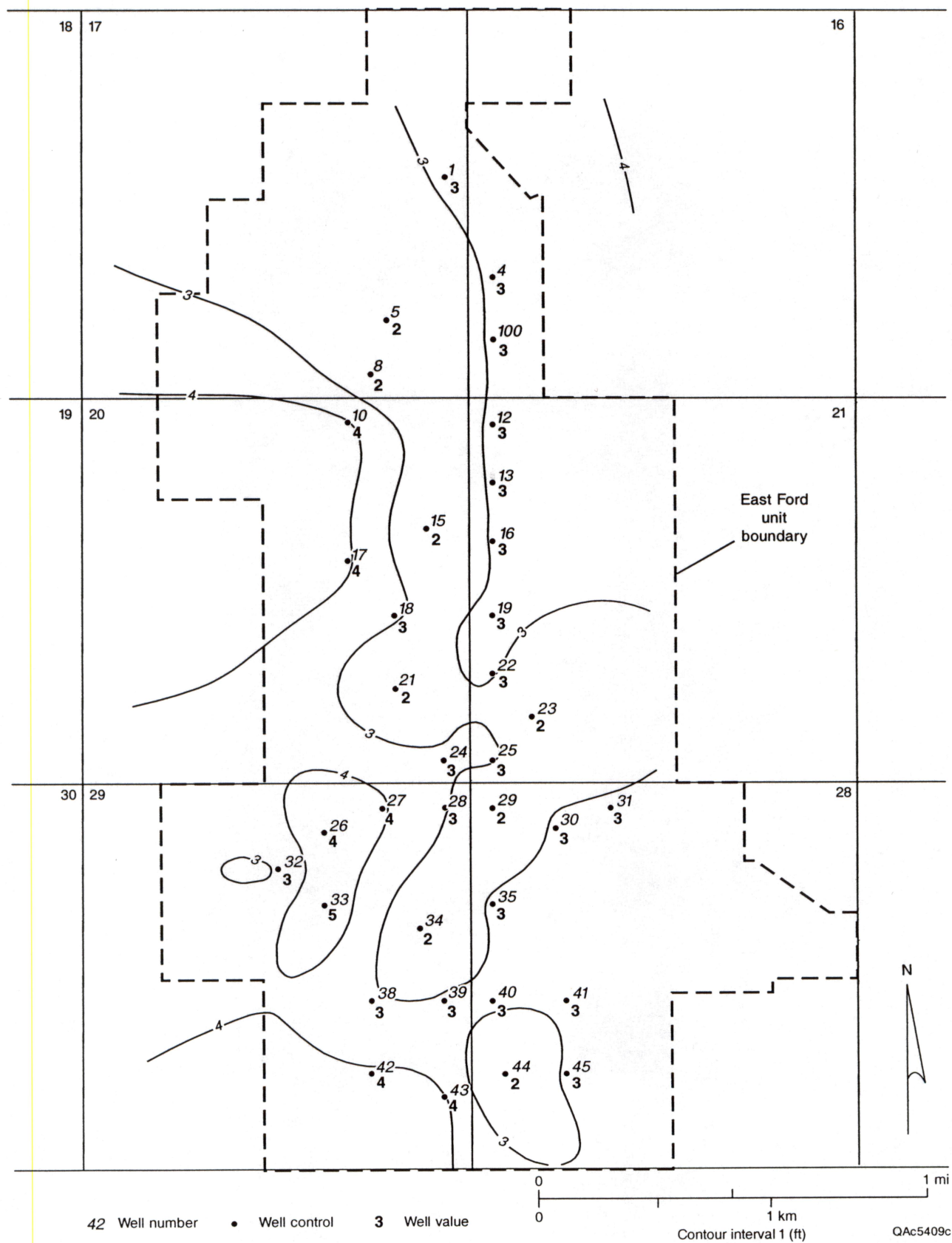


Figure 25. Isopach map of the SH1 laminated siltstone, which was deposited during a break in Ramsey sandstone deposition.

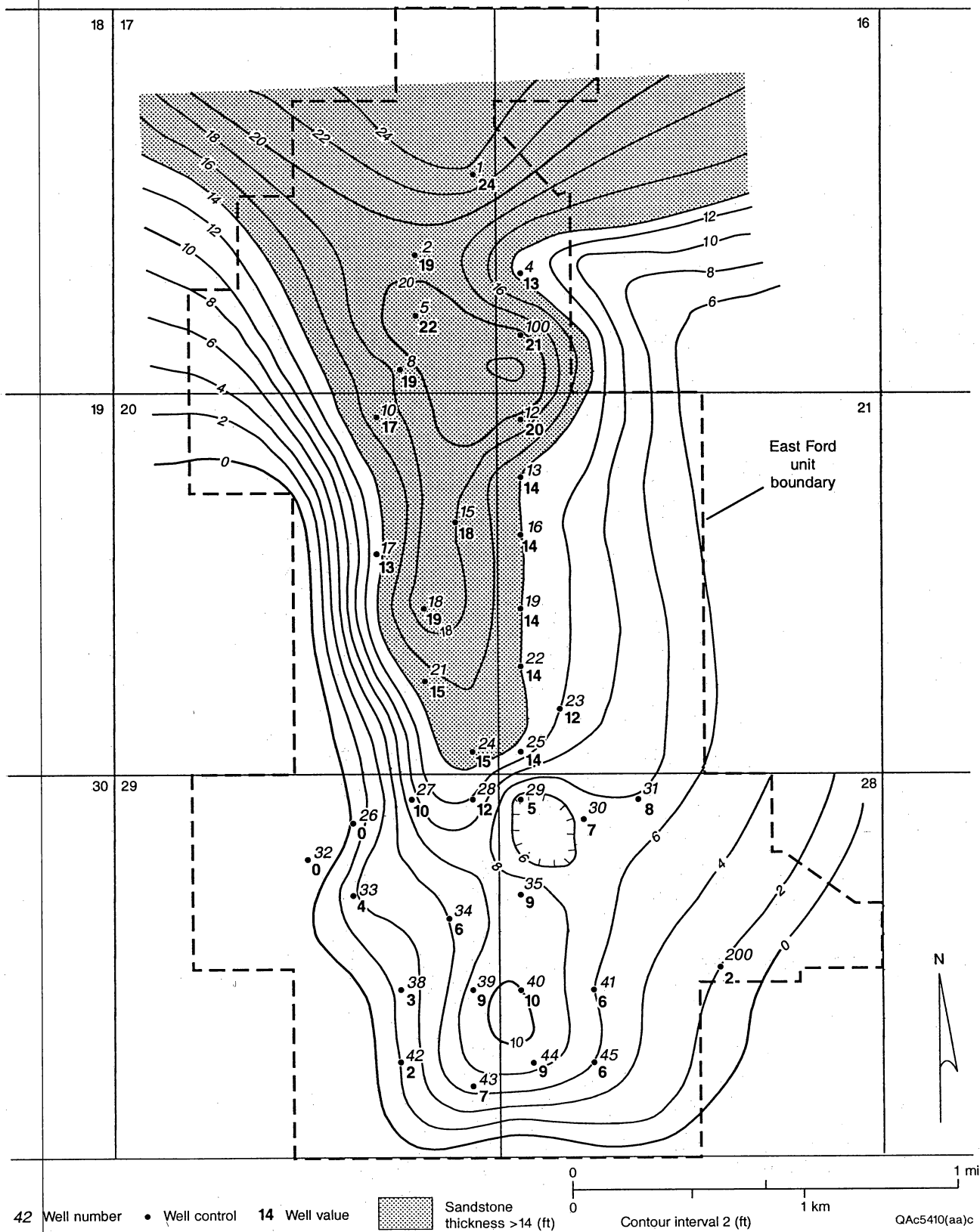


Figure 26. Isopach map of the Ramsey 2 sandstone. The thickest Ramsey 2 sandstone is shifted to the west of the Ramsey 1 sandstone, and the offset of the two sandstones bodies are an example of compensational stacking.

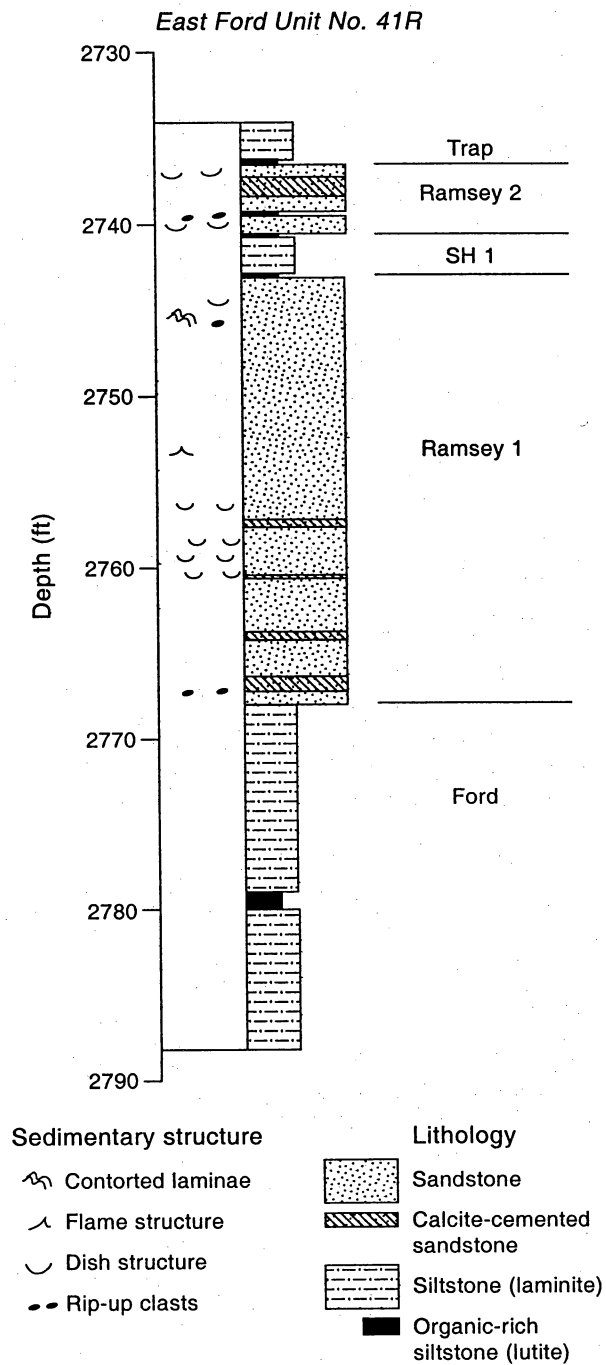
Lower Trap Siltstone

The Ramsey cycle is capped by the Trap laminated siltstone. The lower Trap siltstone, measured from the top of the Ramsey sandstone to the Trap condensed section (fig. 22), forms a broad sheet that is mostly 7 to 8 ft thick (Dutton and others, 1999c). Like the Ford siltstone, the Trap is composed of organic-rich siltstone laminae interbedded on a millimeter scale with organic-poor siltstone laminae. The average grain size of the silt decreases upward from the base of the Trap to the Trap condensed section, and the percentage of sand, amount of burrowing, and the thickness of organic-poor laminae all decrease away from the sandstone. Gamma-ray response increases over this interval as the amount of organic matter increases toward the condensed section. Porosity in the Trap siltstone ranges from 2.9 to 18.8 percent and averages 14.7 percent (table 3). Permeability ranges from 0.01 to 8 md and averages 1 md. Average water saturation measured in Trap siltstone cores is 67 percent.

Ramsey Sandstone Facies

One core from the East Ford unit was available to this study. The well, called the East Ford Unit No. 41R (EFU 41R), is located 100 ft northwest of well EFU 41 (fig. 21). The cored interval extends from the bottom few feet of the Trap siltstone, through the Ramsey 2 sandstone, SH1 siltstone, Ramsey 1 sandstone, and into the upper few feet of the Ford siltstone (fig. 27). Information from this well, combined with analysis of 70 Ramsey sandstone cores from the Ford Geraldine unit, was used to interpret the facies present in the Ramsey sandstone reservoir at the East Ford unit.

Description of sedimentary features of the EFU 41R core shows that the Ramsey 1 and 2 sandstones are very fine grained; many intervals of the sandstone are massive. The most common sedimentary structures are features related to dewatering—dish structures, flame structures, and convolute bedding (fig. 27). Many of the sedimentary structures



QAc8379c

Figure 27. Description of core from East Ford Unit No. 41R (EFU 41R). From Dutton and Flanders (2001).

show up better in UV light than in natural light (fig. 28). In UV light, low-porosity zones are dark because they have no oil-filled porosity, whereas porous sandstones have a bright-yellow fluorescence because of the oil saturation. As a result, slight differences in porosity highlight the sedimentary structures in UV light.

Dish structures are particularly abundant in the EFU 41R core; good examples occur in the core between 2,759 and 2,760 ft (figs. 27, 28). Dish structures form in thick, massive sandstones as fluid escapes during initial compaction (Walker, 1992). They consist of thin, dark, less permeable layers (probably containing more organic matter) and paler, cleaner layers; escaping fluid has broken through the darker layers and curved them upward. These features develop in massive sandstones at the base of turbidity-current deposits, as described by Walker (1992). Similar fluid-escape features were observed in Bell Canyon outcrops in both lobe and overbank-splay sandstones (Barton and Dutton, 1999).

The facies observed in Ramsey sandstone core from EFU 41R are similar to those that were identified in upper Bell Canyon sandstones in outcrop (Dutton and Barton, 1999). The core facies are (1) organic-rich siltstone (lutite); (2) laminated siltstone (laminite); (3) structureless or massive sandstones having few laminations but containing floating siltstone clasts, water escape features, and load structures; and (4) massive sandstone. Two facies that were observed in outcrop and in cores from the Ford Geraldine unit, but not in the EFU 41R core, are cross-stratified sandstone and rippled or convoluted sandstone.

In the Ford Geraldine unit, comparison of sedimentary structures viewed in core with facies identified in outcrop was key to interpreting the Ramsey sandstones as channel-levee and lobe deposits and mapping the facies distribution. Only one core is available from the East Ford unit, but the Ramsey reservoir sandstones in this field are also interpreted to have been deposited by a system of leveed channels having attached lobes and overbank splays (fig. 6a). This interpretation was made on the basis of

(1) interpretation of the EFU 41R core; (2) the similarity of the Ramsey sandstone thickness and geometry to that in the Ford Geraldine unit; (3) the apparent bifurcation of the Ramsey sandstone to the north of both units, resulting in one channel forming the Ford Geraldine reservoir and the other forming the East Ford reservoir; (4) the similarity of log patterns in East Ford field to those in the Ford Geraldine unit; and (5) analysis of pressure and production information. Because of the narrow range of grain sizes in Ramsey sandstones and the absence of detrital clay, log responses are muted, and log patterns are not always reliable for facies identification. When combined with sandstone-thickness data, however, log facies can contribute to facies interpretation at the East Ford unit. The interpreted vertical and lateral distribution of facies is illustrated on representative cross sections through the central and south parts of the East Ford unit (figs. 29, 30).

Channel Facies

Channel facies consist of massive and crossbedded sandstones interpreted to have been deposited from high-density turbidity currents (Lowe, 1982). As interpreted from cross section (fig. 29) and isopach map (fig. 24), channels in the Ramsey 1 sandstone are about 25 ft thick and 950 to perhaps as much as 2,000 ft wide (figs. 29, 31). It is difficult to determine the width of Ramsey 1 channels precisely. The Ramsey 1 sandstone extends east of the unit, but its limits are unknown because of the absence of well control where it dips below the oil–water contact. Ramsey 2 channels are interpreted to be about 15 ft thick and about 1,300 ft wide (fig. 32). In outcrop, many channels were seen to be nested and laterally offset from each other (Barton, 1997; Barton and Dutton, 1999). Similar nesting of multiple channels may occur in the East Ford unit, but the well control is not sufficiently close to distinguish separate channels. The aspect ratio (width:thickness) of Ramsey 1 channel deposits is 40:1 to as much as 80:1. Ramsey 2 channel deposits have aspect ratios of about 85:1. Log response is generally blocky. The thickest part of the

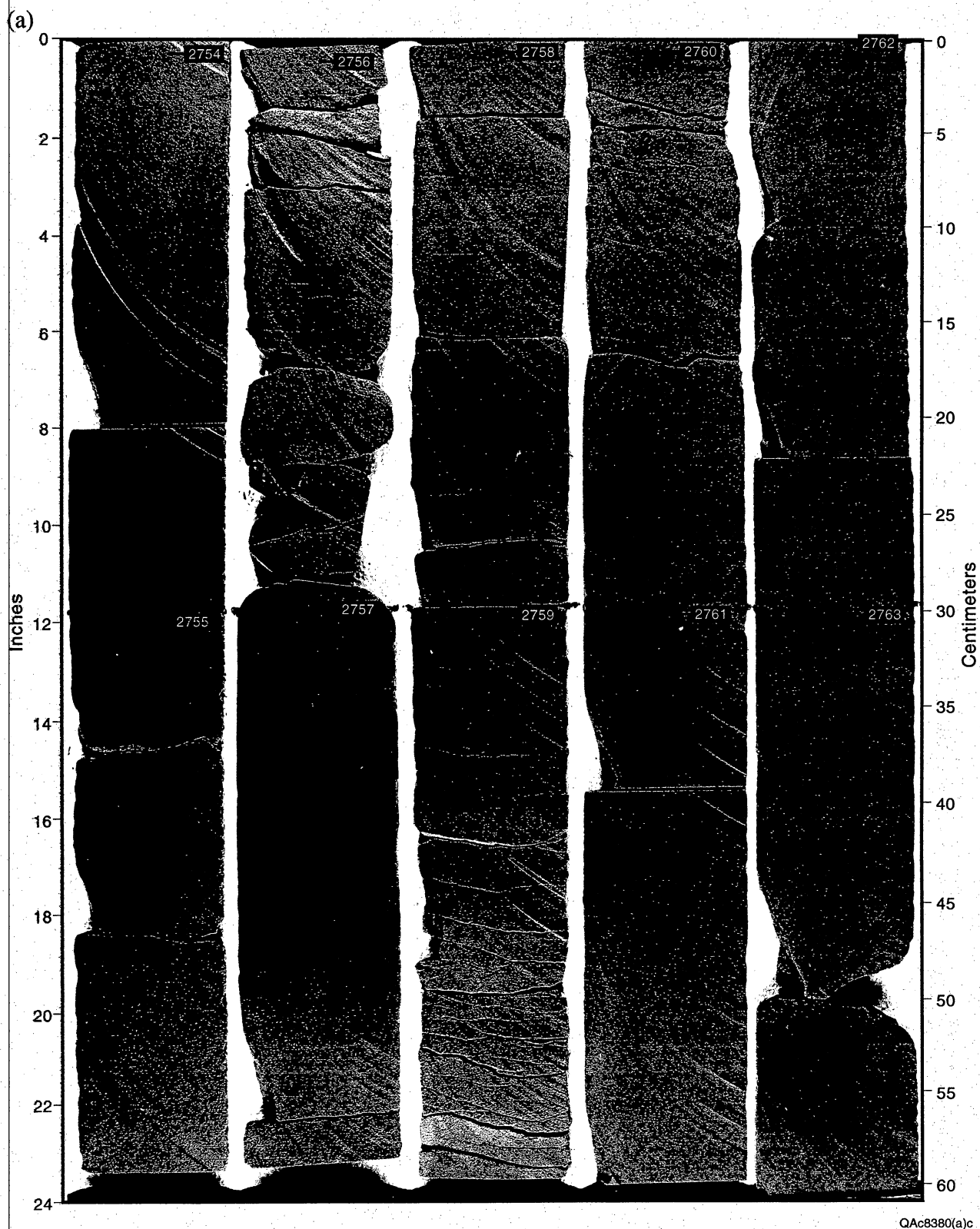
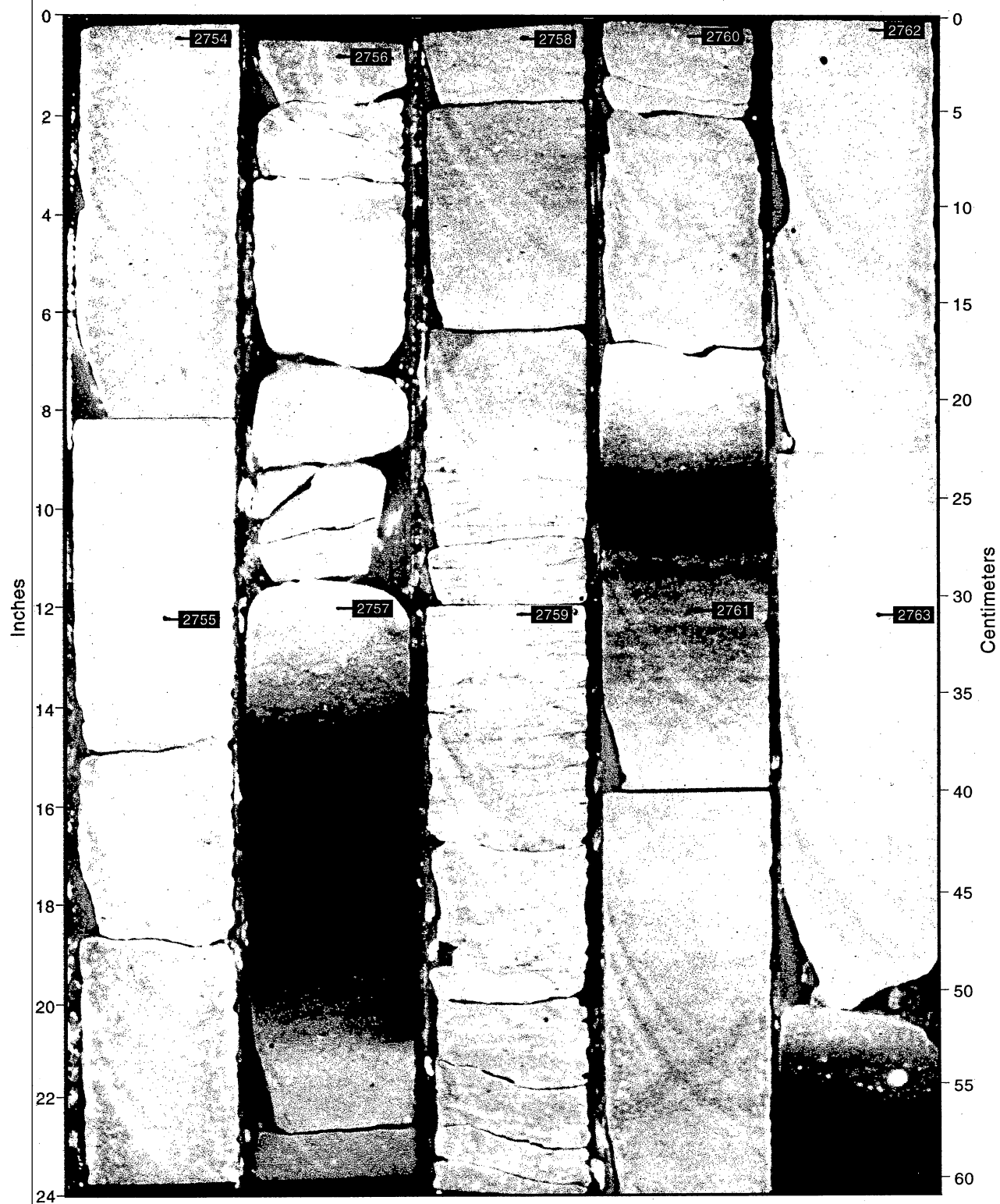


Figure 28. Photograph of core from the EFU 41R well, from a depth of 2,754 to 2,764 ft. (a) Natural-light photograph and (b) ultraviolet-light photograph. Dark intervals in the ultraviolet-light photograph are calcite-cemented layers. From Dutton and Flanders (2001).

(b)



QA68381(a)c

Figure 28. (Cont.)

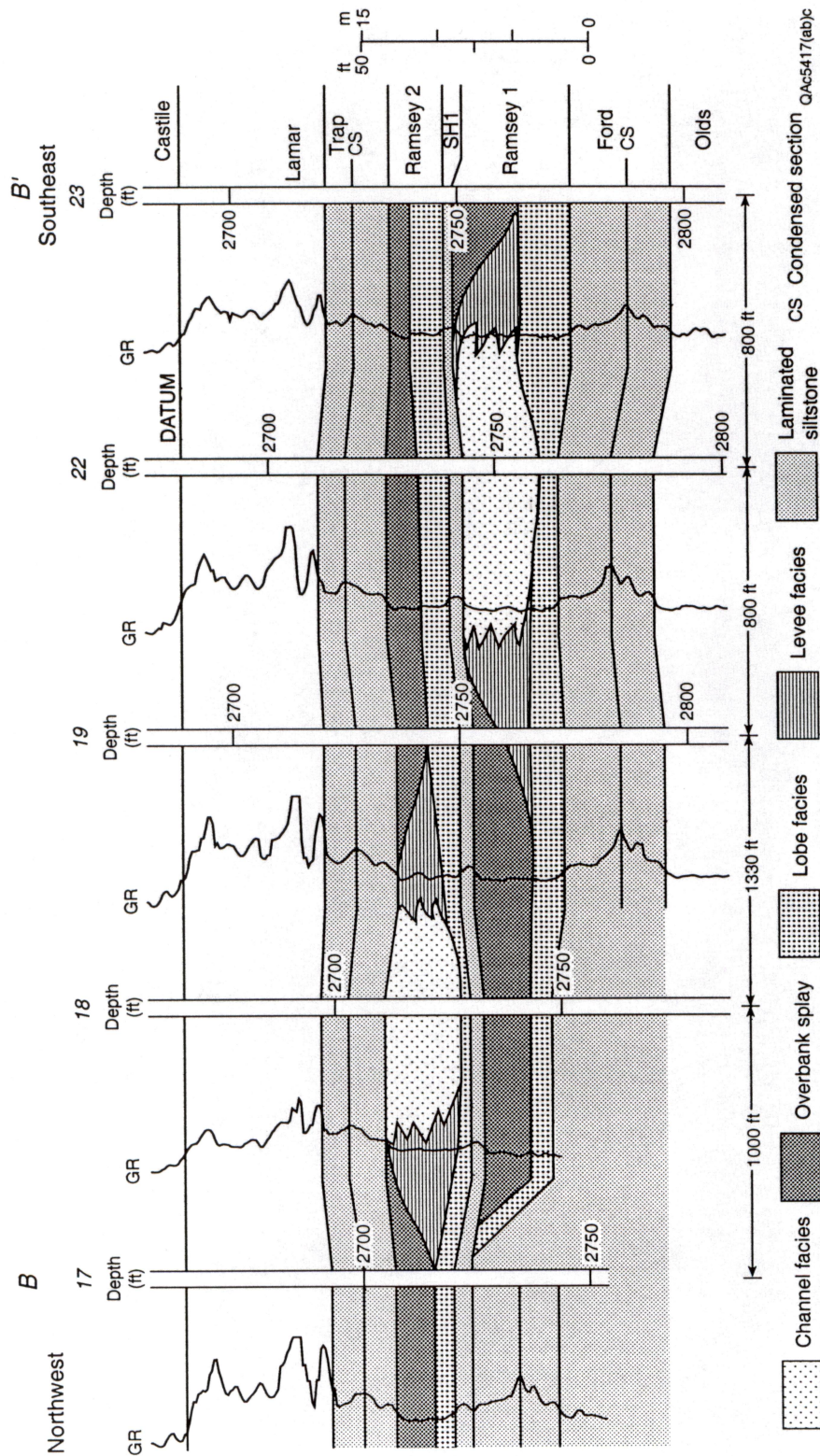


Figure 29. Northwest-southeast strike cross section B-B' of the central part of the East Ford unit. Location of cross section shown in figure 21.

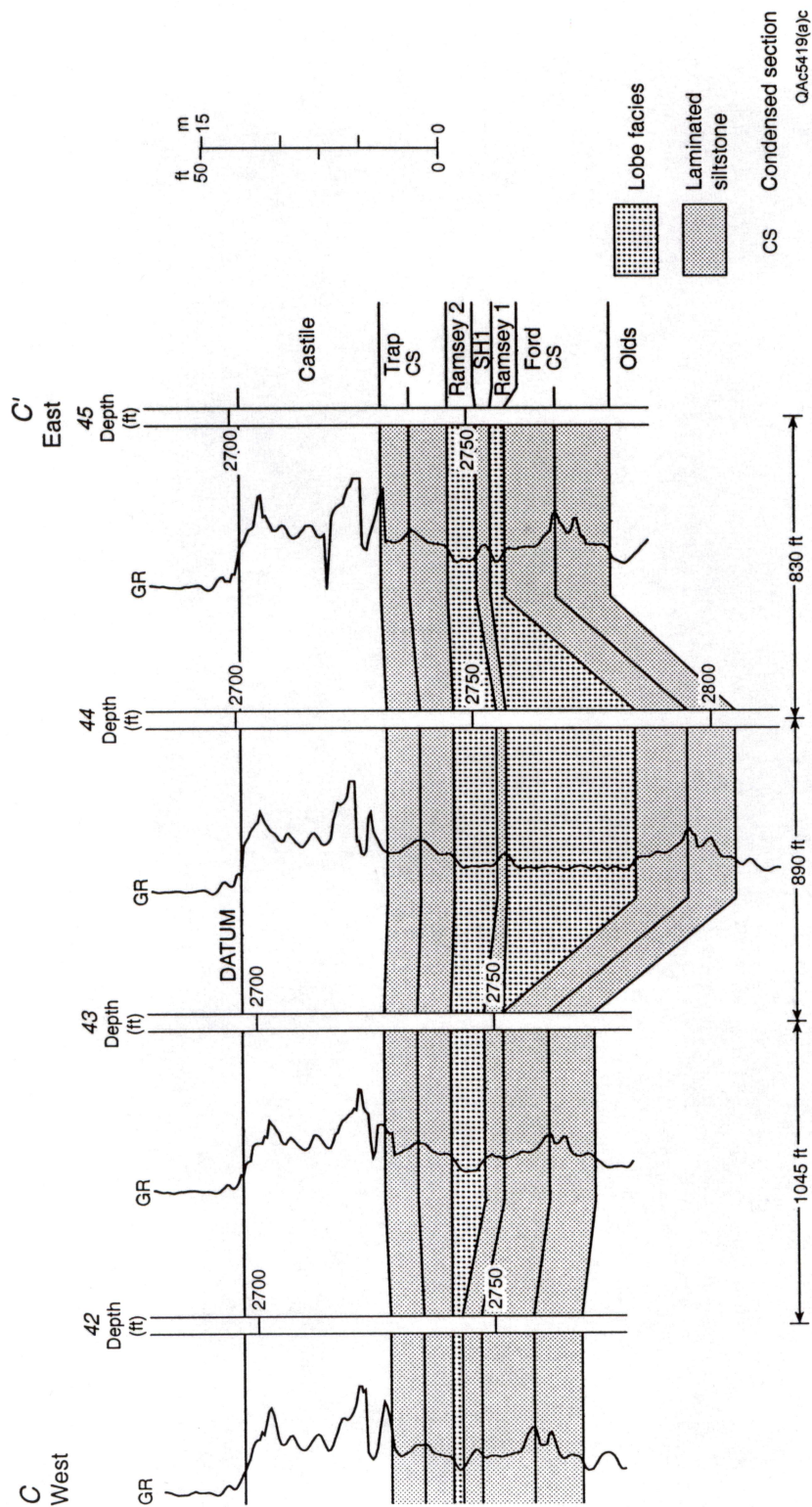


Figure 30. West-east strike cross section C-C' of the south tip of the East Ford unit. Location of cross section shown in figure 21.

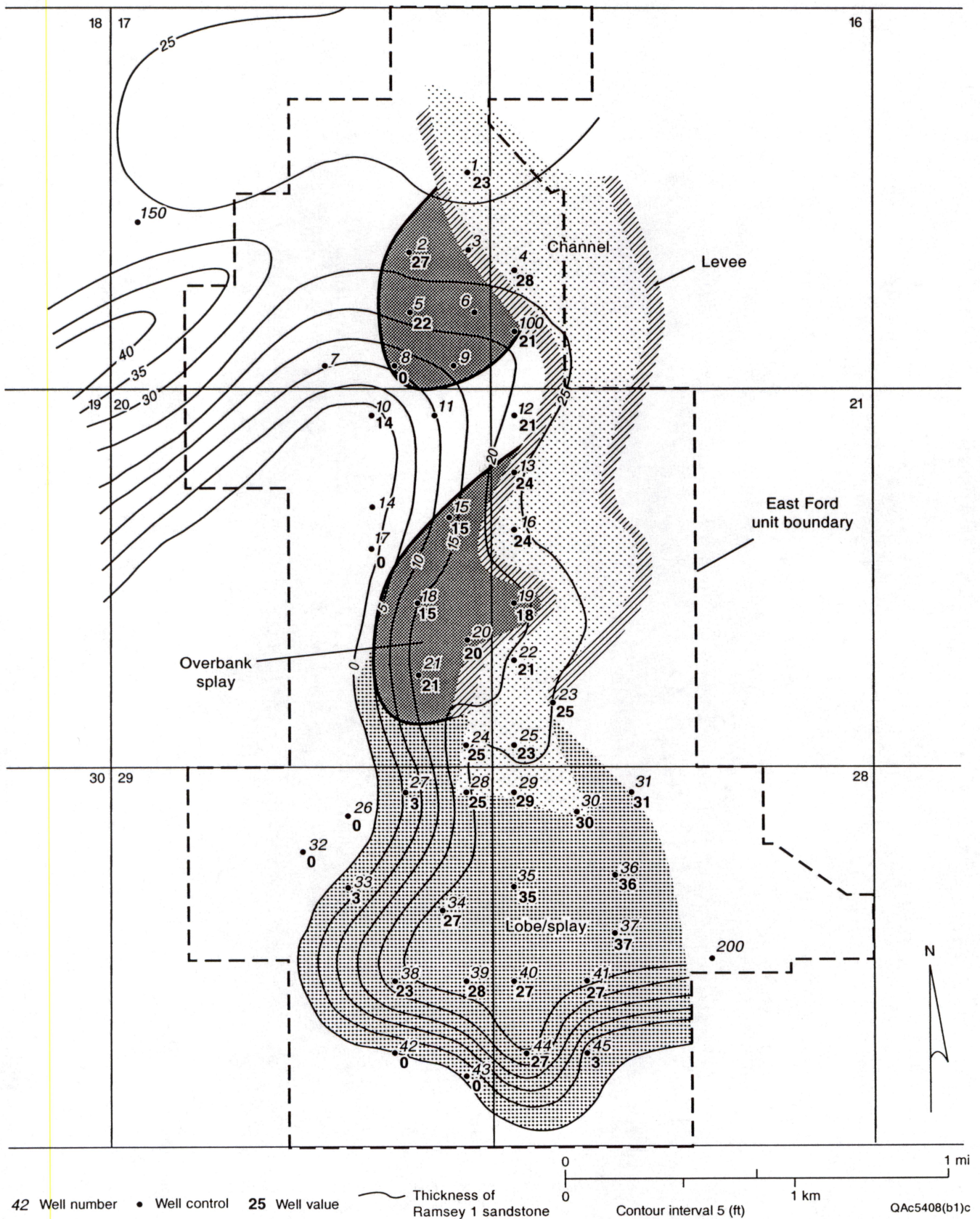


Figure 31. Isopach map of the Ramsey 1 sandstone in the East Ford unit, with interpreted facies distribution shown.

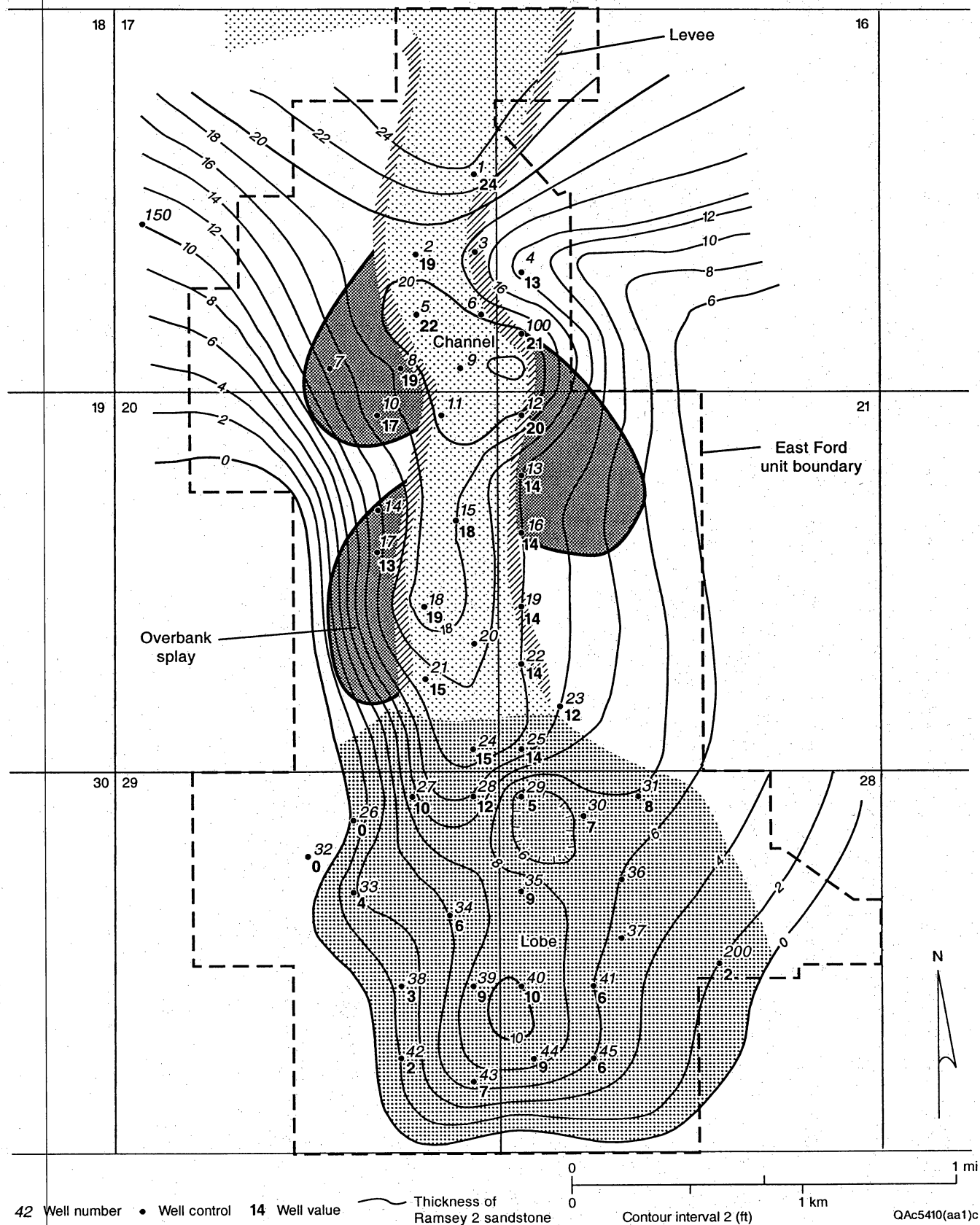


Figure 32. Isopach map of the Ramsey 2 sandstone in the East Ford unit, with interpreted facies distribution shown.

Ramsey 2 sandstone occurs to the west of the Ramsey 1 channel (figs. 31, 32), suggesting that the Ramsey 2 was deposited in the topographic low to the west of the thickest Ramsey 1 sandstone.

Levee Facies

Levee facies occur as narrow wedges that flank the channel margins (figs. 29, 31, 32). In the Ford Geraldine unit, channel-margin deposits consist of sandstones having partial Bouma sequences, particularly ripples and convoluted ripples, and interbedded siltstones. They are interpreted as channel levees formed by overbanking of low-density turbidity currents. The thickness of the levee facies decreases away from the channels, and the volume of interbedded siltstones increases. Log response is more serrated than in the channels because of the presence of interbedded siltstones.

Lobe and Overbank-Splay Facies

Lobe facies, deposited by unconfined, high-density turbidity currents, occur in broad sheets at the mouths of channels. In the Ford Geraldine unit, lobe facies are characterized by massive sandstones and graded sandstones having dewatering features such as dish structures, flame structures, and vertical pipes, features that indicate rapid deposition and fluid escape. They were deposited at high suspended-load fallout rates. In a prograding system such as the Ramsey sandstone, lobe facies would have been deposited first and then overlain and partly eroded by the narrower prograding channel-levee system (fig. 29). Lobe deposits are therefore found at the distal ends of the Ramsey 1 and 2 sandstone channels and also underlying and laterally adjacent to the Ramsey 1 and 2 channels and levees (figs. 29 through 32). Because deposition of lobe sandstones was periodic, laminated siltstones are interbedded with the lobe sandstone sheets. Some lobe deposits

show an upward-coarsening log pattern, but many have a blocky log response (figs. 29, 30).

The sandstones that flank each side of the channel-levee deposits are interpreted to be overbank splays. Volumetrically the splays contain much of the sandstone outside of the channels (figs. 29 through 32). It is difficult to distinguish overbank-splay deposits from lobe deposits by lithofacies alone; the location, shape, and stratigraphic position are needed to differentiate these two facies composed of massive sandstones containing dewatering features. The EFU 41R well is located near the south end of East Ford field. The Ramsey 2 sandstone in this location is interpreted as having been deposited in a broad lobe (fig. 32), and the Ramsey 1 sandstone in a lobe or splay (fig. 31). The presence of massive sandstones and sandstones with fluid-escape structures in the EFU 41R core is consistent with this interpretation.

Laminated Siltstone Facies

The laminated siltstone facies consists of organic-rich siltstone laminae interbedded on a millimeter scale with organic-poor siltstone laminae. The pattern of upward coarsening into the Ramsey sandstone and then upward fining above it suggests that the laminated siltstones are part of the sea-level cycle that resulted in the progradation and retrogradation of the channel levee and lobe. The siltstones may represent windblown silt from the shelf margins that was deposited in the basin by fallout from the wind and settling through the water column, forming widespread, topography-mantling, laminated siltstones of relatively uniform thickness (fig. 25) (Dutton and others, 1999a). Periods of relative sea-level fall may have exposed increasingly larger areas on the shelf, lowered the water table, and allowed the wind to carry away greater volumes of silt, resulting in thicker organic-poor siltstone layers.

Lutite Facies

The organic-rich siltstones are interpreted as condensed sections that formed in the Ford and Trap intervals during times of very slow siltstone deposition. They contain abundant organic matter, including spores. The organic matter is probably derived from settling from suspension of planktonic organisms. In the Ford Geraldine unit, other lutites occur within the Ramsey 1 and 2 sandstone intervals, where they form drapes along the tops of sandstone beds. They probably formed by fallout from suspension of silt and organic matter from a turbulent sediment gravity flow; they are equivalent to the E division of the Bouma sequence.

Sandstone Diagenesis

The composition of Ramsey sandstones in the EFU 41R core was determined by point counts of 25 thin sections made from samples representing a range of permeability in order to quantify the petrographic characteristics of grain size, detrital mineralogy, authigenic cements, and porosity. The chips used to make the thin sections were end trims off core-analysis plugs so that petrographic parameters could be compared with porosity and permeability. Composition was determined by point counts (200 points) of thin sections stained for potassium feldspar and carbonates.

Ramsey sandstones in the EFU 41R well are well-sorted, very fine grained arkoses having an average composition of $Q_{67}F_{26}R_7$. Plagioclase and potassium feldspar are approximately equal in abundance. The most common lithic grains are metamorphic, plutonic, and carbonate rock fragments. Cements and replacive minerals constitute between 1 and 31 percent of the sandstone volume, calcite and chlorite being the most abundant. Calcite cement has an average volume of 7 percent and ranges from 0 to 30 percent. Most of the calcite fills intergranular pores, but an average of 1 percent calcite cement occurs within secondary pores. Chlorite (average = 1 percent) forms rims around detrital grains, extending into pores and pore throats. Primary porosity averages 19 percent and secondary porosity, 2 percent.

Core-plug porosity in Ramsey sandstones in the EFU 41R core ranges from 4.5 to 24.6 percent, and permeability to air from 0.01 to 78 md (fig. 33). Siltstones have porosity ranging from 14.1 to 17.3 percent and permeability from 0.2 to 4.1 md (fig. 33).

Zones of low porosity and permeability in the sandstones occur within highly calcite cemented intervals (Dutton and Flanders, 2001). The cemented zones appear black in ultraviolet light because they have no oil-filled porosity (fig. 28). The rest of the Ramsey sandstones have a bright-yellow fluorescence in ultraviolet light because of the oil saturation. The calcite-cemented layers are 2 to 16 inches thick. Four tightly cemented calcite layers occur in the lower part of the Ramsey 1 sandstone, where they are spaced about 3 ft apart (fig. 27). The Ramsey 2 sandstone contains one cemented layer that is 14 inches thick (fig. 27).

A statistically significant relationship exists between the volume of calcite cement and permeability (fig. 34). In these sandstones, which have little variation in grain size and contain no detrital clay, volume of calcite cement is the dominant control on porosity and permeability (Dutton and Flanders, 2001). In samples having more than 10 percent calcite cement, geometric mean permeability is 0.4 md and average porosity is 11.5 percent. Sandstones having less than 10 percent calcite cement have a geometric mean permeability of 40 md and an average porosity of 22.5 percent.

Detailed permeability measurements were taken on the slabbed core face at about 1-inch intervals above, within, and below the 5-inch-thick cemented zone at 2,757 ft (fig. 28) using a device that measures permeability by an unsteady-state pulse-decay method. (The correlation coefficient comparing 39 steady-state permeability measurements made on core plugs confined in a Hassler rubber sleeve with unsteady-state permeability measured directly on the core plugs is 0.99). The lowest permeability, and presumably the highest volume of calcite cement, occurs between 2,757.5 and 2,757.6 ft (fig. 35).

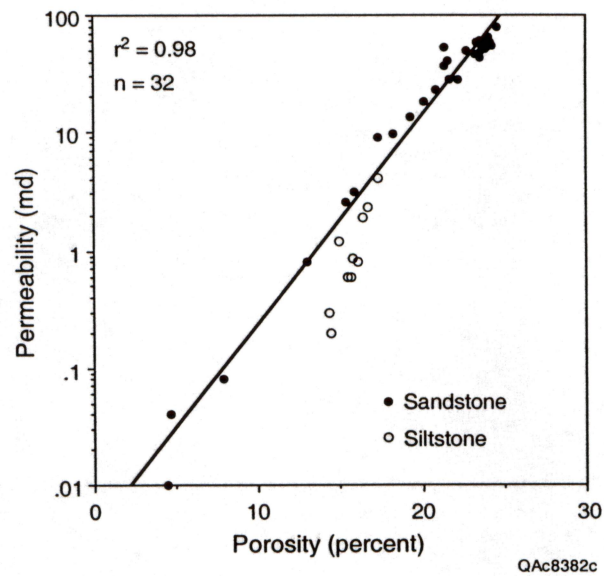


Figure 33. Plot of porosity versus permeability from core-analysis data from the EFU 41R well. From Dutton and Flanders (2001). Regression line calculated from sandstone data only.



77

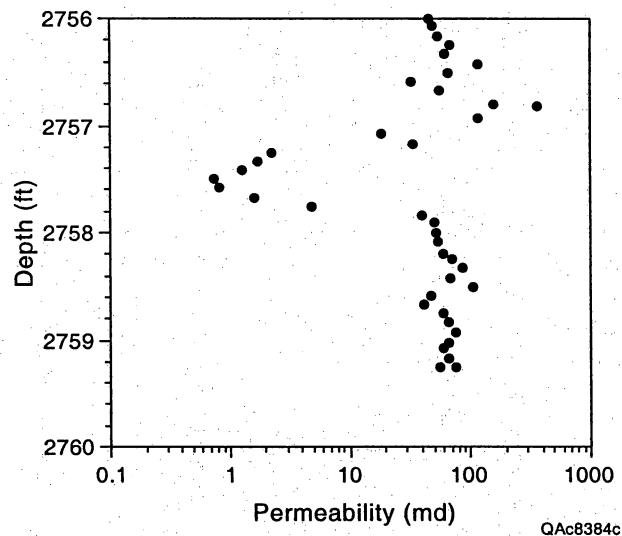


Figure 35. Plot of permeability versus depth across a calcite-cemented layer in the EFU-41R well. From Dutton and Flanders (2001). Permeability was measured at 1-inch intervals directly on the slabbed core face using a device that measures permeability by an unsteady-state pulse-decay method. Permeability has been corrected from air permeability to liquid Klinkenberg permeability.

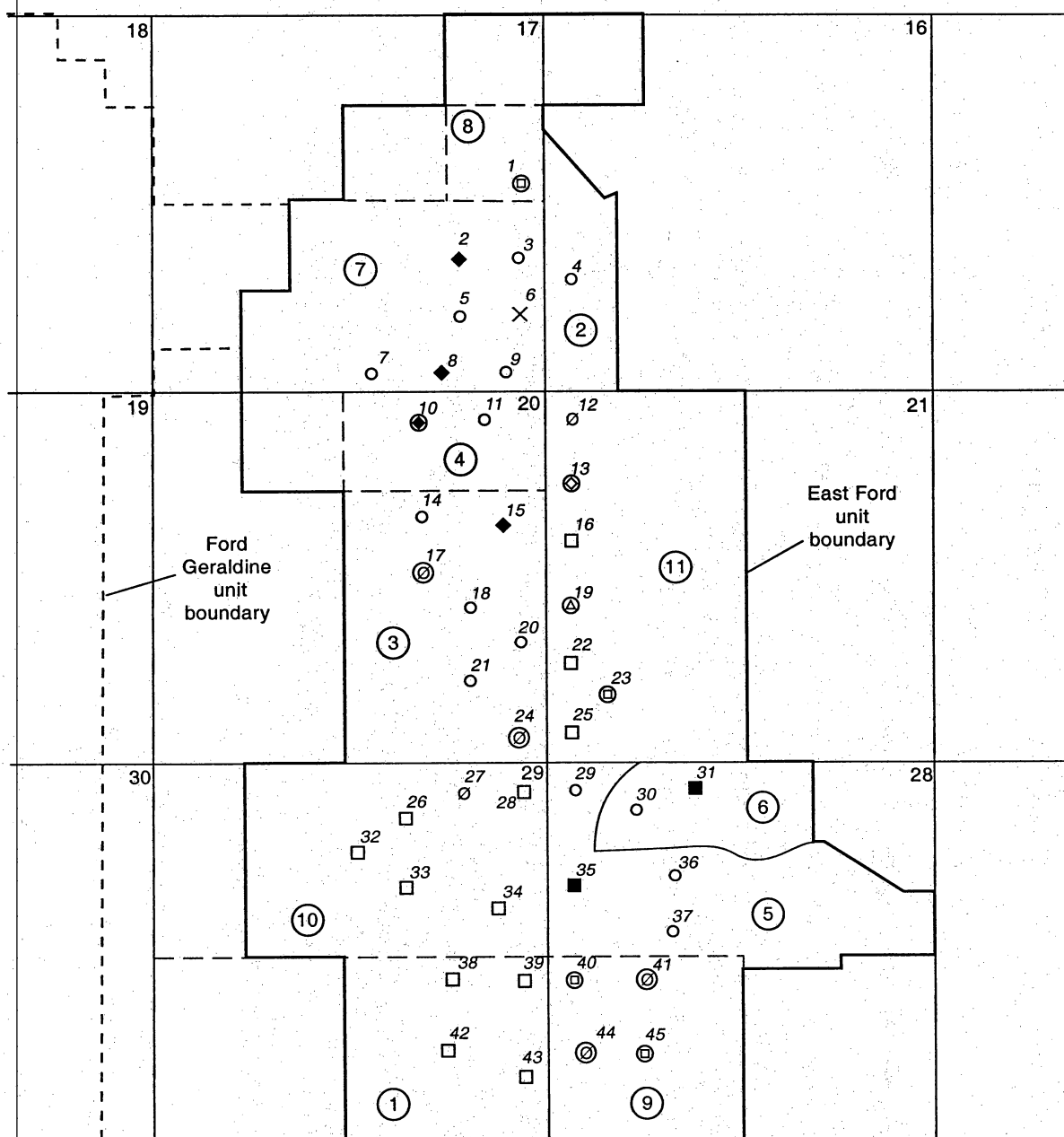
Permeability increases slightly in the 2 inches above and below this depth (fig. 35), but the absence of oil fluorescence in the entire 5-inch-thick zone (fig. 28) suggests that porosity is occluded by calcite cement. Moderate fluorescence in 1-inch-wide zones above and below the completely cemented layer (fig. 28) suggests that there is a thin transition zone in which porosity is somewhat, but not completely, reduced by calcite cement.

Petrophysical Characterization

Reservoir characterization of the East Ford unit provided an opportunity to test the transferability of the log-interpretation methods used in the Ford Geraldine unit to another Delaware sandstone field. Porosity transforms were developed for the East Ford unit, but the $LLD-R_t$ transform and the Archie parameters calculated for the Ford Geraldine unit were used in the petrophysical analysis of the East Ford unit. It was not possible to develop these factors specifically for the East Ford unit because it has a more restricted log suite and no special core analyses.

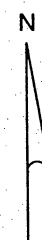
Only 26 wells in the East Ford unit have usable porosity logs (fig. 36). Four other wells have cased-hole neutron logs, which were not used for quantitative petrophysical analysis. Because interval-transit-time (ITT) logs were the most common, only the 23 ITT logs were used for calculating porosity. Seventeen wells have both ITT and resistivity logs.

The gamma-ray logs in the East Ford unit were run in the early 1960's by several different companies at different sensitivities. They could not be directly compared, even though all but one of the logs were recorded in API units, so the gamma-ray logs had to be normalized. High and low GR values were selected for each well, giving them all different normalizing equations.



- 42 East Ford unit well number
- GR only
- ◇ GR-Ø_N (open hole)
- ◆ GR-Ø_N (cased hole)
- ⊙ GR-ITT
- GR-ITT-LL
- △ GR-ITT-LL-MLL
- GR-DEN
- ⊙ Cored well
- × No logs
- ⑩ Tract number

0 1 mi
0 1 km



QA4742(a)c

Figure 36. Distribution of geophysical log suites available in the East Ford unit.

Porosity Transforms

Because core analyses from 334 samples of the Ramsey interval from 11 wells in the East Ford unit were available, new porosity transforms were derived instead of using the equations developed in the Ford Geraldine unit. The least-squares linear regression line relating core porosity and permeability is

$$\text{Permeability (md)} = 0.014 \times 10^{(0.144 \times \text{porosity})} \text{ (fig. 37).}$$

Core depths were shifted to log depths using core-to-log correction factors determined for each cored well. A cross plot of ITT versus core porosity was constructed to determine the ITT-log to core-porosity transform (fig. 38). Several of the ITT logs had zones where the readings went off scale ($>100 \mu\text{sec/ft}$) because of hole washout, and these intervals were omitted from the plot of ITT versus porosity. The reduced-major-axis (RMA) equation relating ITT and core porosity was used to determine porosity in wells having ITT logs. The RMA equation is

$$\text{Porosity (percent)} = 0.533 (\text{ITT}) - 26.5.$$

Because so few ITT logs were available in the East Ford unit, logs from wells with hole washout were used in the petrophysical analysis. ITT values were extrapolated into the washed-out zones from depths where the Ramsey sandstone had good log response, and these extrapolated values were used to calculate porosity from the RMA equation.

Volume of Clay

Volume of clay (V_{cl}) was calculated from gamma-ray logs according to the same method as in the Ford Geraldine unit. From a plot of ITT versus normalized gamma-ray response (GR) from 16 wells in the East Ford unit, a GR_{cl} value of 50 API and GR_{sh} of 89 API was selected. The V_{cl} for the Ramsey sandstone was then calculated by

$$IGR = (GR - 50)/(89 - 50), \text{ and}$$

$$V_{cl} = 0.33[2^{(2 \times IGR)} - 1.0] \text{ (Atlas Wireline, 1985),}$$

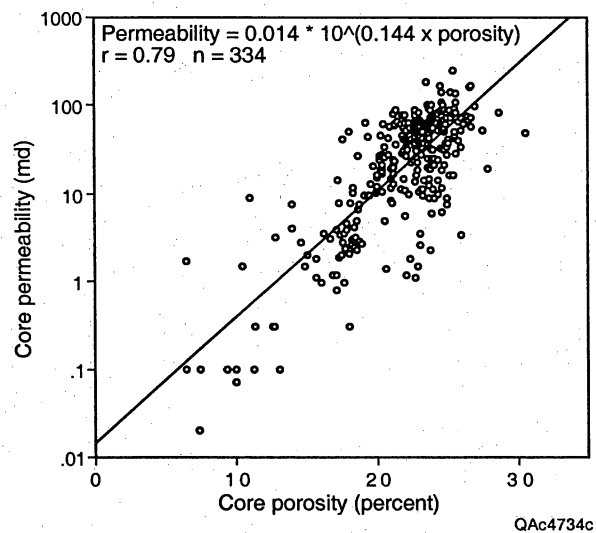


Figure 37. Cross plot of core porosity versus core permeability with porosity-permeability transform for the Ramsey sandstone in the East Ford unit, Reeves County, Texas.

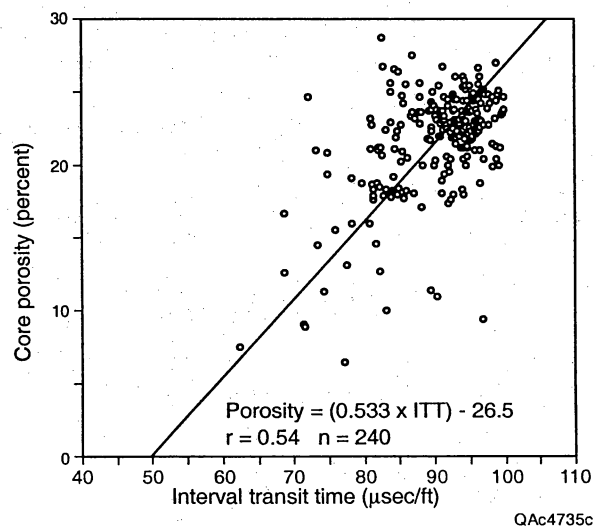


Figure 38. Cross plot of interval transit time (ITT) versus core porosity with porosity transform for the Ramsey sandstone in the East Ford unit.

where IGR is gamma-ray index. A map of V_{cl} distribution shows that low values occur in the center of the East Ford unit and V_{cl} increases toward the margins of the unit, where the Ramsey sandstone pinches out into siltstone.

Calculation of Water Saturation

The same approach for calculating water saturation was followed in the East Ford unit as was developed in the Ford Geraldine unit. Because only one microlaterolog was run in the East Ford unit, we used the transform developed in the Ford Geraldine unit, $R_t = 1.3002 \times LLD + 0.3397$, to correct LLD to R_t in East Ford wells.

Formation-Water Resistivity

In preparation for calculating water saturations (S_w), we estimated formation-water resistivities (R_w) across the Ford East unit from a contour map of formation-water salinities (fig. 39). Salinity data from four wells in the East Ford unit (EFU 1, 9, 24, and 37) were combined with those from the Ford Geraldine unit (Dutton and others, 1997a) to obtain a more regional view of water salinity. The contour map of salinity was used to assign salinity values for each of the East Ford wells. The formation-water resistivity at 75°F was then read from a chart relating NaCl concentration, temperature, and resistivity (Schlumberger, 1995, chart Gen-9, p. 1–5). Values of R_w at 75°F ranged from 0.10 to 0.12 ohm-m in the East Ford unit (fig. 39). Formation temperatures in each well were calculated from the geothermal gradient in the field and the depth of the middle of the Ramsey sandstone. Values of R_w at formation temperature were then calculated by Arp's formula (Asquith and Gibson, 1982): $R_{tf} = R_{temp} \times (Temp + 6.77)/(T_f + 6.77)$, where

R_{tf} = resistivity at formation temperature,

R_{temp} = resistivity at a temperature other than formation temperature,

Temp = temperature at which resistivity was measured, and

T_f = formation temperature.

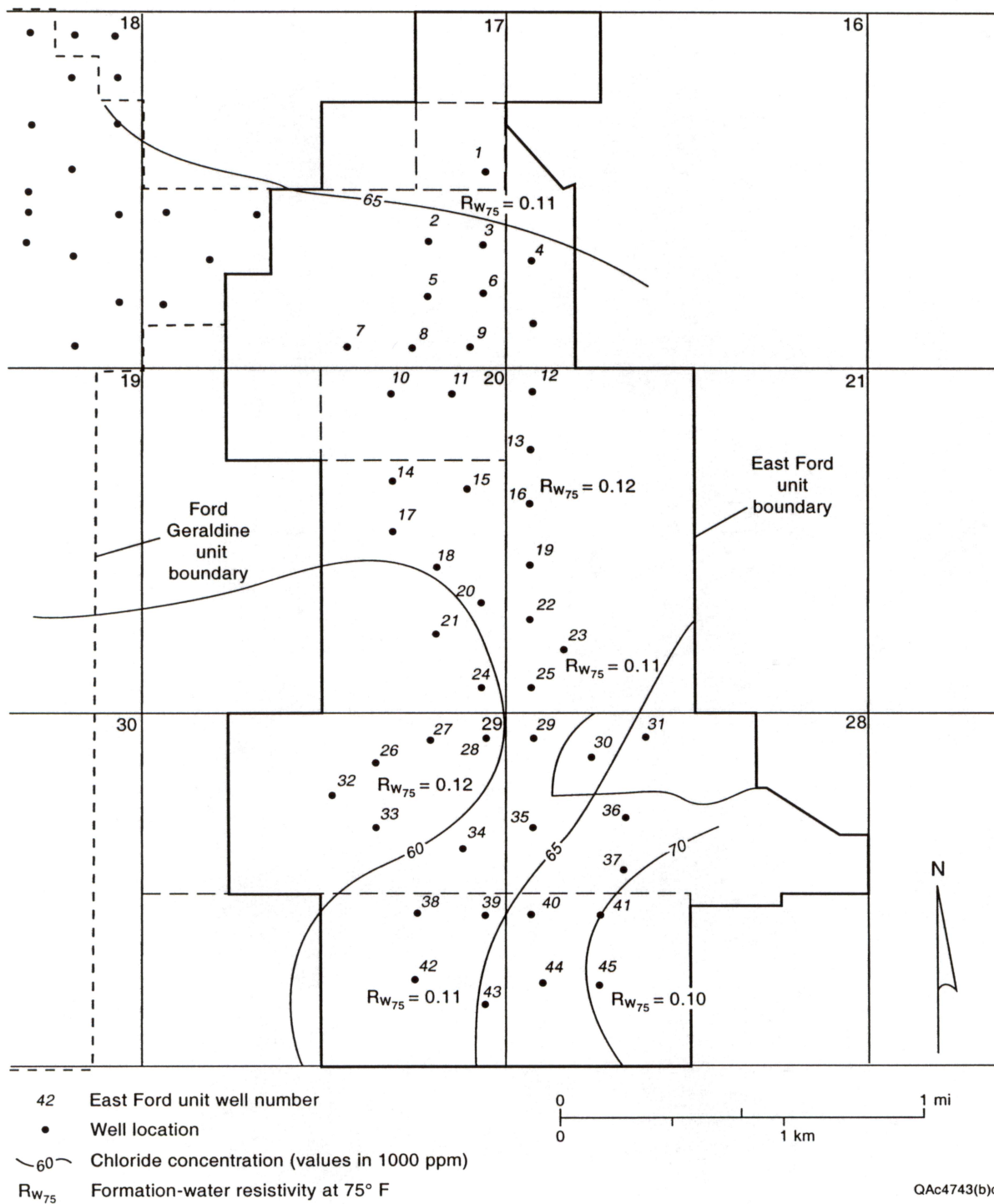


Figure 39. Isosalinity map with formation-water resistivities (R_w) at 75°F for the East Ford unit.

Archie Parameters m and n

No special core analyses of cementation exponent (m) or saturation exponent (n) were available from the East Ford unit, so the values of m and n determined for the Ramsey sandstone in the Ford Geraldine unit (Asquith and others, 1997) were used. Water saturations (S_w) in the East Ford unit were calculated by the same modified Archie equation that was developed for the Ford Geraldine unit:

$$S_w = [(1/\phi^{1.83}) \times (R_w/R_t)]^{1/1.90},$$

where ϕ is porosity.

Net-Pay Cutoffs

Net-pay cutoffs for the Ramsey sandstone in the East Ford Geraldine unit were selected for volume of clay (V_{cl}), porosity (ϕ), and water saturation (S_w). The same V_w cutoff of 15 percent that was used for the Ford Geraldine unit was also applied to the Ford East unit. A porosity cutoff of 17.5 percent, corresponding to a permeability of 5 md (fig. 37), was selected. A change in the slope of the permeability distribution occurs at 5 md, and sandstones having permeability of ≥ 5 md probably represent the floodable Ramsey sandstones (Dutton and others, 1999c). No relative permeability curves were available for the East Ford unit, so the water-saturation cutoff of 60 percent was selected, the same cutoff that was used for the Ford Geraldine unit.

Saturation Distribution

As is common in Delaware sandstone reservoirs, the Ramsey sandstone at the East Ford unit had high initial S_w , and many wells produced some water at discovery. The Ford Geraldine unit averaged 47.7 percent S_w at discovery, well above the irreducible water saturation of 35 percent (Pittaway and Rosato, 1991), and the Ramsey sandstone at the East Ford unit probably also had initial water saturation greater than

irreducible. Average S_w measured in 334 core analyses of the Ramsey sandstones was 47 percent.

Areal distribution of S_w was mapped from geophysical log data supplemented by water-saturation data from cores. First, we mapped the areal distribution of bulk volume water (BVW) according to the formula $S_w = BVW_{ave}/\phi$ using log data from wells having both ITT and resistivity logs (method described in Asquith and others, 1997). On the basis of this map, BVW values were then assigned to wells having porosity logs but no resistivity logs. Average S_w values were calculated in these wells, then combined with S_w data from resistivity logs to map S_w distribution in the East Ford unit. This approach resulted in many wells in the main producing trend of the field having calculated S_w greater than 50 percent. Such high water saturations were considered unreasonable because water cuts in these wells are low, so a new method for calculating water saturation was developed.

A plot of all log-calculated S_w values versus percent water cut in initial potential tests had a large scatter in the data. Data from some wells were thought to be invalid and were eliminated if the wells fell into one of the following categories: (1) Wells completed only in the Olds sandstone; these wells had high water cuts from the Olds sandstone that could not be equated to the S_w calculated from the Ramsey sandstone. (2) Wells completed in both the Olds and Ramsey sandstones having high water cuts; these wells probably produced mainly from the Olds sandstone. (3) Wells without resistivity logs, for which S_w was calculated from the BVW map. These wells had high calculated S_w values that were inconsistent with their low water cuts. (4) Other wells with inconsistent log S_w and water-cut data. For a few wells, it was unclear why the calculated S_w was high despite a low water cut, but these inconsistent wells were also eliminated from the data base. The remaining data were used to calculate a linear regression line relating water cut to S_w . A map of S_w across the East Ford unit (fig. 40) was then made from the valid log-

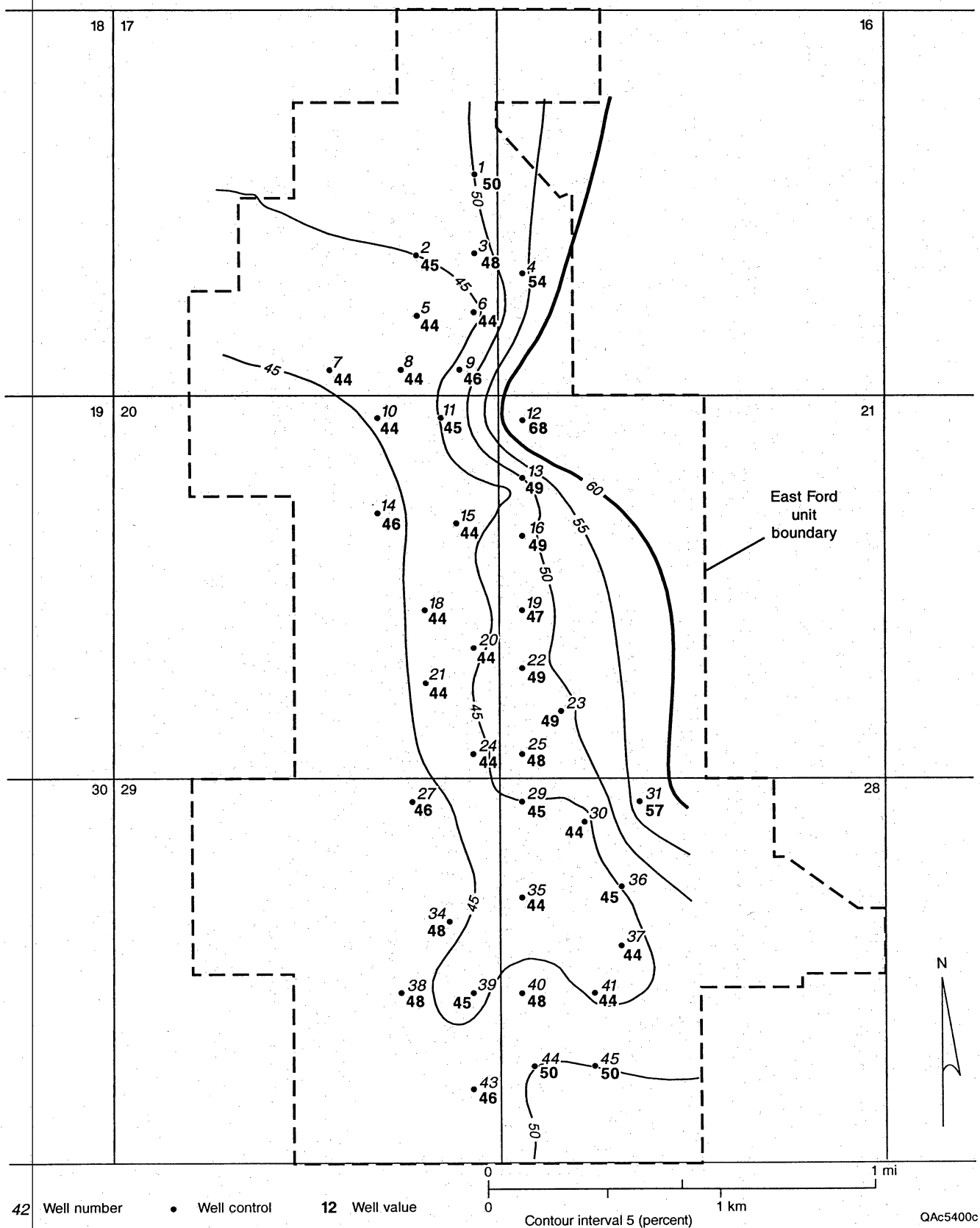


Figure 40. Map of water saturation (S_w) of the Ramsey sandstone in the East Ford unit. The S_w values are either valid log-calculated data or calculated from the water-cut- S_w transform. Dutton and others, 1999c.

calculated S_w data, combined with S_w data calculated from the water-cut- S_w transform. Values of S_w ranged from 44 to 55 percent across most of the field and averaged 48 percent. S_w increases to the east and northeast, which is to be expected because that direction is down structural dip.

Transferability of Log-Interpretation Methods

Most aspects of the log-interpretation methodology developed for the Ford Geraldine unit were used successfully in the East Ford unit. The approach that was used to interpret water saturation from resistivity logs had to be modified because in some East Ford wells, the log-calculated water saturation was too high and inconsistent with the actual production. In addition, the use of bulk-volume water mapping to determine water saturation in wells having no resistivity logs did not yield results consistent with production. A cross plot of valid log-calculated water-saturation versus water-cut data provided a transform that was used to estimate water saturation from water-cut data in wells without good resistivity logs.

The approach to petrophysical analysis that was developed in the Ford Geraldine unit can be used in other fields in the Delaware sandstone play, as demonstrated by the successful transfer of the log-interpretation methods to the East Ford unit. Core-analysis and log data from the field being studied should be used to the greatest extent possible, but where they do not exist, the Ford Geraldine values provide a reasonable substitute. For example, if core-analysis data are available, they should be used to develop core-porosity to log-porosity transforms specific to that field, but in a field having no core analyses, the transforms developed in the Ford Geraldine unit can be used instead. Similarly, if a field has both Laterologs (LLD) and accompanying Microlaterologs, Microspherically Focused Logs, or Shallow Laterologs, an R_t -LLD transform specific to

that field should be developed, but if these logs are not available, the Ford Geraldine equation can be used instead. Unless special core-analyses have determined m and n in a field, the values determined for these parameters in the Ford Geraldine unit are the best data available, and water saturations should be calculated by the following modified Archie equation:

$$S_w = [(1/\phi^{1.83}) \times (R_w/R_t)]^{1/1.90}.$$

When this method of petrophysical analysis is applied to a new field, it is important to compare the results with other field information, such as production data. In fields with poor, incomplete data, there is probably no unique solution to log interpretation that will always be successful. Instead, it is necessary to try a variety of techniques and to test their validity using all available information about the field.

Reservoir Description

The East Ford unit comprises 1,212 acres. The main reservoir is the Ramsey sandstone, but there is also some production from the underlying Olds sandstone (fig. 22). The subsurface database for reservoir characterization includes logs from 44 of the 45 wells in the field, most commonly gamma-ray or gamma-ray and interval-transit-time logs (fig. 36). Core analyses (permeability, porosity, water saturation, and oil saturation) were available from 620 samples from 11 wells throughout the East Ford unit (fig. 21). Because core-analysis data were available from the EFU 41 well, core analyses from adjacent EFU 41R were not added to this database. Areal mapping of reservoir properties across the field was accomplished by means of core-analysis data, geophysical logs, and log-data to core-porosity transforms and core-porosity to core-permeability transforms.

Porosity Distribution

Average porosity in the Ramsey interval is 21.7 percent (fig. 41), as determined by 334 core analyses of Ramsey 1 and 2 sandstones and SH1 siltstones. Standard deviation is 3.9 percent. Ramsey 1 sandstones have higher average porosity than do Ramsey 2 sandstones, 22.5 versus 21.4 percent, respectively (table 3). SH1 siltstones have an average porosity of 18.2 percent, and they range from 17.2 to 20.7 percent. Ramsey sandstones having porosity lower than 17 percent are interpreted to represent calcite-cemented sandstones (fig. 41).

Areal distribution of porosity was mapped by means of porosity data from core analyses, combined with porosities calculated from ITT logs and the log-core porosity transform (fig. 38). The use of core-analysis data increases available well control and provides a more detailed map of porosity distribution than does the use of porosity-log data alone. In wells that have both porosity logs and core-analysis data, the core-analysis data were used. Porosity values for the Ramsey 1 and 2 sandstones (excluding the SH1 siltstone) were calculated on a foot-by-foot basis, and these values were averaged to determine the average porosity in each well.

The map of average porosity (fig. 42) for the Ramsey sandstone in the East Ford unit exhibits a strong north-south trend of high porosity that follows the positions of the Ramsey 1 and 2 sandstone channels (figs. 31, 32). Average porosity for the unit calculated from this map is 22.1 percent. Average porosity was calculated by (1) imposing a 50-ft \times 50-ft grid on the isopach map, (2) summing porosity \times area for each grid block, and (3) dividing total porosity \times area by total area. The zone of highest porosity (>24 percent) is confined to the central part of the field, with slightly lower porosity at the south end.

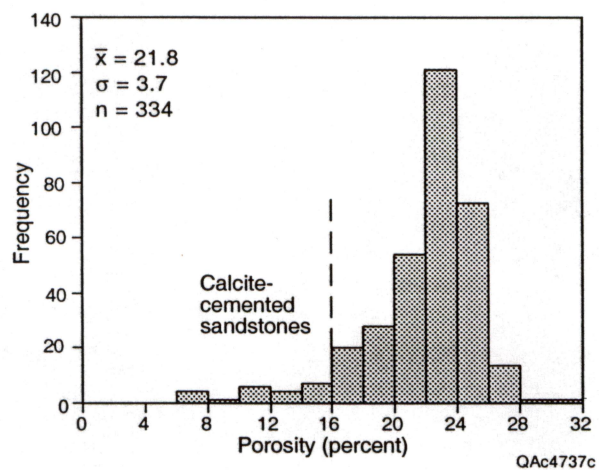


Figure 41. Distribution of porosity in Ramsey 1 and 2 sandstones and SH1 siltstones in the East Ford unit from core analyses. Low porosity values (<16 percent) are probably from calcite-cemented sandstones.

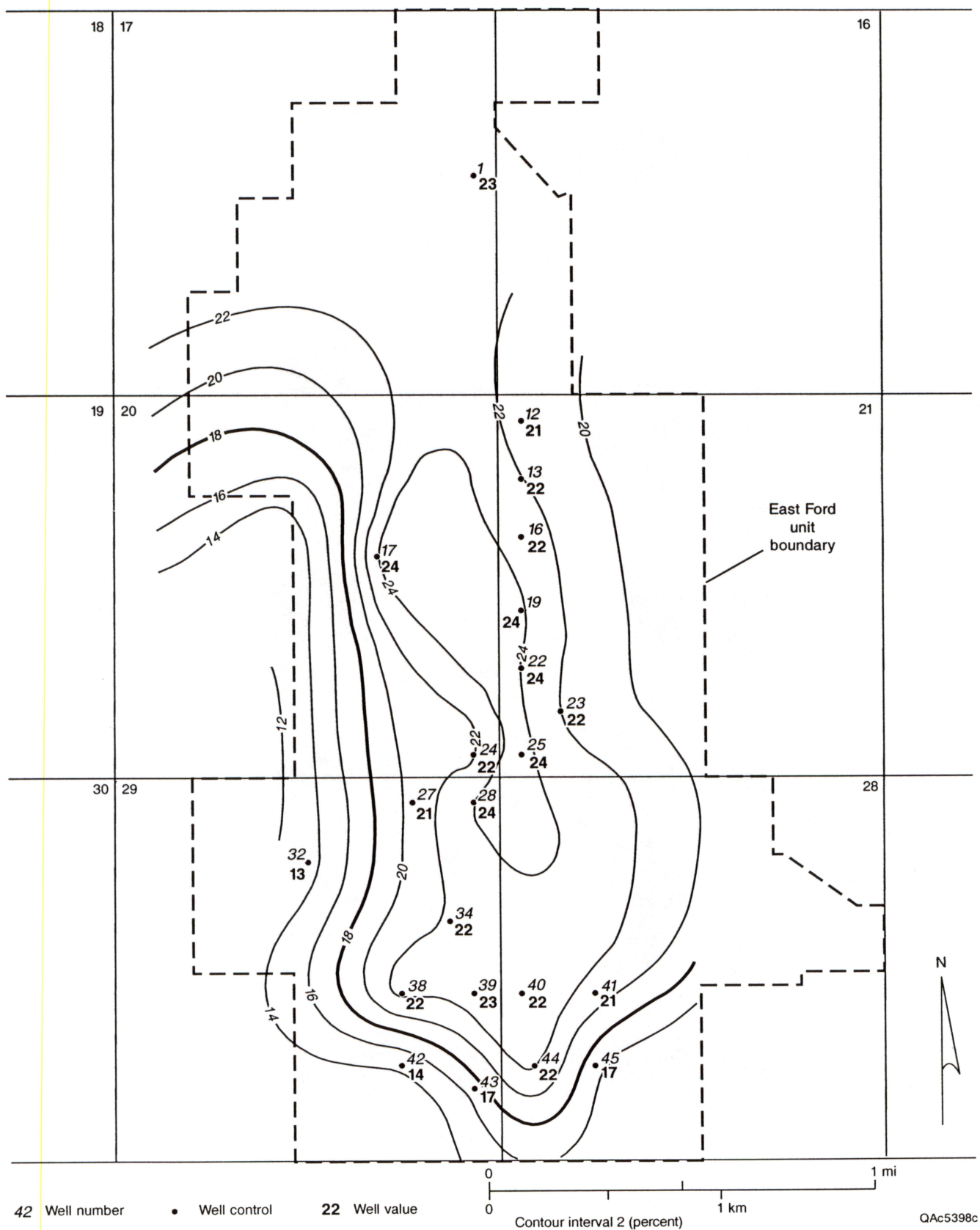


Figure 42. Map of average porosity of the Ramsey sandstone in the East Ford unit. The average porosities were determined from ITT logs and the core-log porosity transform, supplemented by core-analysis data.

Permeability Distribution

Arithmetic average permeability determined by core analyses of Ramsey 1 and 2 sandstones and SH1 siltstones in the East Ford unit is 39 md (fig. 43), and the standard deviation is 35 md. Geometric mean permeability of the Ramsey sandstone is 20 md, with a standard deviation of 5 md. Vertical permeability is typically 90 percent of horizontal permeability (W. A. Flanders, Transpetco Engineering, written communication, 1994). Ramsey 1 sandstones have higher average permeability than do Ramsey 2 sandstones, 46 versus 34 md, respectively (table 3). SH1 siltstones have an average permeability of 4 md.

Plots of the cumulative distribution functions (CDF) of the East Ford permeability data (Ramsey 1 and 2 and total Ramsey sandstones; SH1 siltstones omitted) are close to straight lines on a logarithmic scale (fig. 44), indicating that the permeability data are approximately log normally distributed. All three populations are negatively skewed, having a tail of low permeability values that are interpreted to represent calcite-cemented sandstones. On the basis of the Dykstra–Parsons heterogeneity coefficient (V), a measure of permeability heterogeneity (Dykstra and Parsons, 1950), the Ramsey sandstone in the East Ford unit was found to be moderately homogeneous ($V = 0.52$) (table 2). The Ramsey 2 sandstone is more heterogeneous than is the Ramsey 1 sandstone. The Dykstra–Parsons coefficient for the Ramsey 2 sandstone is 0.57, compared with 0.44 for the Ramsey 1 sandstone (table 3). The Dykstra–Parsons mean permeability of the Ramsey 1 sandstone is 41 md, compared with 29 md for the Ramsey 2 sandstone. The combined Ramsey 1 and 2 sandstones have a Dykstra–Parsons mean permeability of 42 md.

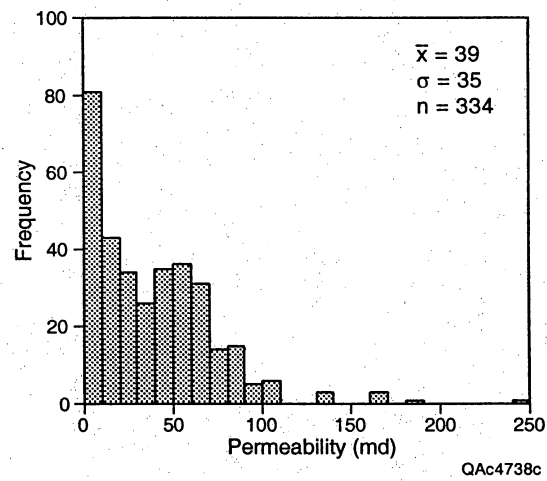


Figure 43. Distribution of permeability in Ramsey 1 and 2 sandstones and SH1 siltstones in the East Ford unit, based on core analyses.

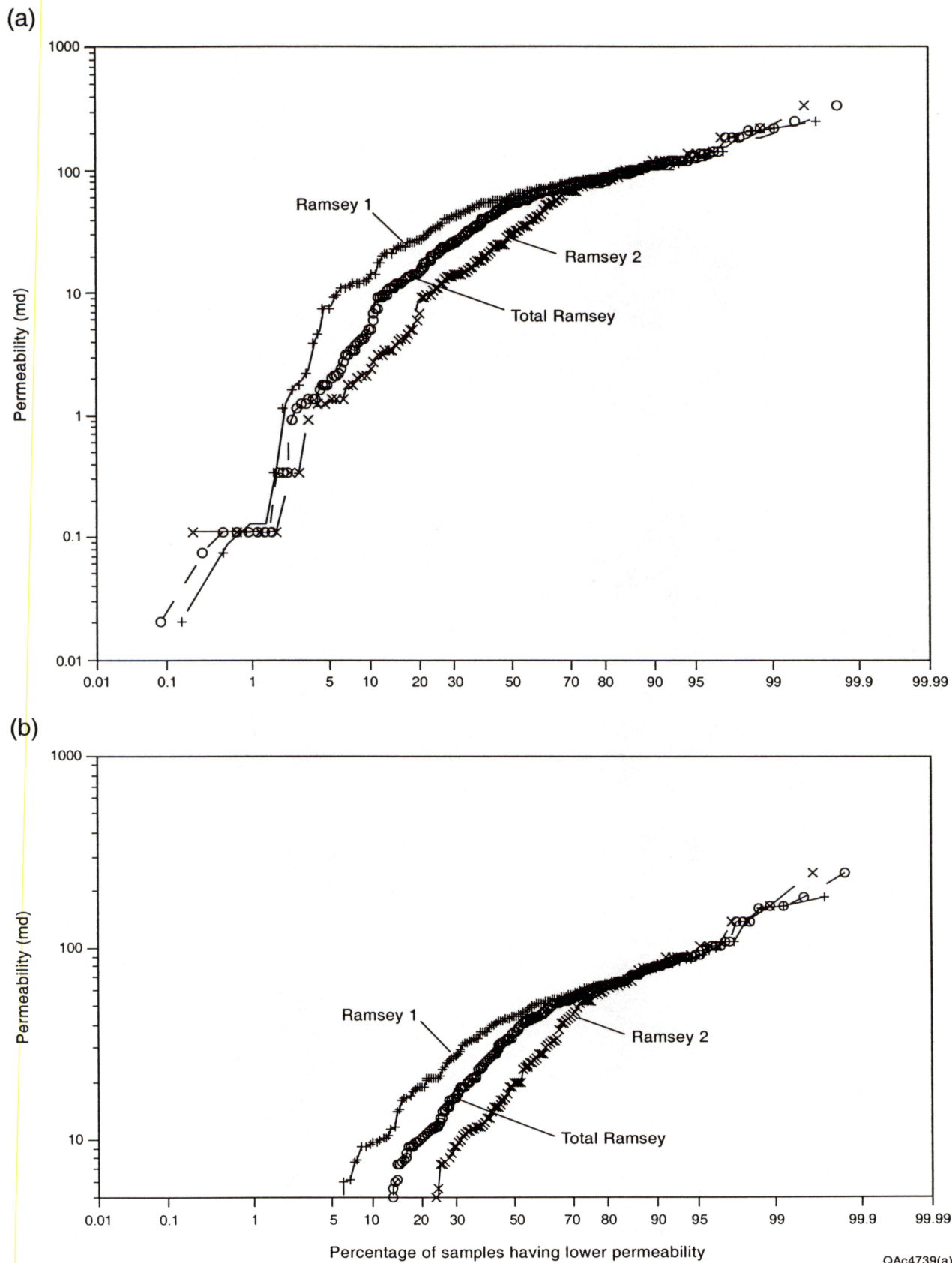


Figure 44. Cumulative distribution function of core-analysis permeability for Ramsey 1 and 2 sandstones in 11 wells in the East Ford unit. (a) All data. (b) Data from floodable Ramsey sandstones only, having permeability ≥ 5 md.

Structure

The Ramsey sandstone at the East Ford unit dips 1° to the east-northeast (fig. 45), almost directly opposite the original depositional dip, because Late Cretaceous movement associated with the Laramide Orogeny tilted the Delaware Basin eastward (Hills, 1984). No faults are interpreted to cut the Ramsey sandstone at the East Ford unit. Production from the East Ford unit and other upper Bell Canyon fields in the Delaware Basin occurs from the distal (southwest) ends of east-dipping, northeast-oriented linear trends of thick Ramsey sandstone deposits (figs. 24, 26). Most hydrocarbons in these fields are trapped by structurally updip facies changes from higher permeability reservoir sandstones to low-permeability siltstones. Several of the fields show minor structural closure because linear trends of thick sandstones formed compactional anticlines by differential compaction during burial (Ruggiero, 1985, 1993).

Net Pay

Net pay in the Ramsey reservoir was calculated from geophysical logs, according to the cutoffs established for volume of clay (≤ 15 percent), porosity (≥ 17.5 percent), and water saturation (< 60 percent). An isopach map of net pay shows that the highest values (>30 ft) follow a north-south trend down the center of the East Ford unit (fig. 46).

The average net pay calculated from the isopach map is 19.6 ft. Net pay decreases to the west, where the Ramsey sandstone pinches out into siltstone, and to the east, where the sandstone dips below the oil–water contact. Gross pay, calculated as the thickness of the total Ramsey sandstone interval (Ramsey 1 sandstone, SH1, and Ramsey 2 sandstone), averages 33 ft.

The map of hydrocarbon pore-feet ($S_o \times \phi \times H$) (fig. 47) shows a strong north-south trend of high values down the central part of the unit. The loss of $S_o \times \phi \times H$ to the east is to be expected because of the structurally lower position of the Ramsey sandstone. The

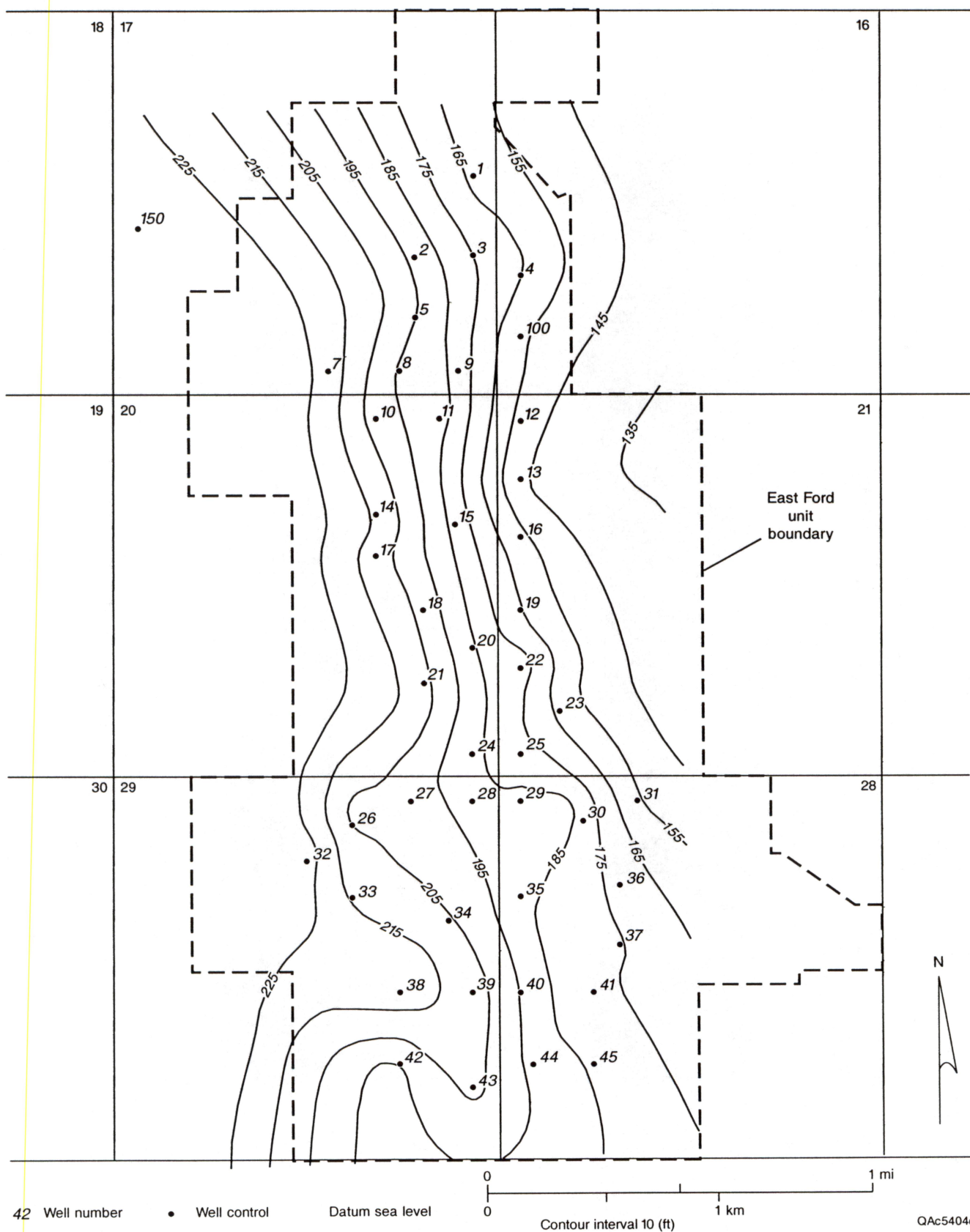


Figure 45. Structure contoured on the top of the Lamar limestone dipping to the east in the East Ford unit. The trap is formed by pinch-out of permeable sandstone into low-permeability siltstone up structural dip.

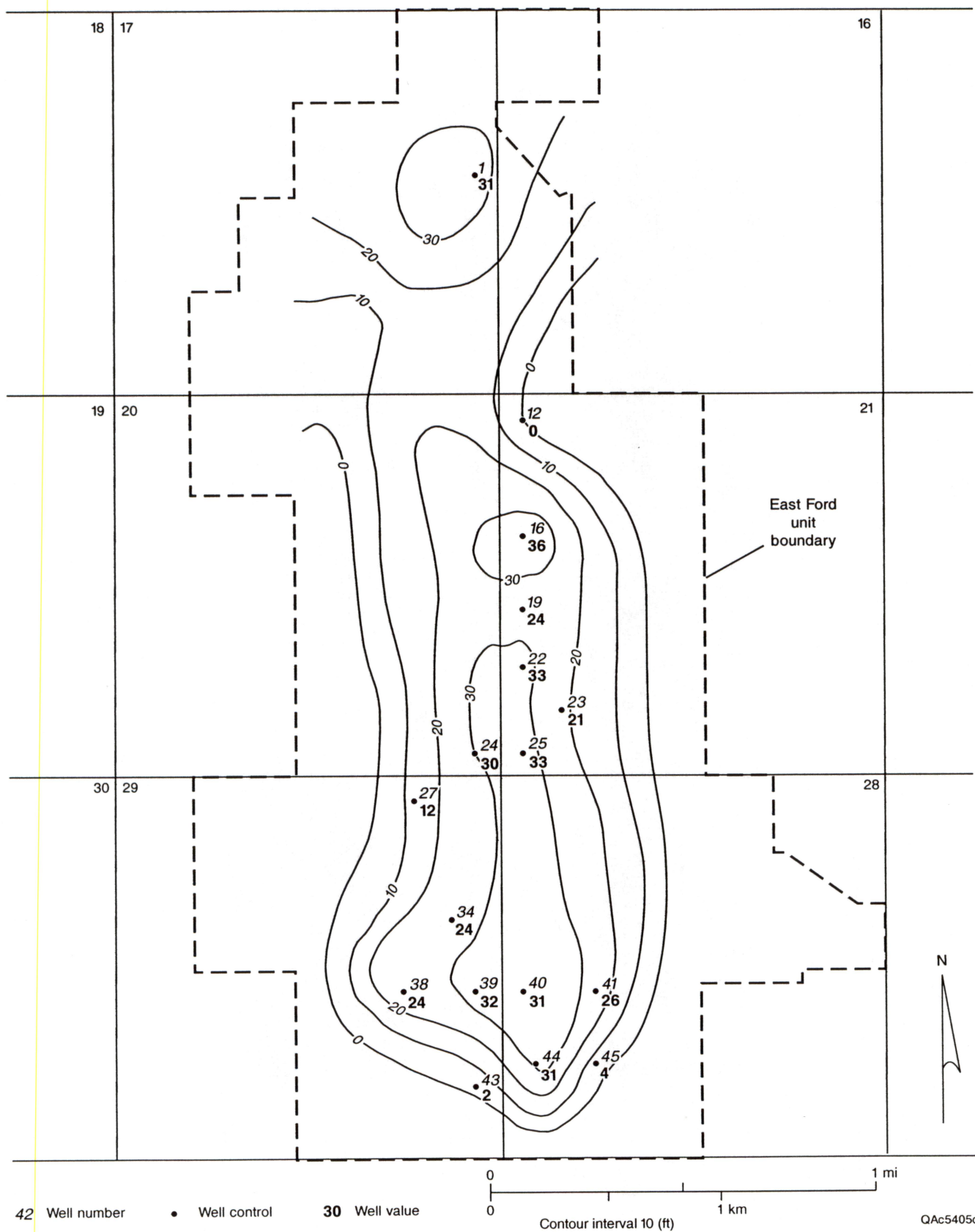


Figure 46. Map of net pay of the Ramsey sandstone in the East Ford unit. The cutoffs for net pay were $V_{cl} \leq 15$ percent, $\phi \geq 17.5$ percent, and $S_w < 60$ percent.

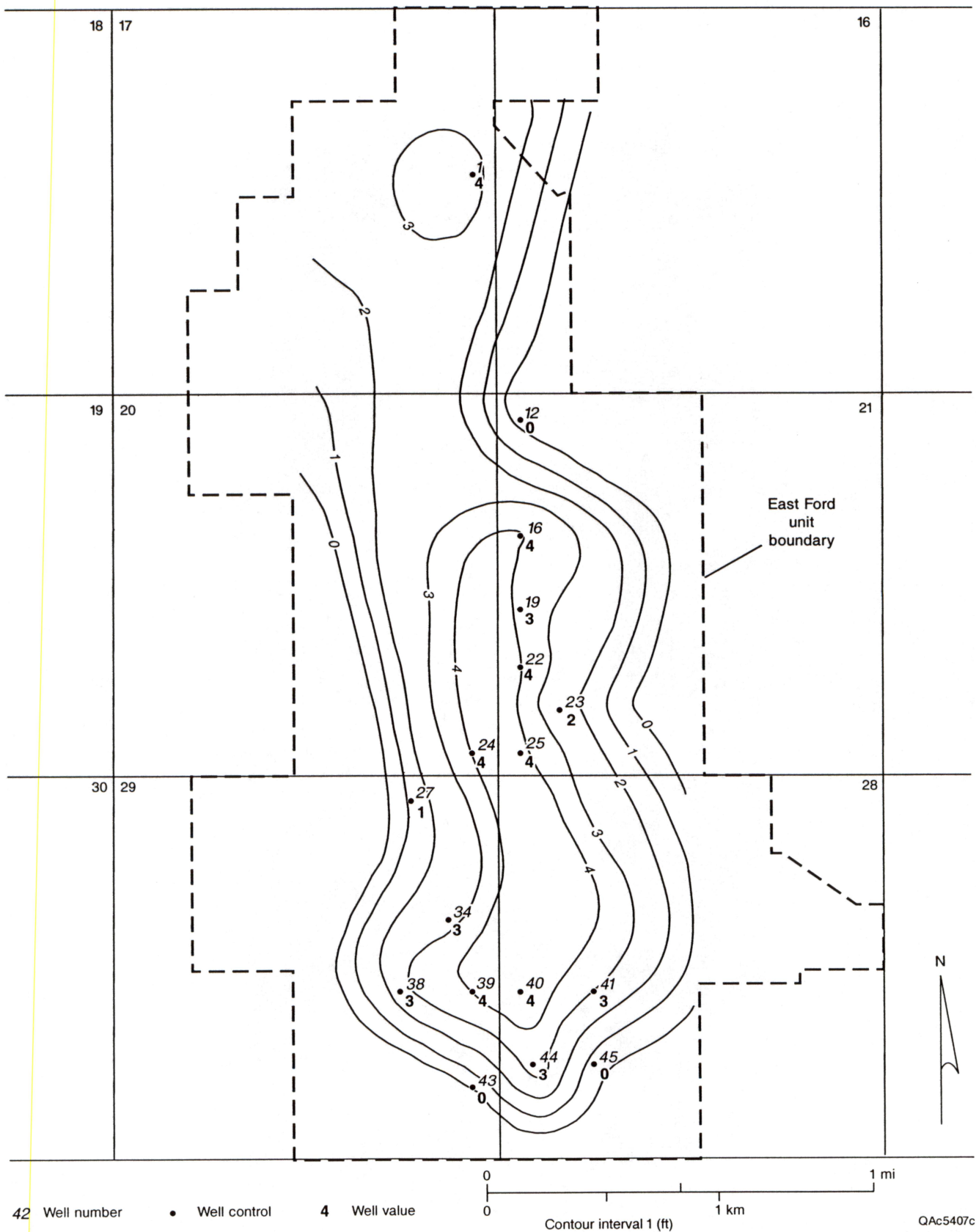


Figure 47. Map of hydrocarbon pore-feet ($S_o \times \emptyset \times H$) of the Ramsey sandstone in the East Ford unit.

$S_o \times \phi \times H$ map was used to calculate OOIP in the East Ford unit and in the area of the CO₂ flood (see section Volumetrics, p. 122).

Natural Water Influx

Low reservoir energy suggests that natural water influx into the field is limited. An oil–water contact was identified at 88 ft above sea level (W. A. Flanders, Transpetco Engineering, written communication, 1994).

Geologic Heterogeneity in East Ford Unit

Heterogeneities within reservoir sandstones, whether formed by depositional processes or by postdepositional diagenesis, have the potential to influence recovery. In many cases these heterogeneities do not have a major influence on primary recovery, but they can have a significant impact on EOR processes, including a CO₂ flood. Some of the most important causes of heterogeneity in the Ramsey sandstone reservoirs in the East Ford unit are the presence of siltstone beds, variations in net:gross sandstone, and calcite-cemented sandstone layers. Logs, core-analysis data, and cores from the EFU 41R well were used to assess and map heterogeneities in the East Ford unit.

Siltstones

Siltstones cause important depositional heterogeneity within Bell Canyon reservoirs because of the grain size and permeability contrast between sandstone and siltstone facies. Because of the low permeability of siltstones, limited cross-flow of fluids will occur between sandstones separated by siltstones. The depositional model provides a way to predict the distribution of siltstones in Bell Canyon deposits. Siltstones occur as (1) widespread sheets that bound high-order depositional cycles; (2) a concentration of

rounded siltstone clasts and, rarely, a drape of massive, organic-rich siltstone along the base of channels; (3) beds interbedded with thin sandstones within the levee deposits that flank both sides of channels and gradually thin and taper away from the channel; and (4) overlying erosion surfaces associated with channel avulsion (Dutton and others, 2000a, b). All of these siltstone beds have the potential to disrupt displacement operations in Delaware sandstone reservoirs. For example, cross-flow of fluids may be limited between a well in an overbank-splay deposit and a well in a channel deposit, not only because of interbedded siltstones in the levee, but also because of a siltstone-pebble lag or thin siltstone drape along the base of the channel (Dutton and others, 2000a, b).

In the East Ford unit, a major geologic heterogeneity is caused by the 1- to 3-ft-thick laminated siltstone (SH1 siltstone [figs. 22, 25]) that divides the Ramsey reservoir into the Ramsey 1 and Ramsey 2 sandstones throughout the field. The SH1 siltstone represents a break in sandstone deposition within the Ramsey interval, when laminated siltstone was deposited over a widespread area. Cross-flow of fluids between the Ramsey 1 and 2 sandstones will be limited because of the SH1 siltstone. Because CO₂ that is injected only into the Ramsey 2 sandstone interval probably will not penetrate the Ramsey 1 sandstone, both injector and producer wells should be perforated above and below the SH1 siltstone.

Net:Gross Sandstone

Another source of heterogeneity in the East Ford unit is variation in reservoir quality between wells. One way to quantify heterogeneity in the Ramsey 1 and 2 sandstones is by mapping the ratio of net:gross sandstone. In the East Ford unit, net pay of an interval was calculated as the number of feet of sandstone having porosity ≥ 17.5 percent, volume of clay (V_{cl}) ≤ 15 percent, and water saturation < 60 percent (Dutton and others, 1999c). Gross sandstone is simply the total thickness of the interval. Because the goal of the

Ramsey 1 and 2 net:gross sandstone maps was to show the ratio of clean sandstone to total sandstone, net sandstone was mapped as sandstone having porosity ≥ 17.5 percent and $V_{cl} \leq 15$ percent, no matter what the water saturation. Clean sandstones on the east side of the field have high water saturation because of their structurally lower position, not because of poorer reservoir quality.

The map of net:gross sandstone for the Ramsey 1 interval (fig. 48) shows high net:gross values (> 90 percent) at the east side of the field, along the inferred trend of the Ramsey 1 channel. The Ramsey 1 channel is interpreted to make a sharp meander east of well EFU 19 because both sandstone thickness (fig. 31) and net:gross values (fig. 48) are lower in EFU 19 than in EFU 16 and 22. Net:gross values decline toward the west side of the field, in the areas that are interpreted to be levee and overbank deposits. Good-quality reservoir sandstone was deposited within the levee and overbank deposits, but these facies also contain interbedded siltstones and silty sandstones and thus have lower net:gross values. High net:gross values at the south end of the field (wells EFU 38, 39, 40, and 41) are interpreted to occur in the center of the lobe facies and decrease toward the margins of the lobe (fig. 31).

The Ramsey 2 sandstone has net:gross sandstone values (fig. 49) somewhat lower than those of the Ramsey 1 sandstone, although few wells have sonic logs where the Ramsey sandstone is thickest and might be expected to have the highest net:gross values. In the center of the field, thick Ramsey 2 sandstone in wells EFU 5, 15, and 18 (fig. 32) are interpreted to follow the channel trend. These wells do not have sonic logs, so net:gross sandstone could not be calculated. The highest values (> 70 percent) of net:gross sandstone occur within the inferred channel and, to a lesser extent, in the lobe (fig. 32). The Ramsey 2 sandstone may have less clean sandstone than does the Ramsey 1 because it was deposited during a time of rising sea level, when there was less clastic input and the thickest sand deposits back-stepped toward the shelf margin (Dutton and others, 1999a). The Ramsey 2 sandstones also contain higher percentages of calcite-cemented

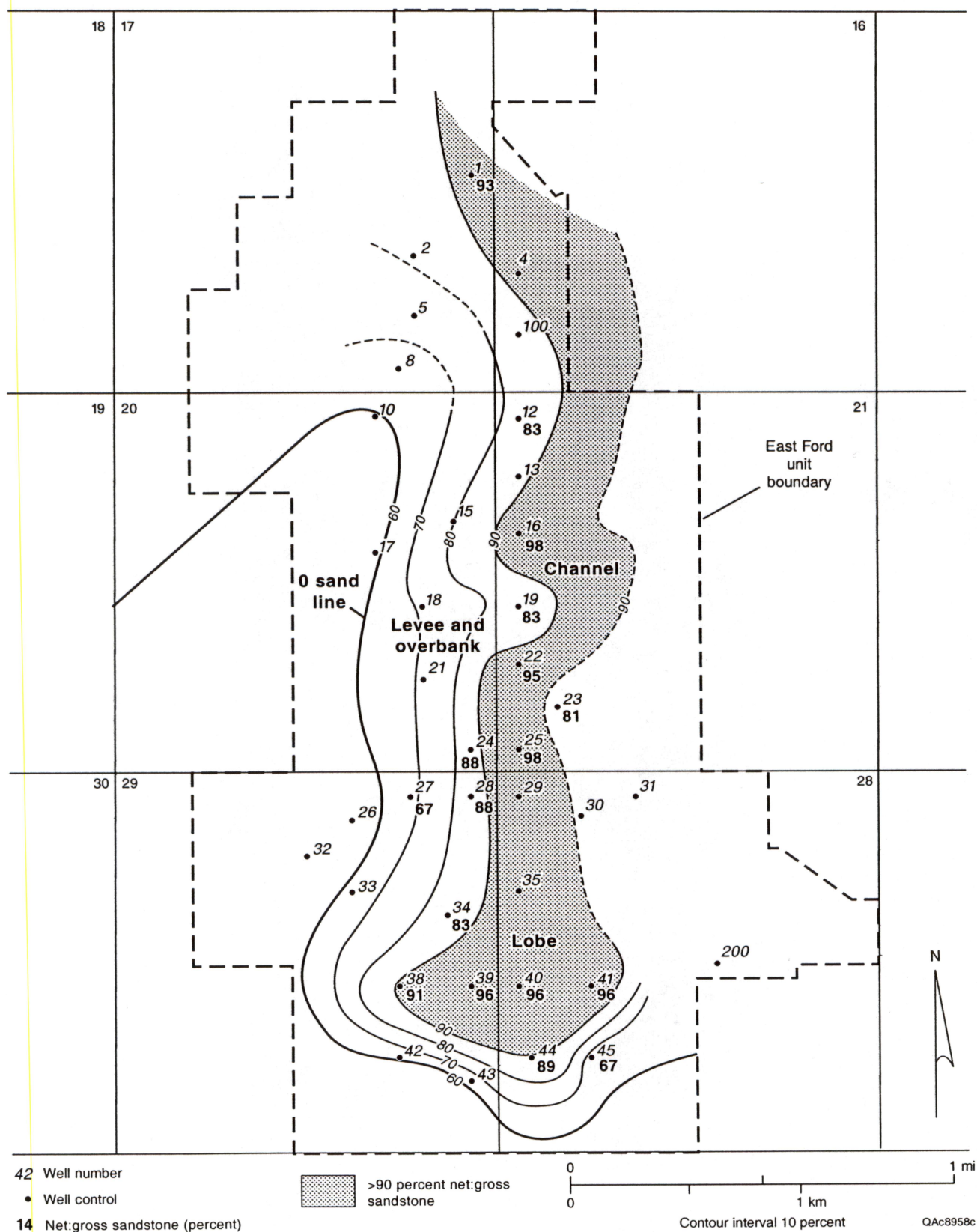


Figure 48. Isopach map of percentage of net:gross sandstone in the Ramsey 1 interval. Net sandstone was determined from sonic and gamma-ray logs as the number of feet of sandstone having volume of clay ≤ 15 percent and porosity ≥ 17.5 percent.

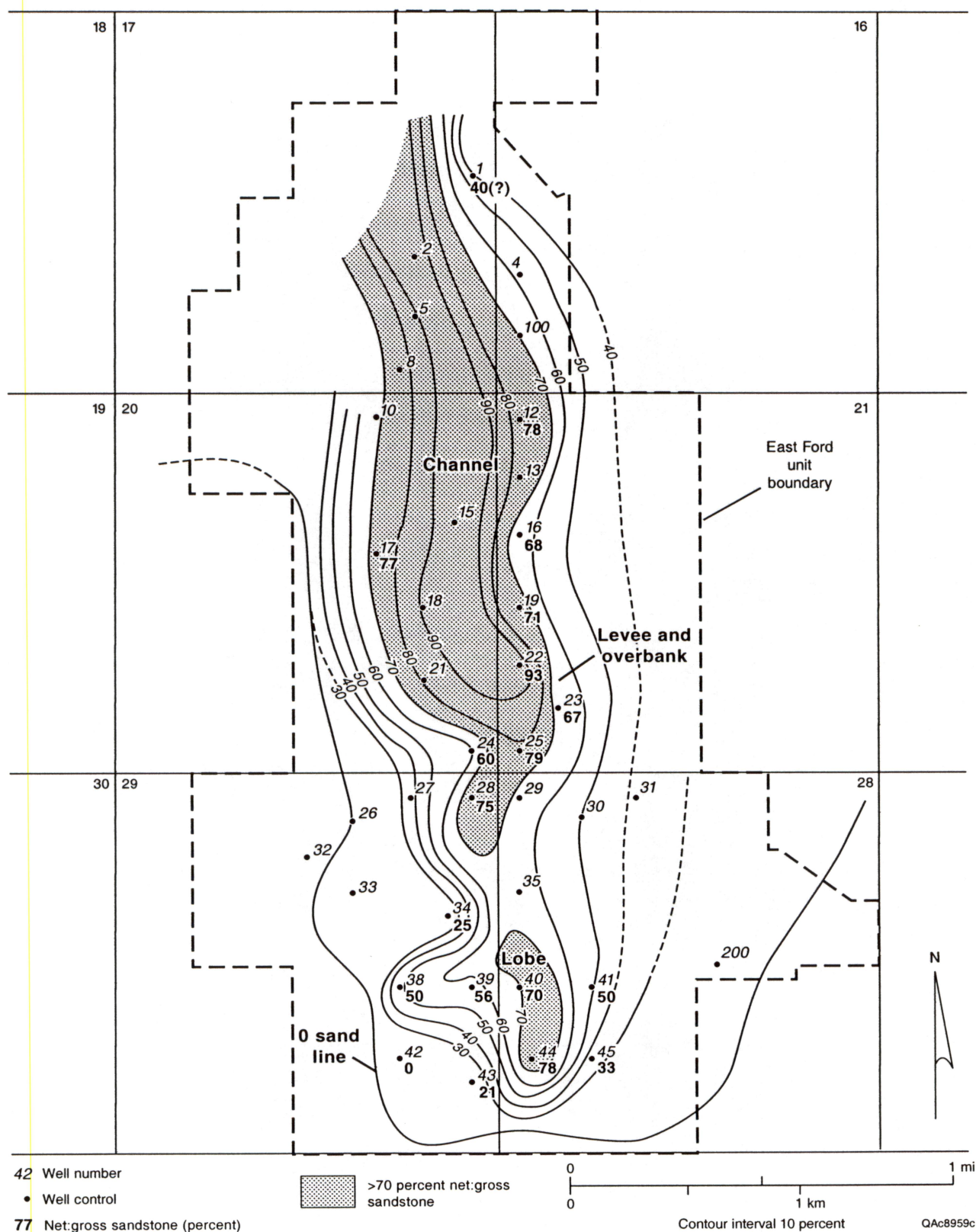


Figure 49. Isopach map of percentage of net:gross sandstone in the Ramsey 2 interval. Net sandstone was determined from sonic and gamma-ray logs as the number of feet of sandstone having volume of clay ≤ 15 percent and porosity ≥ 17.5 percent.

sandstone (see Correlation of Calcite-Cemented Layers, p. 107). As a result of these differences, Ramsey 1 sandstones have higher average permeability than do Ramsey 2 sandstones, 46 versus 34 md, respectively (Dutton and others, 1999c).

Net:gross maps of both Ramsey 1 and 2 intervals provide an indication of geologic heterogeneity in the East Ford unit. The channel and central-lobe deposits are the most homogeneous, consisting mostly of clean, porous sandstone, whereas the levee, overbank, and lobe-margin deposits are more heterogeneous. In general, better communication would be expected between wells within the areas of high net:gross sandstone and poorer communication in areas of low net:gross sandstone or between areas of high and low net:gross sandstone.

Diagenetic Heterogeneity

Diagenetic heterogeneities, particularly the layers of tightly calcite cemented sandstone, also appear to affect the East Ford CO₂ flood. Plots of permeability versus depth show numerous spikes of high and low permeability in Ramsey 1 and 2 sandstones (Dutton and others, 1999c). Petrographic analysis of samples from the EFU 41R well demonstrated that the low-permeability zones correspond to calcite-cemented layers (Dutton and Flanders, 2001).

Gas Effect in EFU 41R Well

Sonic and neutron logs from the EFU 41R well showed a gas effect in the lower 8 to 10 ft of the Ramsey 1 sandstone, in the same interval in which the calcite-cemented layers occur (fig. 50). No gas effect was seen above the uppermost calcite layer. When the well was first completed, it produced a high volume (750 Mcf/d) of high-concentration CO₂ (>90 percent). Production and temperature logs confirmed the gas effect by indicating that inflow to the well bore was essentially all occurring in the

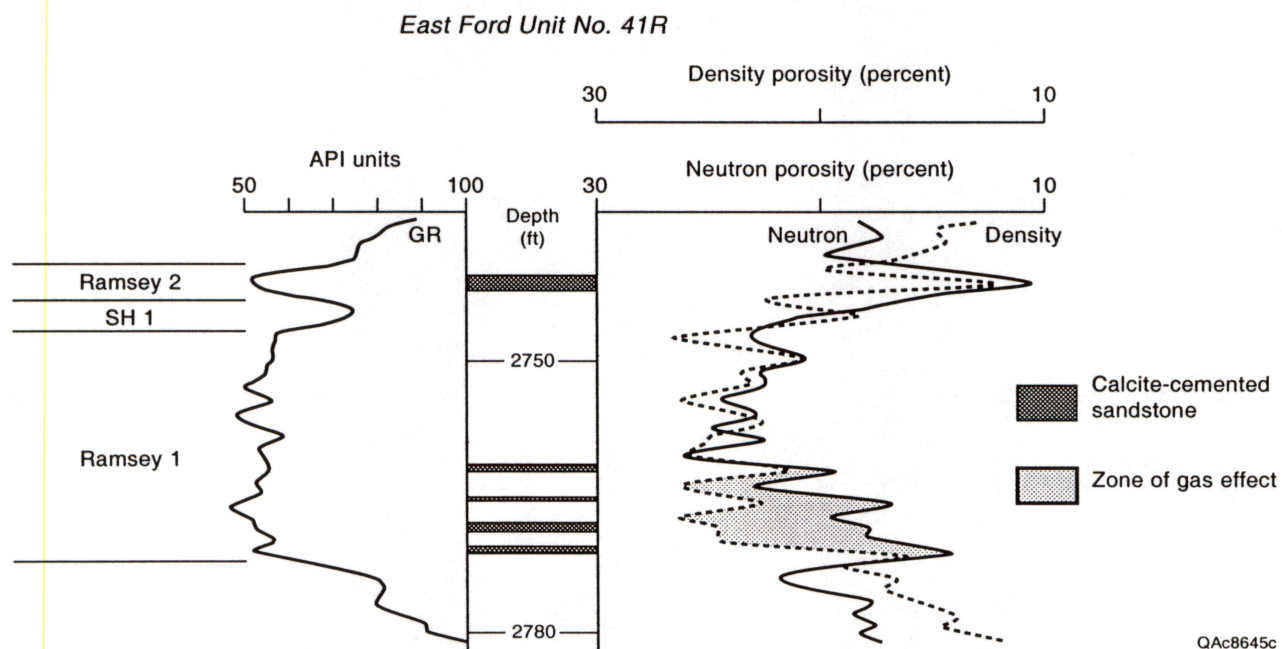


Figure 50. Gamma-ray, neutron, and density logs from the EFU 41R well. The neutron log shows a gas effect in the lower Ramsey 1 sandstone below the uppermost calcite-cemented layer.

bottom 10 ft of the Ramsey 1 sandstone. CO₂ from the nearby injector well EFU 40 (fig. 21) was apparently trapped in the bottom part of the Ramsey 1 sandstone, below the low-permeability, calcite-cemented layers. This trapping suggests that one or more of the calcite layers are laterally continuous between wells 40 and 41R, causing vertical compartmentalization in the Ramsey 1 sandstone.

CO₂ was injected in the EFU 40 well above and below the calcite-cemented layers, but the previous producing wells, EFU 39 and 41, had no perforations in the Ramsey 1 sandstone below the calcite layers. The CO₂ that was produced in the EFU 41R well probably represents banked-up energy that gave a first flush of CO₂ when the well was completed. To control excess gas production, EFU 40 was converted to water injection. The gas-alternating-water (GAW) cycle was apparently successful because gas production was reduced, and the EFU 40 well has been returned to CO₂ injection. Current production suggests that the displacement bank has not reached the EFU 41R well yet. The well has been put on pump and produces 5 to 10 bopd, 50 bbl of water, and 85 Mcf of gas.

Correlation of Calcite-Cemented Layers

Spikes on the EFU 41R sonic log in the lower part of the Ramsey 1 sandstone appear to correlate to those on the EFU 40 and EFU 41 sonic logs (fig. 51), further evidence suggesting lateral continuity of the cement layers. Because the distance between well EFU 40 and wells EFU 41 and 41R is about 1,000 ft, the four calcite layers observed in the EFU 41R core are interpreted as having a lateral extent of at least that distance. Most of these layers did not extend to wells EFU 39 and 38 (fig. 51), which contain fewer calcite-cemented layers in the Ramsey 1 sandstone. However, the cemented zones at the base of the Ramsey 1 sandstone and near the top of the Ramsey 2 sandstone both appear to be continuous across the south part of the unit (fig. 51).

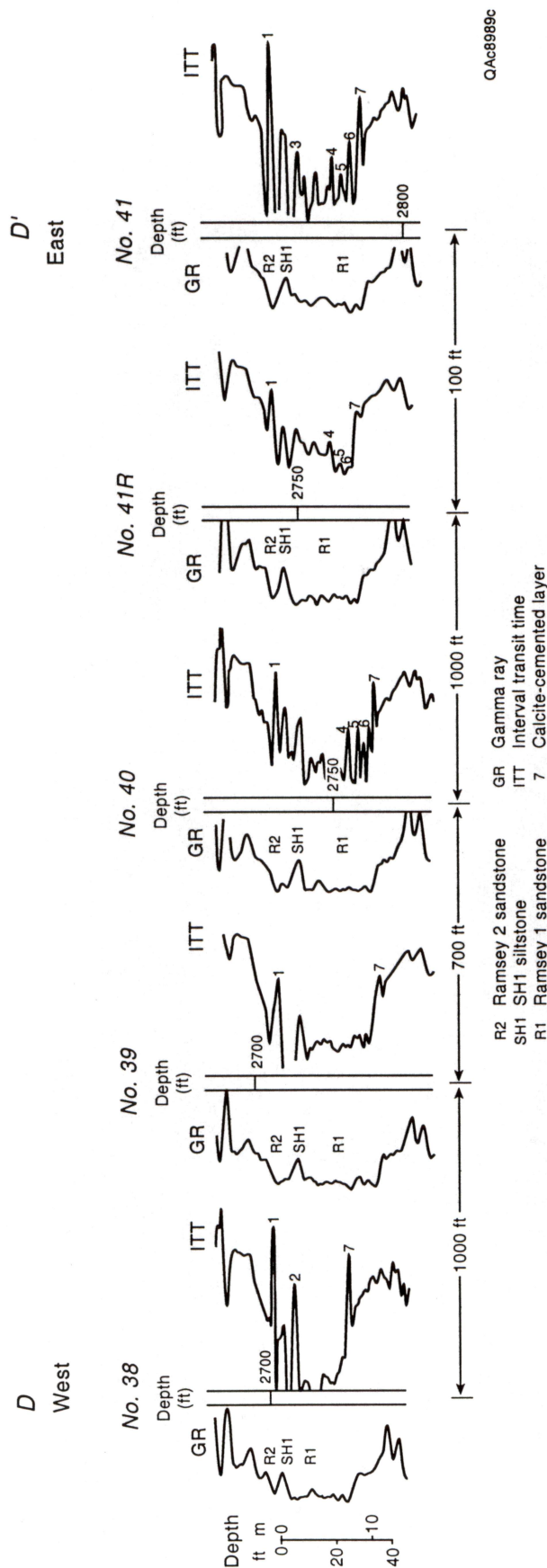


Figure 51. West-east cross section D-D' of south end of the East Ford unit. Four calcite-cemented layers in the lower Ramsey 1 sandstone can be correlated in the EFU 40, 41, and 41R wells. The layer at the base of the Ramsey 1 sandstone and another near the top of the Ramsey 2 sandstone occur in all five wells. Location of cross section shown in figure 21.

Calcite-cemented layers were identified throughout the East Ford unit by using core-analysis data and sonic and resistivity logs to identify cemented intervals. The cemented thicknesses are probably overestimated because cemented zones appear thicker on the logs than they really are (see fig. 50, for example). Wells EFU 24 and 28 contain several calcite-cemented layers in the bottom of the Ramsey 1 sandstone that appear to correlate between the two wells, a distance of about 735 ft. In addition, a 1- to 2-ft-thick calcite-cemented zone was observed in most wells just below the top of the Ramsey 2 sandstone and just above the base of the Ramsey 1 sandstone. In most wells, including EFU 41R, these layers are not at the very top or bottom of the sandstone, but about 6 inches from the contact with the siltstone.

Maps of the percentage of calcite-cemented sandstone in the Ramsey 1 and Ramsey 2 intervals (figs. 52, 53, respectively) show variations across the field. In general, the percentage of calcite-cemented sandstone is lower in the Ramsey 1 than in the Ramsey 2 sandstone. In both sandstones, the areas having the lowest percentage of calcite-cemented sandstone (<10 percent) occur where the sandstone is thickest, in what is interpreted to be the channel facies. Areas having high percentages of calcite-cemented sandstone (>20 percent) occur along the margins of the sandstones, in levee, overbank, and lobe deposits.

In a study of turbidite reservoirs in Upanema field in the Potiguar Basin, Brazil, Moraes and Surdam (1993) observed carbonate cement (calcite and dolomite) in both channel and lobes facies. Carbonate-cemented layers in channel sandstones were dispersed and of short lateral extent, whereas in the lobe facies carbonate layers were more numerous and laterally extensive (fig. 54). They interpreted the carbonate cement to be associated with shaly zones between turbidite depositional packages. Because shaly zones were more likely to be deposited and preserved in the lobe facies than in the channel facies, carbonate-cemented layers are longer and more abundant in lobe deposits (fig. 54). Moraes and Surdam (1993) noted that the laterally extensive calcite-cemented layers can form significant vertical permeability baffles in a reservoir.

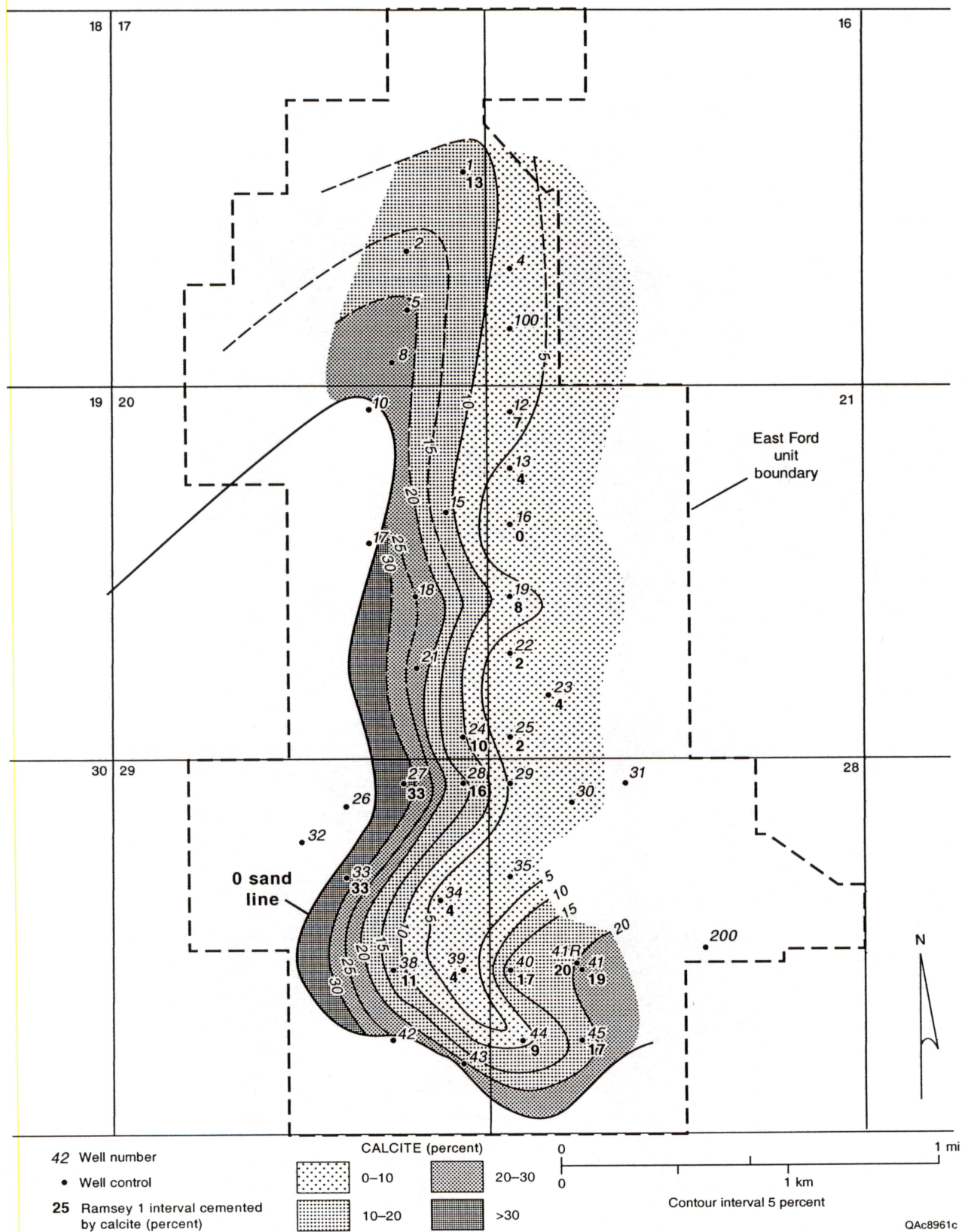


Figure 52. Map of percentage of the Ramsey 1 sandstone that is cemented by calcite.

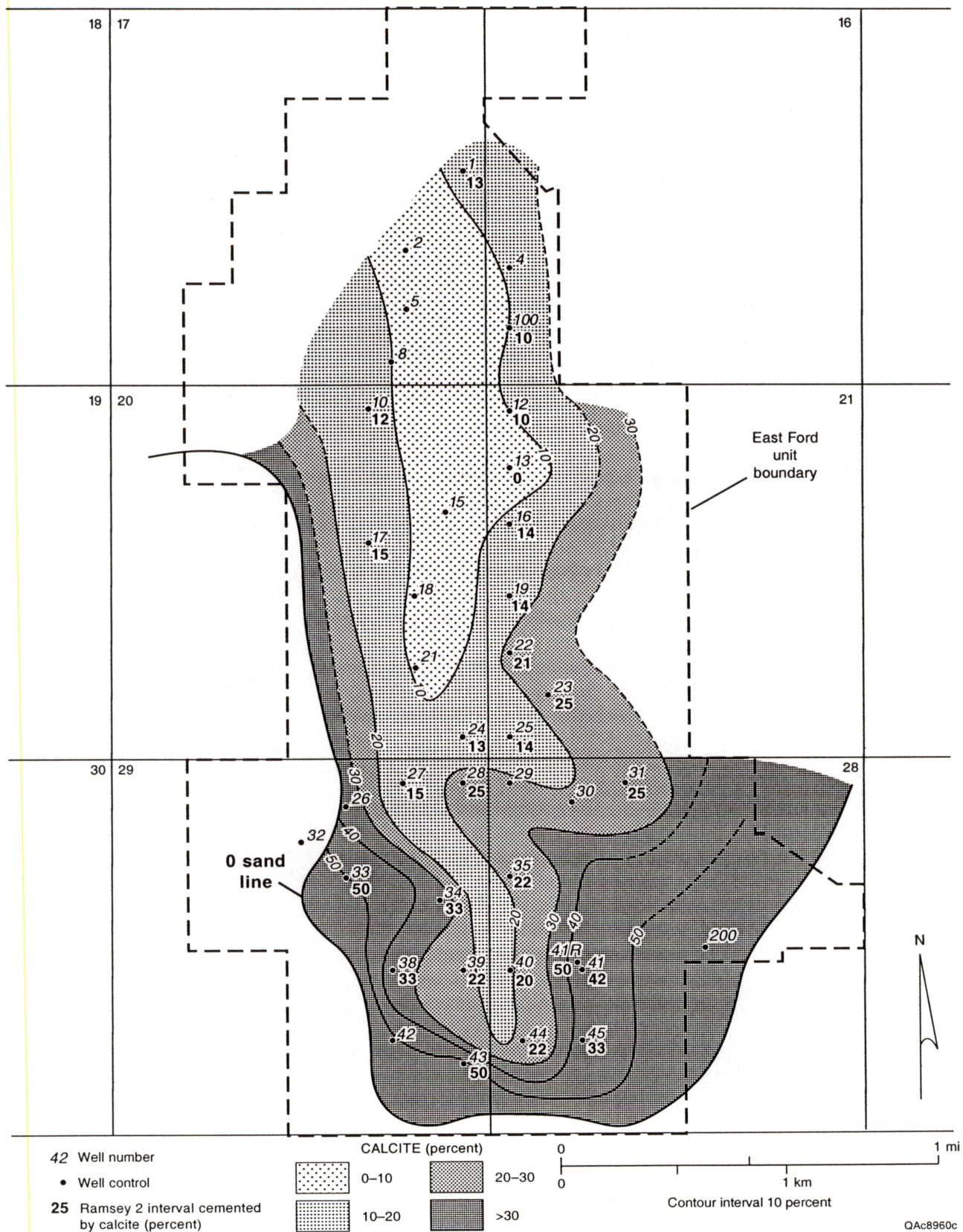


Figure 53. Map of percentage of the Ramsey 2 sandstone that is cemented by calcite.

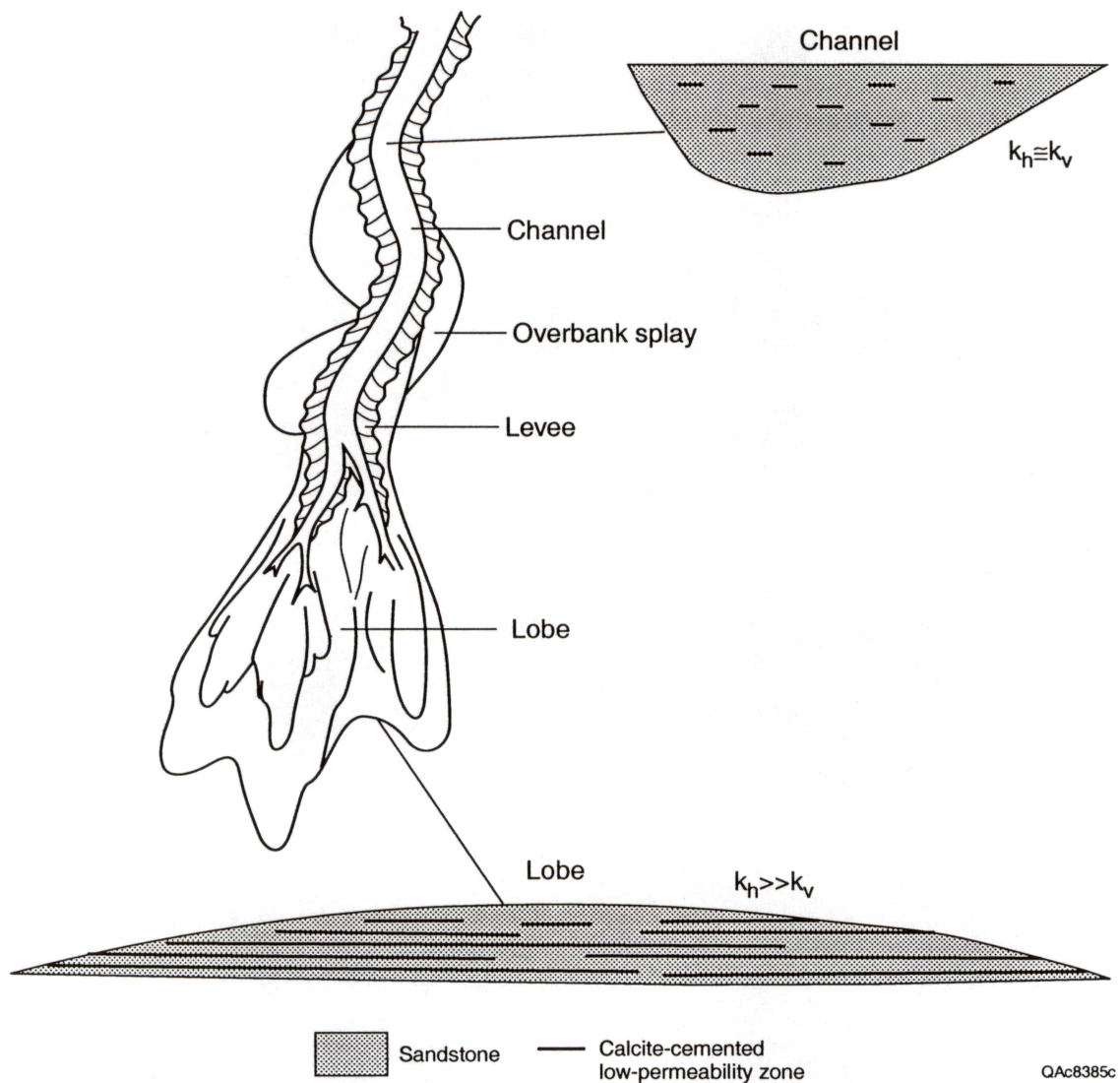


Figure 54. Interpretive model of possible calcite-cement distribution in turbidite sandstones in the East Ford unit. Model of calcite-cement distribution in channel and lobe sandstones and inferred horizontal (k_h) and vertical (k_v) permeability relationship from Moraes and Surdam (1993), superimposed on turbidite depositional model after Galloway and Hobday (1996) and Barton (1997).

The model that Moraes and Surdam (1993) developed for calcite cementation in lobe sandstones may explain the apparent lateral continuity of calcite layers in sandstones at the south end of East Ford field. The calcite layers may be associated with pulses of turbidite deposition, although the uniform grain size in East Ford sandstones makes it difficult to differentiate turbidite packages. The source of calcium carbonate that forms the cement is probably dissolution and reprecipitation of detrital carbonate rock fragments and fossils that occur in both the sandstones and siltstones. The common occurrence of calcite cement near the sandstone-siltstone contacts would be explained if some of the calcite had been derived from the siltstones.

Chlorite Cement

Chlorite cement is the second-most-abundant authigenic mineral in Ramsey sandstones in the EFU 41R core. Chlorite has an average volume of 1 percent and ranges from 0 to 3 percent. Forming rims around detrital grains and extending into pores and pore throats, it can thus have an effect on permeability in these very fine grained sandstones greater than its volume alone might indicate.

Authigenic chlorite has been identified in many other Delaware sandstone reservoirs. In El Mar field in Loving County, chlorite and mixed-layer illite-smectite compose a maximum of 10 percent of the bulk rock volume (Williamson, 1978). Authigenic clays compose 1 to 10 percent of the bulk rock volume of Delaware sandstones in Waha field, southeast Reeves County; the most abundant clays are chlorite and an interlayered chlorite/expandable clay (Hays and Tieh, 1992; Walling and others, 1992). Clay minerals make up 5 to 6 weight percent of the Delaware sandstone samples in Twofreds field in Loving and Ward Counties. The clays are mainly mixed-layer chlorite/smectite (76 to 91 percent), with lesser amounts of illite/mica (9 to 24 percent)

(W. A. Flanders, Transpetco Engineering, written communication, 1994). The mixed-layer chlorite contains about 30 to 35 percent expandable interlayers.

EAST FORD FIELD PRIMARY DEVELOPMENT HISTORY

East Ford field was discovered in 1960. The field was originally developed on 20-acre spacing at the north end, then drilled on 40-acre spacing throughout the rest of the field (fig. 21). There are currently 44 usable well bores in the field, including 15 producer and 7 injector wells (fig. 21). Approximately half of the East Ford wells are open-hole completions. The open-hole wells, most drilled by cable tools, initially only penetrated 10 to 15 ft into the Ramsey 2 sandstone. Some were later deepened into the Ramsey 1 sandstone. Cased-hole wells were generally perforated only in the Ramsey 2 sandstone because it was assumed that fracture stimulation would open communication between the Ramsey 1 and 2 sandstones across the SH1 siltstone (fig. 22).

Wells in East Ford field were stimulated by a small fracture treatment of 1,000 gal of lease oil and 1,500 lb of sand. Many wells were restimulated between 1970 and 1987 by 3,000 gal of lease oil and 4,500 lb of sand. The restimulations were marginally successful in increasing production, possibly by opening communication between the Ramsey 1 and 2 sandstones in some wells. Several wells were initially completed in the Olds sandstone (fig. 22). Production from the Olds and Ramsey sandstones was commingled.

Oil gravity is 43° (API), and viscosity is 0.775 cp at reservoir temperature. Average current reservoir pressure is 850 psi. An oil–water contact occurs at an elevation of 88 ft above sea level. The sandstones are water wet.

Primary Development

Primary recovery in East Ford field began in October 1960 and continued until June 1995. The drive mechanism was solution-gas drive. A total of 45 wells were drilled for primary production. Oil production peaked at 965 bbl of oil per day (bopd) in May 1966. Cumulative production by the end of primary recovery in June 1995 was 3,209,655 bbl. An estimated 10 percent of the total production, or 320,966 bbl, was from the Olds sandstone (W. A. Flanders, Transpetco Engineering, written communication, 1994). The estimated 2,888,690 bbl produced from the Ramsey sandstone represents 15.7 percent of the 18.4 MMbbl of OOIP (Dutton and others, 1999c).

Primary production data in the East Ford unit were collected by lease, not by individual well. To map primary oil production, we plotted production for each lease (fig. 21) at the geographic center of the wells that produced from the Ramsey sandstone (fig. 55). All production was assumed to be from the Ramsey sandstone. Highest production at the north end of the field occurs along the position of the Ramsey 2 channel, but in the south part of the field the highest production is shifted to the east, at the position of the Ramsey 1 channel and lobe.

The map of total primary production by lease (fig. 55) gives a somewhat misleading view of where the best production occurs because the leases are different sizes (fig. 21). Production was normalized, therefore, by dividing total production for each lease by the size of the lease. The map of normalized production in bbl/acre indicates that the highest production rates occur on the east side of the unit (fig. 56). High production rates from leases 6 and 9 (fig. 21) suggest that there may be some aquifer support to production that is bringing in oil from the water–oil transition zone to the east of those leases.

The highest production generally follows the trend of low-percentage water cut during initial-potential (IP) tests (fig. 57). In the Ford Geraldine unit, the percentage of water produced during IP tests was the single best predictor of eventual total production

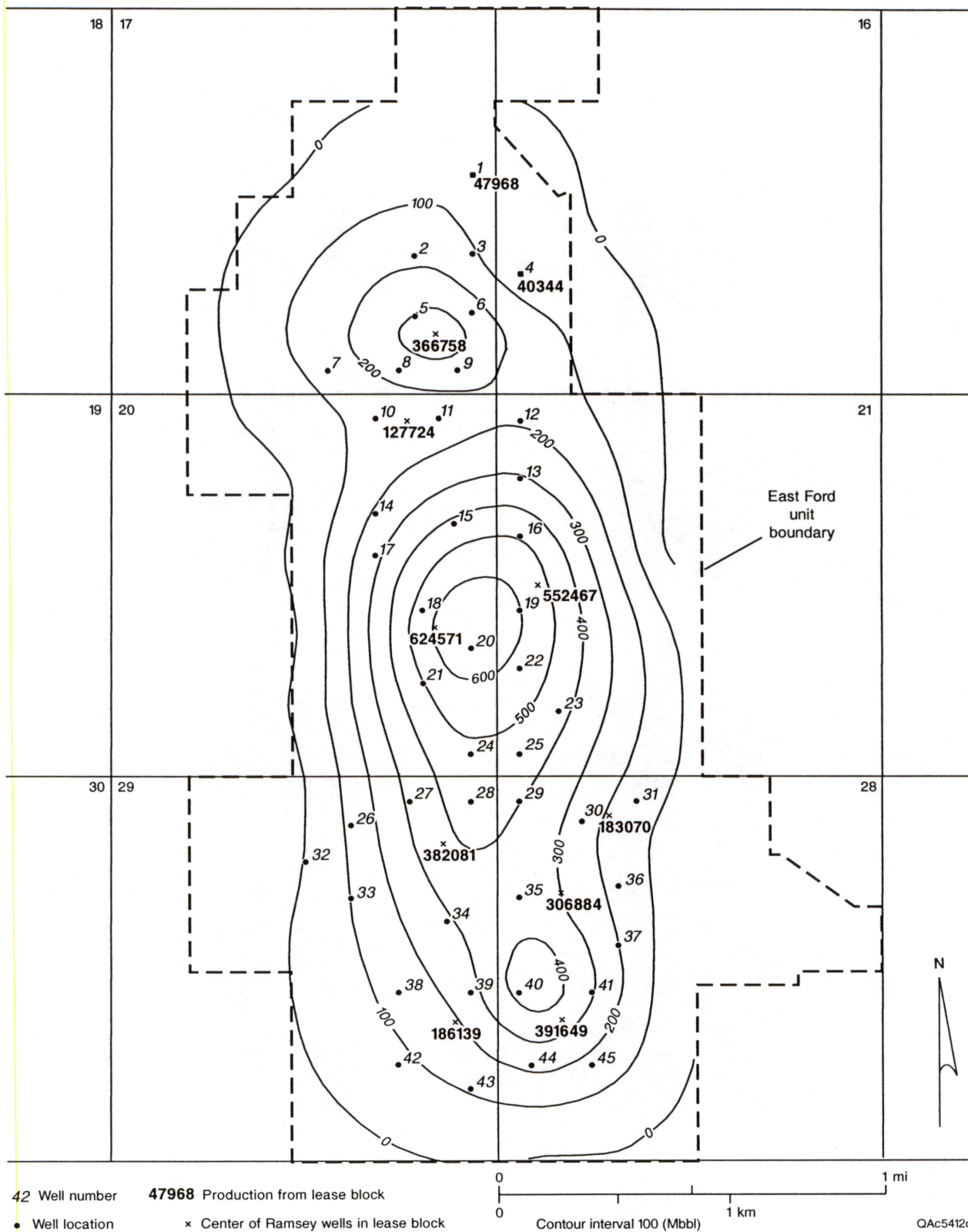


Figure 55. Map of primary oil production from the Ramsey sandstone in the East Ford unit. Production for each lease was plotted at the geographic center of the wells producing from the Ramsey sandstone within the lease.

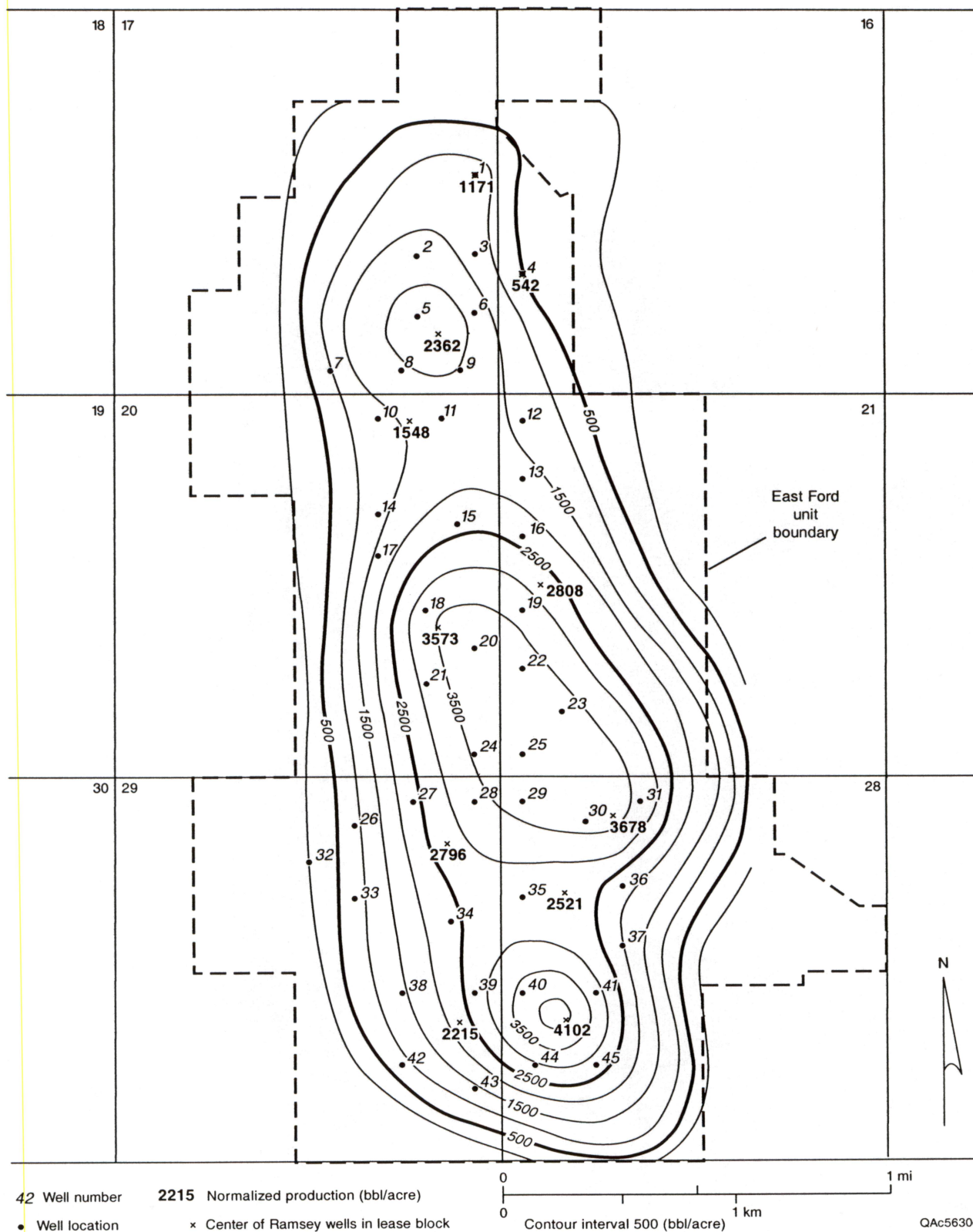


Figure 56. Map of normalized production in the East Ford unit in barrels/acre. Normalized production for each lease was plotted at the geographic center of the wells producing from the Ramsey sandstone within the lease.

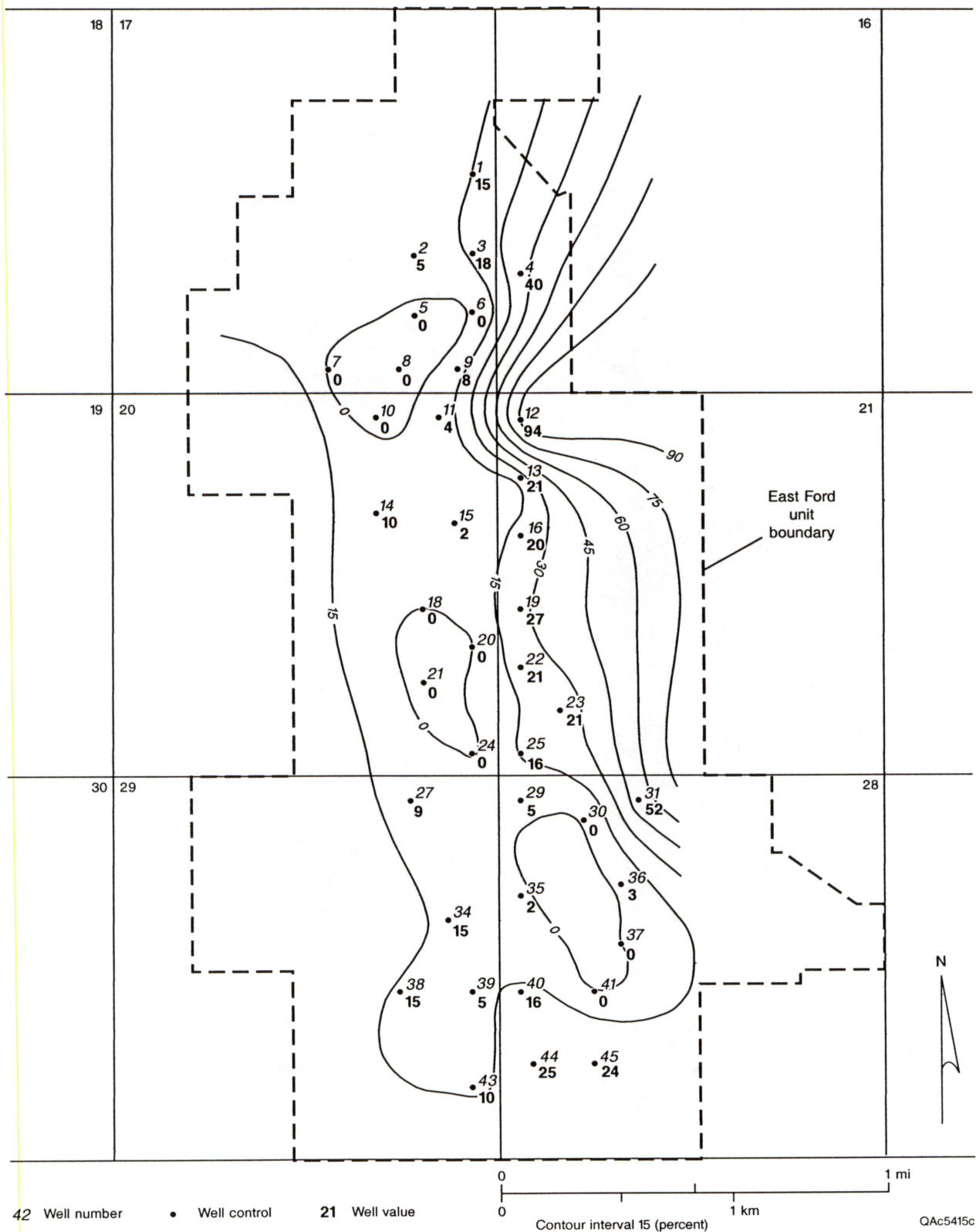


Figure 57. Map of the percentage of water (water cut) produced during initial-potential tests.

from a well (Dutton and others, 1997b), and it appears to be a good predictor in the East Ford unit as well.

In the second method, production from each lease was apportioned among the wells on the lease by initial-potential (IP) test data (fig. 58). For each lease, the barrels of oil per day (bopd) produced by each well during IP tests were summed to get a total value of bopd for the lease, then the percentage contribution of each well to the total was calculated. That fraction was used to apportion total production from the lease to individual wells. Four wells produce only from the Olds sandstone (EFU-26, 32, 33, and 42), so none of the production from those wells was included in the map of Ramsey primary production. Six other wells (EFU-17, 27, 28, 34, 39, and 45) produce from both the Ramsey and Olds zones, and Ramsey production is interpreted as being 90 percent of the total. Total primary production assigned to those wells was reduced by 10 percent to account for the Olds production. The map of primary production generated by this method (fig. 59) shows that most of the better wells in the north part of the field (for example, EFU-2, 15, 18, and 20) penetrate the Ramsey 2 channel facies (fig. 32). The better wells from the south part of the unit (EFU-25, 30, 40, and 41) are offset toward the east, where the Ramsey 1 sandstone is thickest (fig. 31) and where aquifer support may contribute toward production.

The East Ford unit, like other Delaware sandstone reservoirs, was characterized by relatively high amounts of mobile water at the time of discovery. Primary recovery by solution-gas drive was low, less than 16 percent. Among the reasons for the low primary production are (1) the solution gas:oil ratio of only 400 to 600 scf/bbl, which resulted in limited natural drive energy; (2) the expenditure of considerable solution-gas drive energy in the recovery of water from the reservoir; and (3) the lack of pressure support from the aquifer owing to the limited water influx (W. Flanders, written communication, 1994).

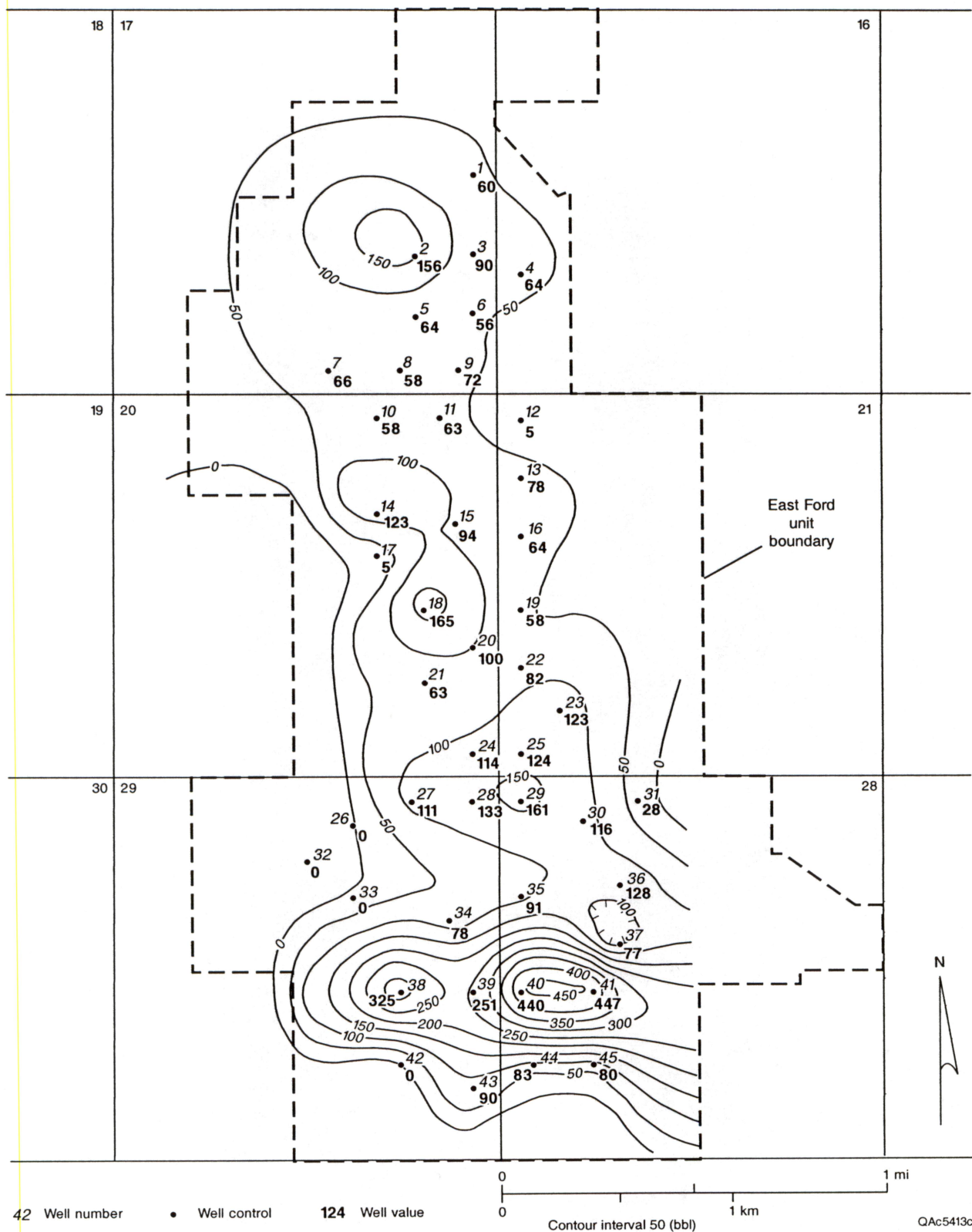


Figure 58. Map of oil produced during initial-potential tests in wells of the East Ford unit.

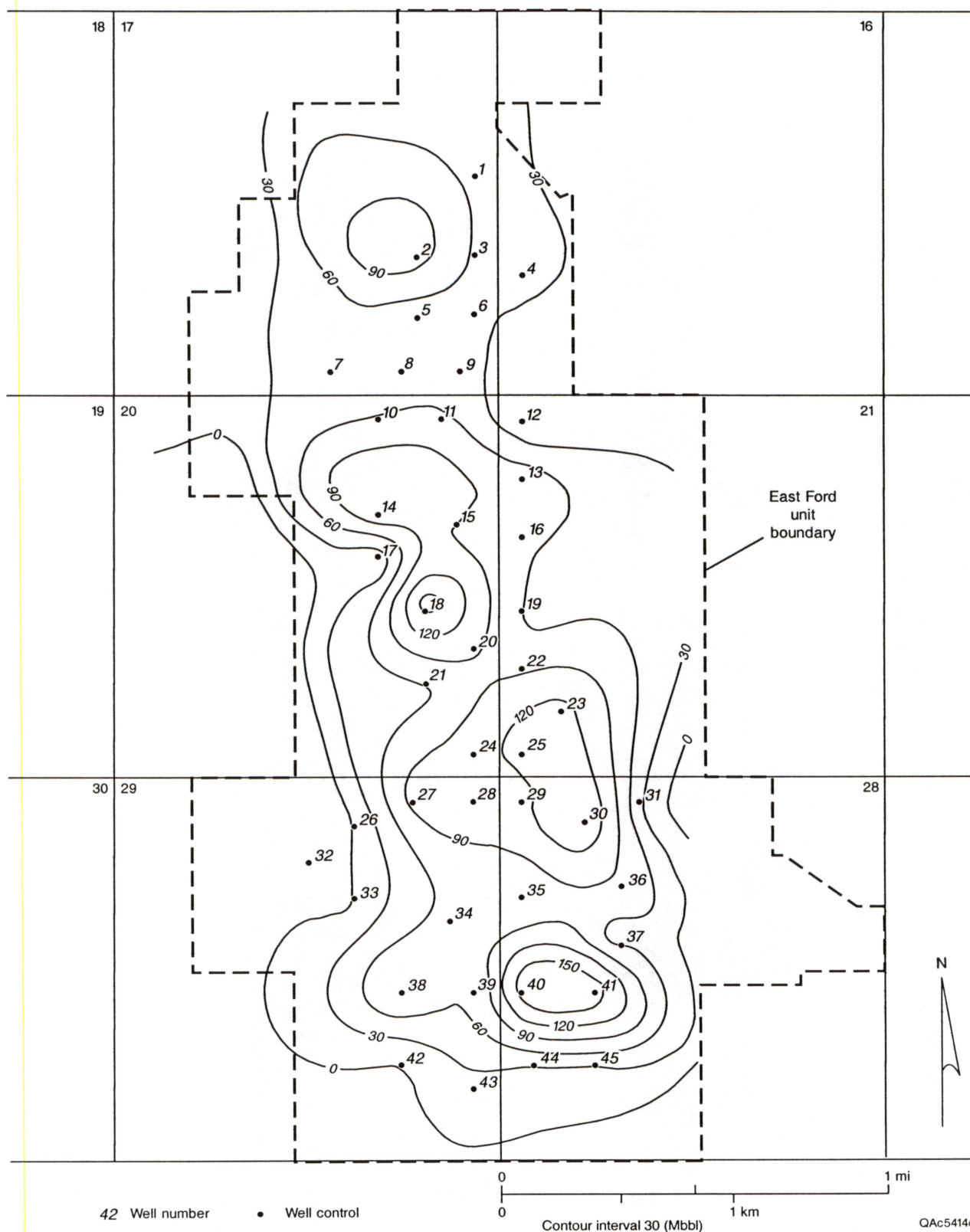


Figure 59. Map of primary oil production from the Ramsey sandstone in East Ford field. Production from each lease was apportioned among the wells on the lease according to the volume of oil produced during initial-potential tests.

Secondary Recovery

The East Ford unit did not undergo secondary recovery by waterflooding. In Ramsey sandstone reservoirs in other fields, waterflooding has not been very successful. In the Ford Geraldine unit, waterflooding added only about 4 percent of the OOIP to the total recovery by the end of secondary development (Pittaway and Rosato, 1991). Low secondary recovery is not unique to the Ford Geraldine unit; secondary recovery from Twofreds field was only 4 percent (Kirkpatrick and others, 1985; Flanders and DePauw, 1993). Waterflood recoveries in Ramsey sandstones have been low because of poor sweep efficiency caused by (1) abundant mobile water present when the waterflood was started and (2) water injection above the formation parting pressure (W. Flanders, written communication, 1994).

Volumetrics

To calculate OOIP and remaining oil in place (ROIP) in the East Ford unit after primary production, the $S_o \times \phi \times H$ map (fig. 47) was divided into 50-ft \times 50-ft grid blocks, and the volume of oil in each grid block was summed. The 1,212 acres of the East Ford unit contained an estimated 18,445,101 bbl of OOIP (table 4). The lease outlines were then superimposed on the $S_o \times \phi \times H$ map to calculate OOIP in each lease (fig. 60) (Dutton and others, 1999c). Primary production was known for each lease, so ROIP was calculated by subtracting primary production from OOIP (table 4). The percentage of OOIP remaining in most leases is about 82 to 89 percent (table 4), but leases 6, 9, and 11 apparently contain lower percentages of ROIP, from 65 to 78 percent. The lower values may reflect additional oil production from the oil–water transition zone to the east of these leases, making it appear that they have produced a higher percentage of their OOIP, whereas it actually reflects oil entering the leases from the east by aquifer support.

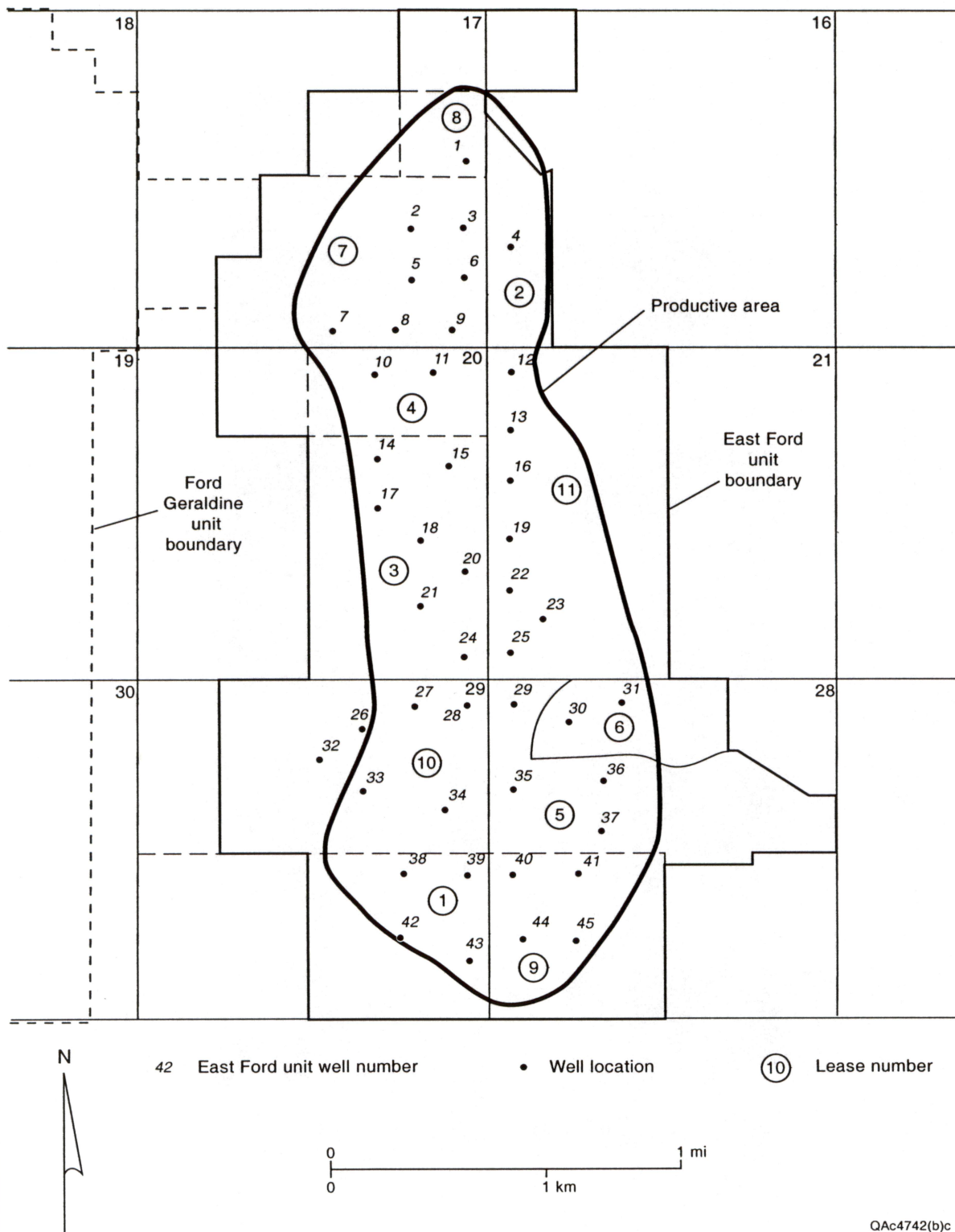


Figure 60. Outline of the producing area of the East Ford unit and individual leases.

Table 4. Volume of original oil in place in the East Ford Unit. Oil volumes are in stock tank barrels (STB).

Lease no.	Area (acres)	OOIP (STB)	Primary prod. (STB)	ROIP (STB)	ROIP/OOIP (percent)
1	84	1,307,025	186,139	1,120,886	86
2	74	361,882	40,344	321,538	89
3	175	3,484,483	624,571	2,859,912	82
4	83	1,013,064	127,724	885,340	87
5	122	2,579,520	306,884	2,272,636	88
6	50	614,927	183,070	431,857	70
7	155	2,249,600	366,758	1,882,842	84
8	41	777,984	47,968	730,016	94
9	95	1,117,527	391,649	725,878	65
10	137	2,395,441	382,081	2,013,360	84
11	197	2,543,647	552,467	1,991,180	78
Total unit	1212	18,445,101	3,209,655	15,235,446	82

The area influenced by the CO₂ flood is smaller than the total productive area of the East Ford unit. A streamline model developed to determine the optimal injection pattern for the East Ford unit (W. A. Flanders, Transpetco Engineering, written communication, 1994) was used to estimate the size of the CO₂ flood area as 842 acres (fig. 61). The outline of the flooded area was superimposed on the $S_o \times \phi \times H$ map to calculate the OOIP of 14.7 MMbbl (table 5). Although the area of the CO₂ flood is only 69 percent of the total producing area, it contained 80 percent of the OOIP in the unit.

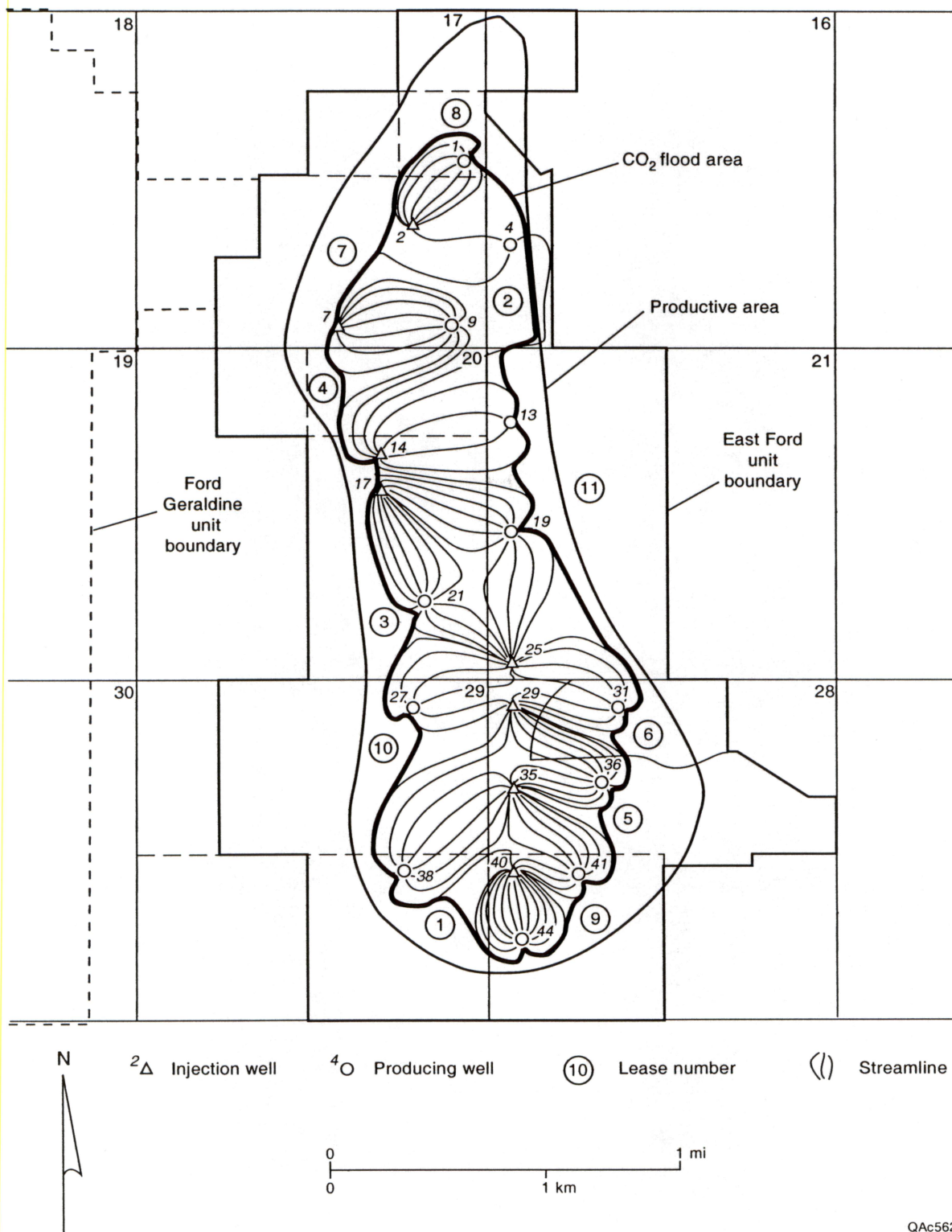
The size of the flooded area within each lease and the OOIP in the flooded area were estimated from the streamline and $S_o \times \phi \times H$ maps (table 5). To estimate primary production from the flooded area of the lease, primary production from each lease was multiplied by the ratio of OOIP in the flooded area to OOIP in the total lease (table 5). ROIP was then calculated by subtracting primary production from the flooded area from the OOIP in the flooded area (table 5). The average percentage of ROIP after primary production in the areas of the leases that would be flooded was 83 percent (table 5). The 12.2 MMbbl of ROIP in the CO₂ flood area represents the target for tertiary recovery.

CO₂ FLOOD OF EAST FORD UNIT

Results

The CO₂ flood of the East Ford unit began in July 1995 with eight injector wells. In the north part of the unit the injectors were positioned on the west side, but to the south the injectors were located centrally (fig. 62a). The number of active wells in the unit was minimized to reduce costs. The unit currently has 7 injectors and 15 producers (fig. 21).

Average bottom-hole pressure in the unit at the start of the project was 723 psi, whereas minimum miscibility pressure is 900 psi. Somewhat higher pressure occurred around wells 7, 12, 36, and 37 (fig. 62a). The low pressure in the East Ford unit at the



QAc5629c

Figure 61. Outline of the CO₂ flood area within the East Ford unit, superimposed on a streamline-pattern model of the flood.

Table 5. Volume of original oil in place in the CO₂ flood area within the East Ford Unit. Oil volumes are in stock tank barrels (STB).

Lease no.	Area (acres)	OOIP (STB)	Primary prod. (STB)	ROIP (STB)	ROIP/OOIP (percent)
1	55	1,120,062	159,513	960,549	86
2	40	153,690	17,134	136,556	89
3	169	3,402,474	609,871	2,792,602	82
4	83	1,017,090	128,232	888,858	87
5	82	2,054,109	244,376	1,809,732	88
6	28	430,576	128,187	302,389	70
7	123	1,811,034	295,257	1,515,776	84
8	13	276,153	17,027	259,127	94
9	38	771,981	270,549	501,432	65
10	120	2,304,745	367,615	1,937,130	84
11	91	1,400,226	304,122	1,096,104	78
Total area	842	14,742,138	2,541,882	12,200,256	83

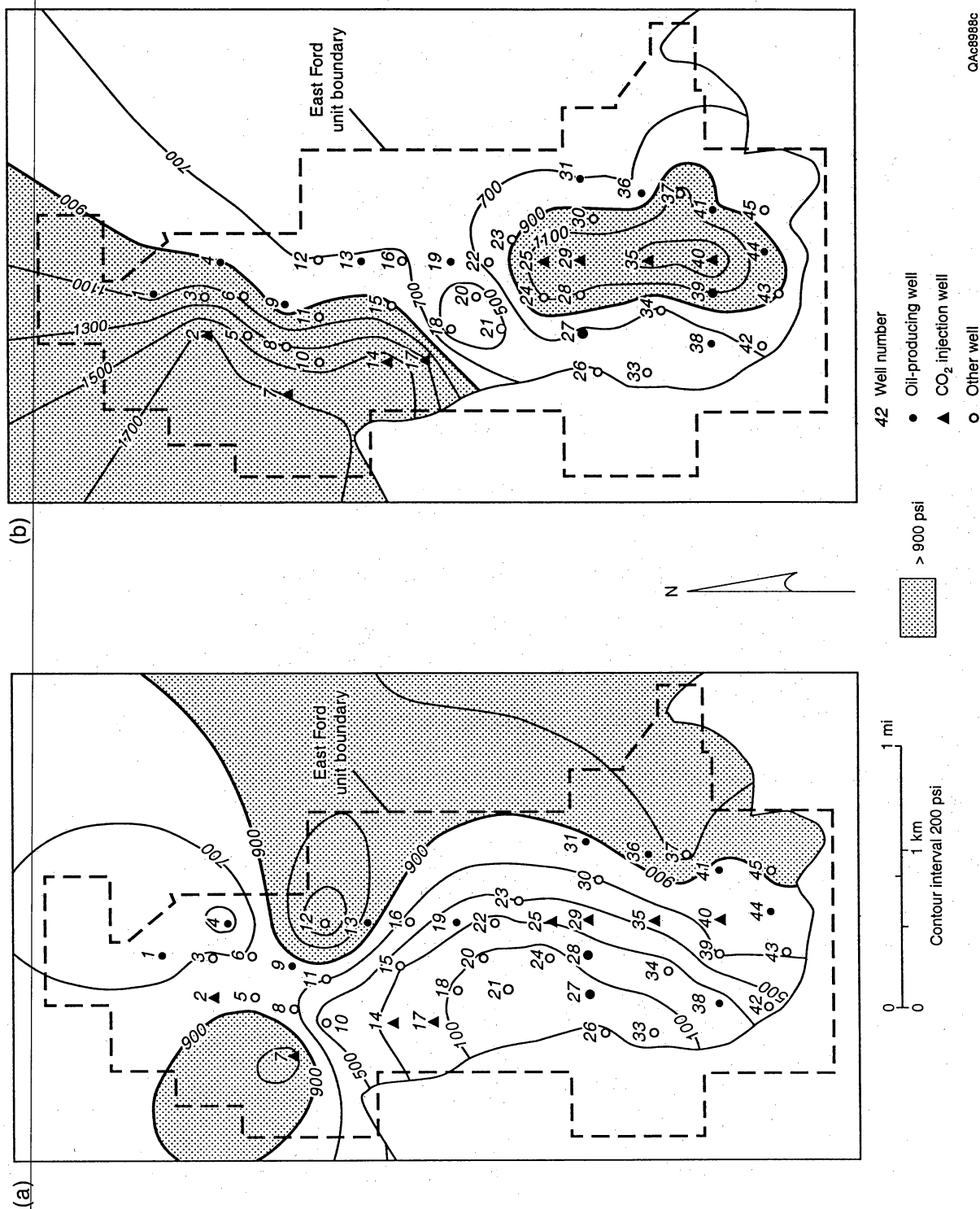


Figure 62. Bottom-hole pressure in the East Ford unit in (a) July 1995 and (b) January 1999. Miscibility pressure is 900 psi.

start of the CO₂ flood, combined with the low reservoir temperature of 83°F, meant that CO₂ would exist as both vapor and liquid phases under these conditions. Response to CO₂ injection in the field may have been delayed as a result. At these low temperatures and pressures, liquid CO₂ can occur on both the injection side as well as the production side. For comparison, CO₂ injected in the Ford Geraldine unit was entirely in the vapor phase at the temperature and pressure conditions in that unit. The higher pressure in the Ford Geraldine unit resulted from repressuring by a waterflood prior to CO₂ flooding.

The first response to the CO₂ flood was observed in April 1996 in well EFU No. 28, and major production response in the unit began in December 1997 (fig. 63). The production rate in May 2001 in the East Ford unit was 185 bopd, 345 barrels of water per day (bwpd), and 1.7 MMcf/d of gas (hydrocarbon gases and CO₂) (table 6, fig. 64). Cumulative production through May 2001 was 180,097 stock tank barrels of oil, 518,000 bbl of water, and 1,344 MMcf of gas (table 6). Most of the produced gas and water are reinjected. Injection rates in May 2001 were 3,100 Mcf/d of purchased CO₂, 1,425 Mcf/d of recycled CO₂, and 375 bwpd (table 6, fig. 65). Cumulative injection through May 2001 was 9,057 MMcf of purchased CO₂, 1,075 MMcf of recycled CO₂, and 670,000 bbl of water (table 6). As a result of the CO₂ flood, production from the East Ford unit increased from 30 bbl/d at the end of primary production to 185 bbl/d in 2001. The unit has produced 180,097 bbl of oil from the start of tertiary recovery through May 2001, and total production in 2000 was 62,190 bbl.

Production during 1994, the last full year of primary production, was 9,734 bbl. The primary production decline rate, calculated by using an exponential least-squares fit of the production data from April 1991 through September 1994, was 10.1 percent (from "Application for an EOR Positive Production Response Certification for the East Ford Unit," form H-13, filed by Orla Petco, Inc., with the Railroad Commission of Texas, March 1998; application was approved in June 1998). At that rate of decline, the economic limit of the field would have been reached within the next few years if the CO₂

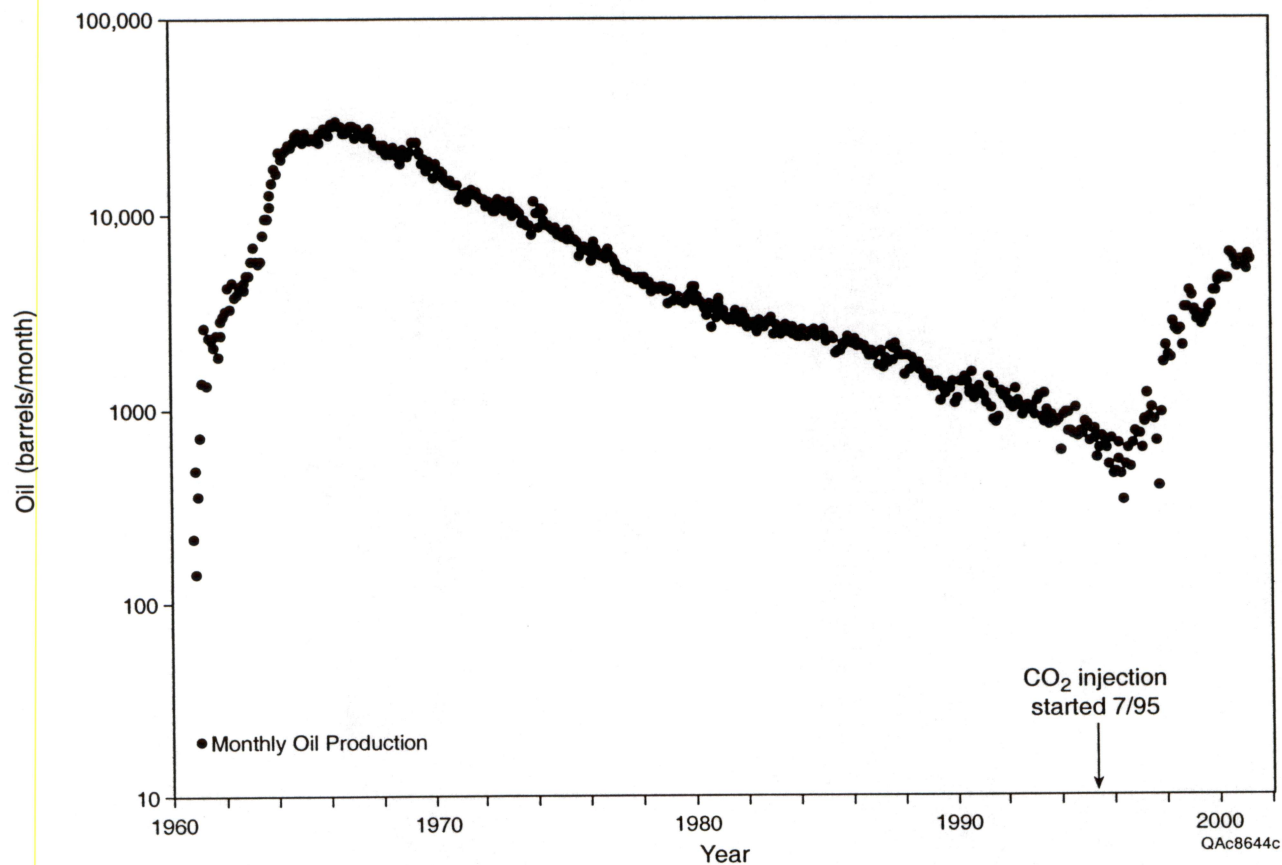


Figure 63. Plot of monthly oil production from the East Ford unit since the field was discovered in 1960. The field was on primary production until a CO₂ flood was begun in July 1995.

Table 6. Injection and production data from East Ford CO₂ flood.

Production

Current production rate (May 2001)

Oil (bopd)	185
Water (bwpd)	345
Gas (MMcf/d)	1.70

Cumulative production (through May 2001)

Oil (STB)	180,097
Water (bbl)	518,000
Gas (MMcf)	1,344

Injection

Current injection rate (May 2001)

Purchased CO ₂ (MMcf/d)	3,100
Recycled CO ₂ (MMcf/d)	1,425
Water (bwpd)	375

Cumulative injection (through May 2001)

Purchased CO ₂ (MMcf)	9,057
Recycled CO ₂ (MMcf)	1,075
Water (bbl)	670,000

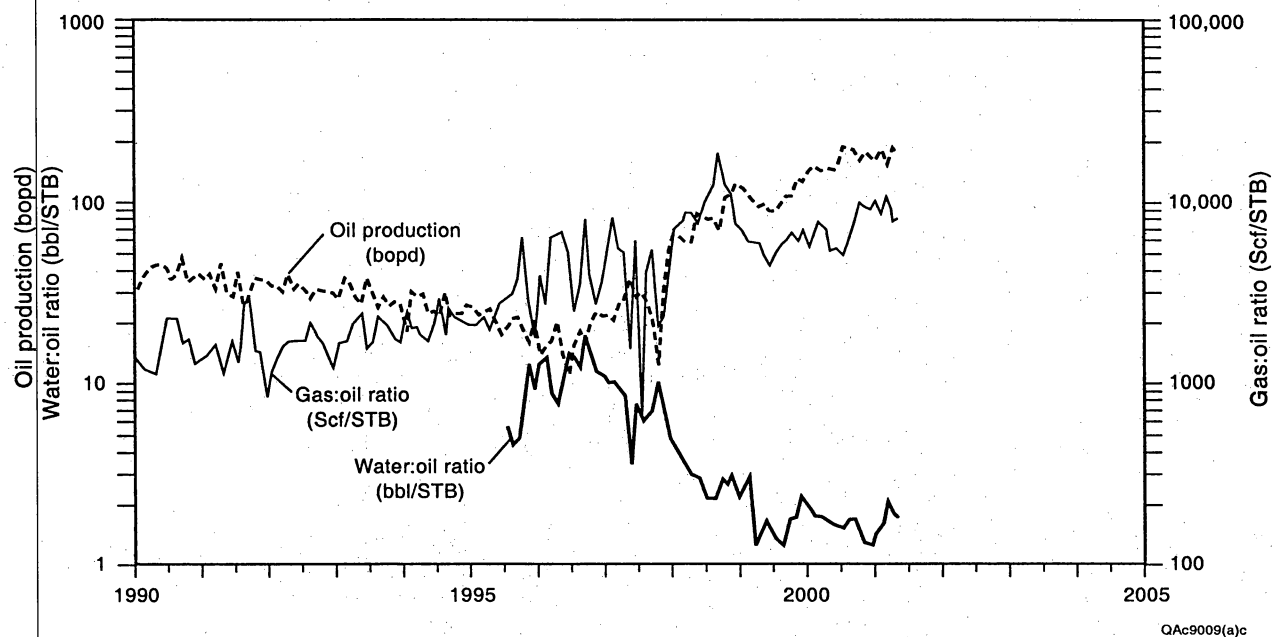


Figure 64. Plot of oil production, water:oil ratio (WOR), and gas:oil ratio (GOR) in the East Ford unit since 1990.

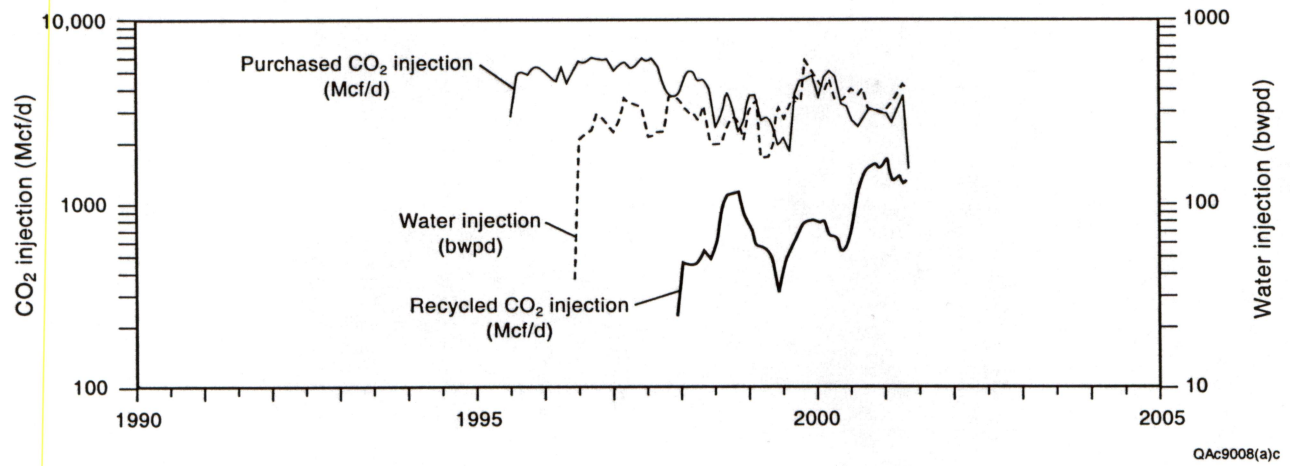


Figure 65. Plot of gas and water injection in the East Ford unit since 1995.

flood had not started. Essentially all the production since the start of the CO₂ flood—180,097 bbl through May 2001—can thus be attributed to the EOR project.

The CO₂ flood has increased production from the East Ford unit substantially, but several production abnormalities have been observed: (1) low pressure in the center of the field, (2) low production rates, (3) severe reduction in transmissibility indicated by a bottom-hole pressure-buildup test, and (4) low gas production rates in key wells. Some of these abnormalities may be caused by mechanical problems, but others may result from the effect of geologic heterogeneity in the field.

Although pressure at the north and south ends of the field has increased during CO₂ injection, low pressure has persisted in the center of the field (fig. 62b). The pressure data were collected in wells used as observation wells (fig. 21); injection wells were shut in for 48 h, and the decline in pressure was observed. The pressure distribution suggests that communication is poor between wells in the center of the field (EFU 18, 19, 20, and 21) and the nearest injectors (EFU 14 and 25) (figs. 21, 62b).

The production rate in some wells, including EFU 3 and 4 (fig. 21), is lower than would be expected from their initial potential. For example, well 4 made 106 bbl of liquids (oil + water) per day (blpd) during initial-potential tests, so the current production of about 20 blpd is surprisingly low. In addition, gas production from EFU 4 has leveled off. Well EFU 3 has a similarly low production rate of 10 blpd (whereas it flowed 110 blpd during the initial-potential test), and pressure in the well now is >1,200 psi. Gas production from EFU 3 is also low, even though the well is close to the injector EFU 2.

Influence of Geologic Heterogeneity on East Ford Production

Oil recovery has been improved by the CO₂ flood, but not as much as had been expected. Production abnormalities, such as those listed earlier, may indicate that geologic heterogeneities are affecting reservoir displacement operations. In many cases there seem to be restrictions between injector and producer wells that are causing production to be lower than expected, and these restrictions may be caused by depositional and diagenetic heterogeneities.

The East Ford unit appears to be divided into three areas of better interwell communication (fig. 66); communication between wells in different areas is restricted. The areas may result from facies changes, subtle structural or bathymetric controls on deposition, or variations in sediment transport direction. The three areas are shown in figure 66, superimposed on an isopach map of the total Ramsey sandstone interval.

North Part of East Ford Unit

The area at the north end of the unit contains three injector wells located along the west side of the area (EFU 2, 7, and 14) and seven producers (EFU 1, 3, 4, 9, 10, 13 and 17) (fig. 66). In this part of the field, the Ramsey 2 sandstone is the main target (fig. 32). The Ramsey 1 sandstone is thin in EFU 7 and not present in EFU 10 (fig. 31). EFU 2 was deepened into the Ramsey 1 sandstone, but the bottom of the well filled in with sand and injection pressure went up, indicating that CO₂ is not going into the Ramsey 1 sandstone. Although the well has been cleaned out, it is too early to determine the results.

EFU 1 has responded well to the flood and is one of the better wells in the field, producing about 26 bopd in March 2000 (fig. 67a). The 40-percent net:gross sandstone value for the Ramsey 2 in this well (fig. 49) is surprisingly low and is based on gamma-ray log values that calculated 14.5 ft of sandstone (out of 24 ft gross sandstone) having $V_{cl} > 15$ percent. Core-analysis data from this well showed that 18 ft of the Ramsey 2

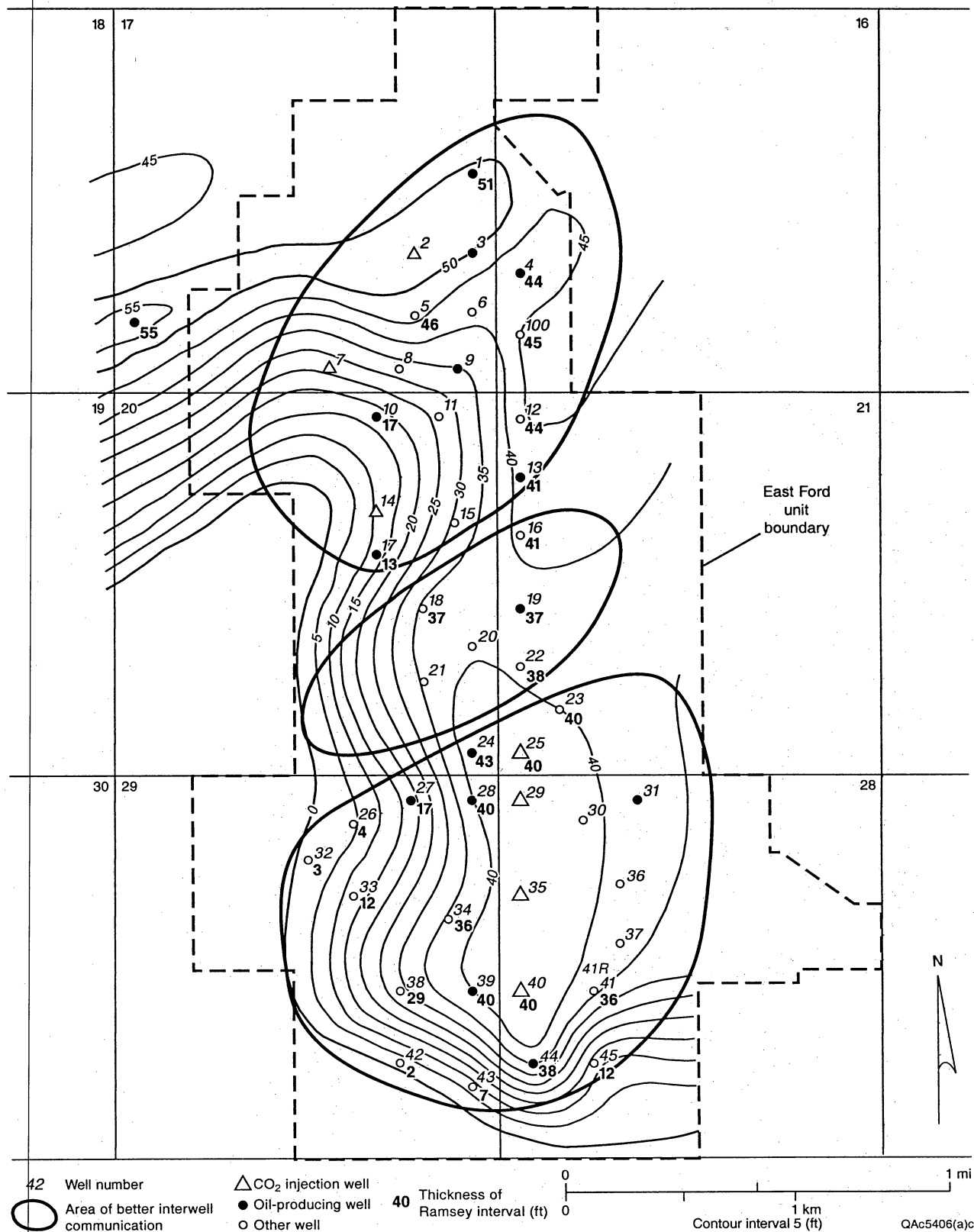


Figure 66. Outlines of the three areas of better interwell communication within the East Ford unit; communication between wells in different areas is restricted. The outlines are superimposed on a map of thickness of the total Ramsey sandstone interval, from the base of the Trap siltstone to the top of the Ford siltstone.

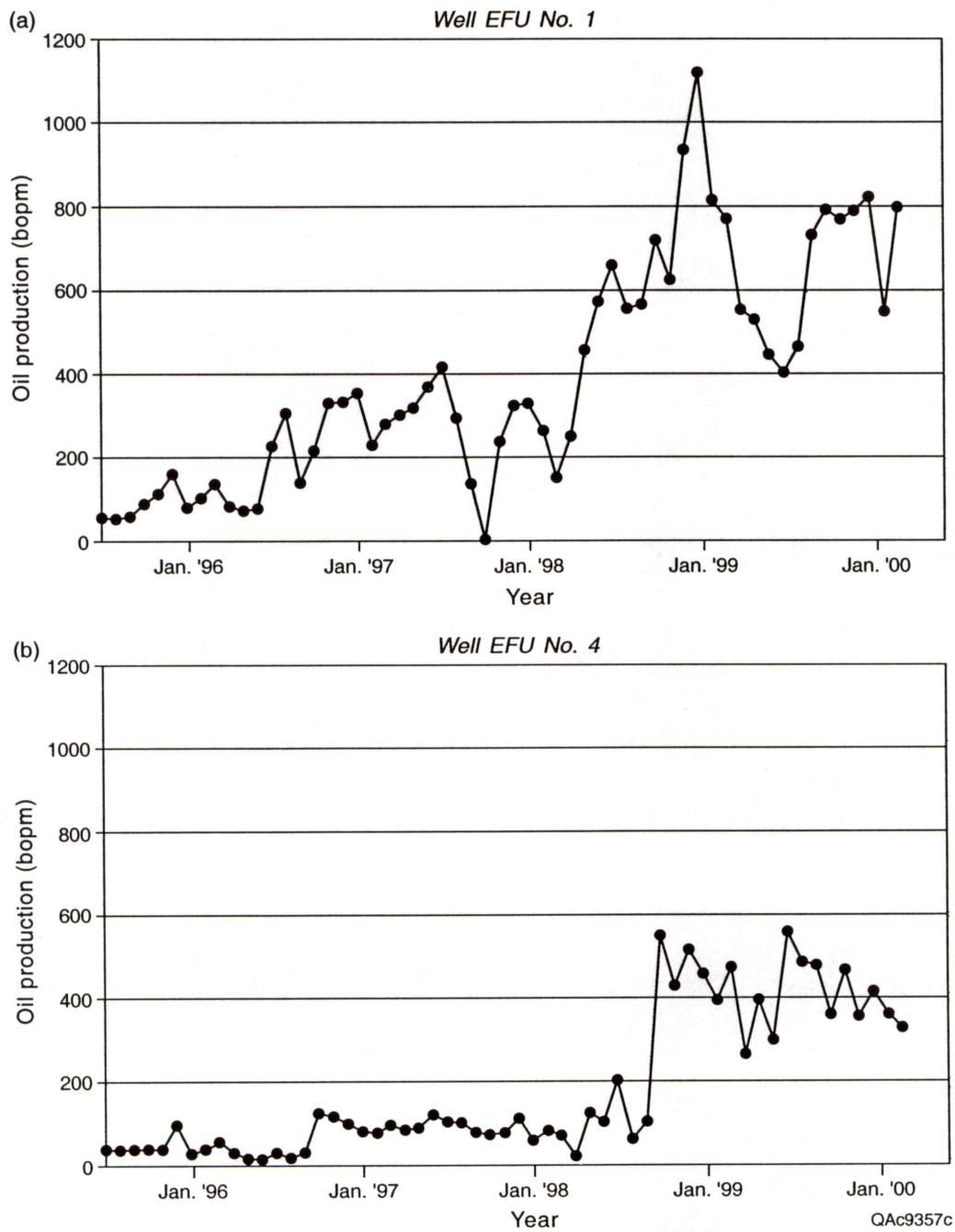


Figure 67. Plots of oil production from the (a) EFU 1 and (b) EFU 4 wells.

sandstone has permeability >10 md and porosity >17.5 percent, so a net:gross sandstone value of 75 percent might be more accurate.

Production from EFU 4 is lower, about 15 bopd (fig. 67b). One possible explanation for the lower production is that a barrier may restrict communication between this producing well and EFU 2. Geologic interpretations suggest the presence of a channel-levee boundary between wells 2 and 4 in the Ramsey 2 sandstone.

EFU 10, which is interpreted to be in the same overbank-splay sandstone as injector EFU 7 (fig. 32), is a moderately good well, producing about 19 bopd in March 2000. EFU 9 is a poor well, even though it is located in the thickest part of the Ramsey 2 sandstone. The presence of a levee between injector well 7 and producer well 9 may explain the poor response of well 9. However, EFU 9 has a shallow casing leak and mechanical problems, so it may be replaced by EFU 8.

Wells 14 and 17 are interpreted as being in a different splay sandstone that is not in pressure communication with the splay to the north (fig. 32). Communication between wells in this southern splay and wells in the channel also appears to be restricted by levee deposits. Well 17 was converted from an injector to a producing well, and wells 14 and 17 apparently penetrate the same splay. The depositional model suggests that each separate splay sandstone, as well as the channel sandstone, must contain both injector and producer wells to be produced effectively.

Locating a new injector in a north-south orientation with the existing producers, following the channel trend, might improve recovery from the thick Ramsey 2 channel sandstones in this north area. EFU 6 could be converted into an injector and increase the response of EFU 9; both of these wells are in the thickest part of the Ramsey 2 sandstone channel.

Middle Part of East Ford Unit

Both Ramsey 1 and 2 sandstones are targets in this part of the unit. The pressure response in the middle part of the unit has been slow during the CO₂ flood (fig. 62b), suggesting that this area is in poor communication with injector EFU 14 (and EFU 17 when it was an injector) to the north and EFU 25 to the south. The south boundary of the central area is quite sharp and can be delineated easily by the high pressure in EFU 24, which is in the south part of the unit. The bottom-hole pressure in EFU 24 was 1,246 psi on June 14, 2000.

No injectors are located in this area, and well 19 is the only producer (fig. 66). EFU 19 is not responding to injection in EFU 14 or 25; production during March 2000 was only 4 bopd.

Communication between EFU 25 and 19 may be limited in the Ramsey 1 sandstone because the channel apparently makes a large bend to the east in this part of the field (fig. 31). The Ramsey 1 sandstone is thinner in EFU 19 (fig. 31), net:gross sandstone is lower than in the wells to the north and south (fig. 48), and the percentage of calcite-cemented sandstone is higher (fig. 52). All these factors may restrict communication between EFU 19 and 25.

Adding an injector well to this area, such as EFU 20, and making EFU 18, 21, and 22 producers may improve production from this apparently isolated area. One approach would be first to inject water into the Ramsey 2 sandstone in EFU 20 and then to see whether the pressure increases in the surrounding wells. If it does, EFU 20 could be deepened into the Ramsey 1 sandstone and converted to a CO₂ injector.

South Part of East Ford Unit

The south area of the field is mostly in the lobe facies of the Ramsey 1 sandstone (fig. 31), but lobe deposits of the Ramsey 2 sandstone probably also contribute to

production. This area is responding well to the existing north-south line of injectors EFU 25, 29, 35, and 40; current producers are EFU 24, 27, 28, 31, 39, 41R, and 44. Wells EFU 27, 28, and 31 are among the best wells in the field. Recovery in this area is interpreted to be good because the lobe sandstones are less laterally heterogeneous than are the channel-levee and splay sandstones to the north.

Recovery might be improved by bringing on additional producers; this could be accomplished by overcoming mechanical problems with some of the shut-in wells. EFU 31 was not responding well, so it was refractured. Production increased but then fell off quickly. It was determined that there was a problem with the pump, which has since been replaced, and production has improved. Well 36 is shut in because of a casing leak and could be brought on line as a producer when the leak is fixed. Well 34 needs to have injected water produced back, and EFU 39 needs to be fractured in the Ramsey 1 sandstone.

TECHNOLOGY TRANSFER ACTIVITIES

This project has demonstrated that (1) enhanced oil recovery by CO₂ flood can increase production from slope and basin clastic reservoirs of the Delaware Mountain Group, and (2) reservoir characterization can improve EOR projects. Slope and basin clastic reservoirs in sandstones of the Delaware Mountain Group in the Delaware Basin of West Texas and New Mexico contained more than 1.8 billion barrels (Bbbl) of oil at discovery. Recovery efficiencies of these reservoirs have averaged less than 20 percent since production began in the 1920's, and, therefore, a substantial amount of the original oil in place remains unproduced. Many of these mature fields are nearing the end of primary or secondary production and are in danger of abandonment unless effective, economic methods of enhanced oil recovery (EOR) can be implemented. For this reason, a key component of this project has been technology transfer of the project results and

methodologies to operators of Delaware Basin reservoirs. The results are also broadly applicable to slope and basin clastic reservoirs across the United States.

Through the course of this study, 29 presentations have been made at regional or national meetings of geological and engineering professional societies and at universities (app. 1). Results have been widely distributed in 33 publications, including articles, abstracts, and major contract reports (app. 2). Three workshops, a field trip, and a project Web site (http://www.utexas.edu/research/beg/delaware_project) presented study results directly to operators (app. 3).

Presentations

Oral and poster presentations of project methods and results at regional and national technical conferences and universities are one way to transfer information quickly, as soon as it becomes available, to operators of slope and basin clastic reservoirs. Project scientists and engineers have provided 29 such presentations over the life of the project (app. 1). Audiences at presentations to technical societies have ranged from 50 senior independent operators at the smaller, monthly society meetings to hundreds of geoscientists and engineers at the larger, annual meetings. All presentations received positive audience response, and two presentations received Best Paper Awards. The paper "Petrophysics of the Ramsey Sandstone, Ford Geraldine Unit, Reeves and Culberson Counties, Texas," presented by Dr. George B. Asquith at the 1997 Fall Symposium of the West Texas Geological Society, in Midland, Texas received the WTGS Best Paper Award. The paper "Characterization of reservoir heterogeneity in slope and basin clastic reservoirs, Bell Canyon Formation, Delaware Basin, Texas," presented by Dr. Shirley P. Dutton at the 2000 Annual Meeting of the Southwest Section of the American Association of Petroleum Geologists (AAPG) in Midland, Texas received the A. I. Levorsen Memorial Award from AAPG for the best paper presented at the meeting.

Publications

In addition to presentations, project results have been published in several forms to provide a more permanent and widely circulated documentation of ways to increase production from mature slope and basin clastic reservoirs. Articles in transactions volumes for meetings where presentations have been made provide details and figures so that attendees and those unable to attend can fully comprehend the methods and results developed during the project. Abstracts in convention volumes can entice operators to presentations and provide summaries for those unable to attend. In-depth information on project details and results has been presented in quarterly, annual, and topical project reports to the DOE, and project results were highlighted in the Summer 1999 edition of the DOE publication *The Class Act*.

Appendix 2 lists all publications produced by this project. Twelve full-length articles have been published: one Report of Investigations published by the Bureau of Economic Geology, three papers in the Transactions volume of the 1997 West Texas Geology Society Fall Symposium, two papers in the Transactions volumes of the 2000 and 2001 Southwest Section of the AAPG, one paper in the Transactions volume of the 1998 Society of Petroleum Engineers Permian Basin Oil and Gas Recovery Conference, and two papers in the Transactions volume of a special Gulf Coast Section SEPM research conference on Advanced Reservoir Characterization. In addition, an article was published in the Proceedings of the 1999 Oil & Gas Conference on Technology Options for Producer Survival, sponsored by DOE. A total of 12 abstracts have been published in convention volumes, including volumes accompanying the 1997, 1998, 1999, and 2001 national AAPG meetings. Project reports to DOE have included six annual reports, two topical reports (one focused on the Ford Geraldine unit and one on the East Ford unit), and this final report.

Workshops

Workshops provide an opportunity to meet and train operators who are interested in applying the methods and results developed in this project to their reservoirs. It is a forum for providing detailed information and conducting question-and-answer sessions, thus ensuring a deeper understanding of the information presented. Three workshops and a 2-day field trip associated with one of the workshops were held during the project (app. 3). Attendees at each of these workshops were provided course notebooks containing figures and text for annotation and future reference. The guidebook provided to the field-trip participants contains geological background and data (maps, photographs, measured sections, and cross sections) and discussions relevant to each field-trip stop.

The first workshop, held in Midland, Texas, on March 25, 1997, at the Midland Convention Center, was hosted by the West Texas Geological Society. The second workshop took place at the Stevens Motel in Carlsbad, New Mexico, on November 21, 1997. All of the participants in this workshop also attended the field trip on November 22–23 to outcrops of the Bell Canyon sandstone. The final workshop, which focused on the results of the CO₂ flood of the East Ford unit, was held in Midland on May 2, 2000. This workshop was sponsored by the Permian Basin Petroleum Association.

CONCLUSIONS

This project has demonstrated that (1) enhanced oil recovery by CO₂ flood can increase production from slope and basin clastic reservoirs of the Delaware Mountain Group and (2) reservoir characterization can improve EOR projects. CO₂ injection in the East Ford unit began in July 1995, and production response was observed in December 1997. As a result of the CO₂ flood, production from the East Ford unit increased from 30 bbl/d at the end of primary production to more than 185 bbl/d in 2001. The unit has produced 180,097 bbl of oil from the start of tertiary recovery through May 2001, and

total production in 2000 was 62,190 bbl. Essentially all the production since the start of the CO₂ flood—180,097 bbl through May 2001—can be attributed to the EOR project.

Geologic heterogeneities appear to influence response to the CO₂ flood in the East Ford unit. The upper and lower Ramsey sandstones were deposited in a channel-levee system that terminated in broad lobes; overbank splays filled topographically low interchannel areas. CO₂ injector wells in splay sandstones apparently have poor communication with wells in channel sandstones, perhaps because communication is restricted through levee deposits. Diagenetic heterogeneity may also influence fluid-displacement operations by trapping CO₂ below low-permeability, calcite-cemented layers that can form significant vertical permeability baffles in a reservoir.

The East Ford unit appears to be divided into three areas of better interwell communication; communication between wells in different areas is restricted. The areas may result from facies changes, subtle structural or bathymetric controls on deposition, or variations in sediment transport direction. Modification of the existing east-west alignment of injectors and producers at the north end of the unit may overcome the problem of apparently restricted communication between splay sandstones and channel sandstones. Pressure response in the central area of the unit has been slow, suggesting that communication is restricted between the wells in this area and the injectors that are located in the north and south parts of the unit. Adding an injector in the central area may overcome this problem. The south area of the unit is responding well to the existing north-south line of injectors. Recovery might be improved in this area by bringing on additional producers; this could be accomplished by overcoming mechanical problems with some of the shut-in wells.

- Galloway, W. E., and Hobday, D. K., 1996, Terrigenous clastic depositional systems: applications to fossil fuel and groundwater resources, 2d ed.: New York, Springer-Verlag, 489 p.
- Gardner, M. H., 1992, Sequence stratigraphy of eolian-derived turbidites: patterns of deep water sedimentation along an arid carbonate platform, Permian (Guadalupian) Delaware Mountain Group, West Texas, *in* Mruk, D. H., and Curran, B. C., eds., Permian Basin exploration and production strategies: applications of sequence stratigraphic and reservoir characterization concepts: West Texas Geological Society Publication 92-91, p. 7–12.
- Gardner, M. H., 1997a, Characterization of deep-water siliciclastic reservoirs in the upper Bell Canyon and Cherry Canyon Formations of the northern Delaware Basin, Culberson and Reeves Counties, Texas, *in* Major, R. P., ed., Oil and gas on Texas State Lands: an assessment of the resource and characterization of type reservoirs: The University of Texas, Bureau of Economic Geology Report of Investigations No. 241, p. 137–146.
- Gardner, M. H., 1997b, Sequence stratigraphy and hydrocarbon habitat of the Permian (Guadalupian) Delaware Mountain Group, Delaware Basin, West Texas, *in* Major, R. P., ed., Oil and gas on Texas State Lands: an assessment of the resource and characterization of type reservoirs: The University of Texas, Bureau of Economic Geology Report of Investigations No. 241, p. 147–157.
- Grant, P. R., Jr., and Foster, R. W., 1989, Future petroleum provinces in New Mexico—discovering new reserves: New Mexico Bureau of Mines & Mineral Resources, 94 p.
- Green, K. M., Frailey, S. M., and Asquith, G. B., 1996, Water-flood feasibility study of the Brushy Canyon K-2 zone Red Tank field, Lea County, New Mexico, *in* DeMis,

- W. D., and Cole, A. G., eds., The Brushy Canyon play in outcrop and subsurface: concepts and examples: Permian Basin Section, SEPM, Publication No. 96-38, p. 165–171.
- Hays, P. D., and Tieh, T. T., 1992, Organic geochemistry and diagenesis of the Delaware Mountain Group, West Texas and southeast New Mexico: American Association of Petroleum Geologists Southwest Section, Publication SWS 92–90, p. 155–175.
- Hills, J. M., 1984, Sedimentation, tectonism, and hydrocarbon generation in Delaware Basin, west Texas and southeastern New Mexico: American Association of Petroleum Geologists Bulletin, v. 68, p. 250–267.
- Jacka, A. D., 1979, Deposition and entrapment of hydrocarbons in Bell Canyon and Cherry Canyon deep-sea fans of the Delaware Basin, *in* Sullivan, N. M., ed., Guadalupian Delaware Mountain Group of West Texas and Southeast New Mexico: Society of Economic Paleontologists and Mineralogists (Permian Basin Section) Publication 79-18, p. 104–120.
- Jacka, A. D., Beck, R. H., St. Germain, L. C., and Harrison, S. C., 1968, Permian deep-sea fans of the Delaware Mountain Group (Guadalupian), Delaware Basin, *in* Guadalupian facies, Apache Mountain area, west Texas: Society of Economic Paleontologists and Mineralogists (Permian Basin Section) Publication 68-11, p. 49–90.
- Kerans, Charles, and Fitchen, W. M., 1995, Sequence hierarchy and facies architecture of a carbonate-ramp system: San Andres Formation of Algerita Escarpment and western Guadalupe Mountains, West Texas and New Mexico: The University of Texas at Austin, Bureau of Economic Geology Report of Investigations No. 235, 86 p.

- Kerans, Charles, Fitchen, W. M., Gardner, M. H., Sonnenfeld, M. D., Tinker, S. W., and Wardlaw, B. R., 1992, Styles of sequence development within uppermost Leonardian through Guadalupian strata of the Guadalupe Mountains, Texas and New Mexico, *in* Mruk, D. H., and Curran, B. C., eds., Permian Basin exploration and production strategies: applications of sequence stratigraphic and reservoir characterization concepts: West Texas Geological Society Publication 92-91, p. 1–6.
- Khan, S. A., 1992, An expert system to aid in compositional simulation of miscible gas flooding: The University of Texas at Austin, Ph.D. dissertation, 470 p.
- Kirkpatrick, R. K., Flanders, W. A., and DePauw, R. M., 1985, Performance of the Twofreds CO₂ injection project: Proceedings, 1985 SPE Annual Technical Conference: Society of Petroleum Engineers, Paper 14439.
- Kosters, E. C., and others, 1989, Atlas of major Texas gas reservoirs: The University of Texas at Austin, Bureau of Economic Geology Special Publication, 161 p.
- Lewis, Paul, Cross, Scott, and Hoose, Gary, 1996, Delaware Mountain Group production map, *in* DeMis, W. D., and Cole, A. G., eds., The Brushy Canyon play in outcrop and subsurface: concepts and examples: Permian Basin Section SEPM, Publication No. 96-38, separate map in back pocket.
- Linn, A. M., 1985, Depositional environment and hydrodynamic flow in Guadalupian Cherry Canyon Sandstone, West Ford and West Geraldine fields, Delaware Basin, Texas: Texas A&M University, Master's thesis, 152 p.
- Lowe, D. R., 1982, Sediment gravity flows: II. depositional models with special reference to the deposits of high-density turbidity currents: *Journal of Sedimentary Research*, v. 52, p. 279–297.

- Malik, M. A., 1998, Compositional simulations of a CO₂ flood in Ford Geraldine unit, Texas, *in* Proceedings, SPE Permian Basin Oil and Gas Recovery Conference: Society of Petroleum Engineers, Paper 39794, p. 375–383.
- Meissner, F. F., 1972, Cyclic sedimentation in Middle Permian strata of the Permian Basin, west Texas and New Mexico, *in* Cyclic sedimentation in the Permian Basin, 2d ed.: West Texas Geological Society, p. 203–232.
- Moraes, M. A. S., and Surdam, R. C., 1993, Diagenetic heterogeneity and reservoir quality: fluvial, deltaic, and turbiditic sandstone reservoirs, Potiguar and Reconcavo rift basins, Brazil: American Association of Petroleum Geologists Bulletin, v. 77, p. 1142–1158.
- Payne, M. W., 1973, Basinal sandstone facies of the Delaware Mountain Group, west Texas and southeast New Mexico: Texas A&M University, Ph.D. dissertation, 150 p.
- _____, 1976, Basinal sandstone facies, Delaware Basin, west Texas and southeast New Mexico: American Association of Petroleum Geologists Bulletin, v. 60, p. 517–527.
- Peng, D. Y., and Robinson, D. B., 1976, A new two-constant equation of state: Industrial and Engineering Chemistry Fundamentals, v. 15, p. 59–64.
- Pittaway, K. R., and Rosato, R. J., 1991, The Ford Geraldine unit CO₂ flood—update 1990: Society of Petroleum Engineers Reservoir Engineering, v. 6, no. 4, p. 410–414.
- Ross, C. A., and Ross, J. R. P., 1987, Late Paleozoic sea levels and depositional sequences, *in* Ross, C. A., and Haman, D., eds., Timing and depositional history of

- eustatic sequences: constraints on seismic stratigraphy: Cushman Foundation for Foraminiferal Research, Special Publication 24, p. 137–149.
- Ruggiero, R. W., 1985, Depositional history and performance of a Bell Canyon sandstone reservoir, Ford-Geraldine field, West Texas: The University of Texas at Austin, Master's thesis, 242 p.
- _____ 1993, Depositional history and performance of a Permian Bell Canyon sandstone reservoir, Ford-Geraldine field, West Texas, *in* Rhodes, E. G., and Moslow, T. F., eds., Marine clastic reservoirs: New York, Springer-Verlag, p. 201–229.
- Schlumberger, 1995, Log interpretation charts: Houston, Schlumberger Wireline & Testing, variously paginated.
- Schneider, F. N., 1987, Three procedures enhance relative permeability data: Tulsa, Oil and Gas Journal, March, p. 45–51.
- Silver, B. A., and Todd, R. G., 1969, Permian cyclic strata, northern Midland and Delaware Basins, west Texas and southeastern New Mexico: American Association of Petroleum Geologists Bulletin, v. 53, no. 11, p. 2223–2251.
- Thomerson, M. D., 1992, Petrophysical analysis of the Brushy Canyon Formation, Hat Mesa Delaware field, Lea County, New Mexico: Texas Tech University, Master's thesis, 124 p.
- Walling, S. D., 1992, Authigenic clay minerals in sandstones of the Delaware Mountain Group: Bell Canyon and Cherry Canyon Formations, Waha field, West Texas: Texas A&M University, Master's thesis, 63 p.

- Walker, R. G., 1992, Turbidites and submarine fans, *in* Walker, R. G., and James, N. P., eds., Facies models response to sea level change: Geological Association of Canada, p. 239–263.
- Walling, S. D., Hays, P. D., and Tieh, T. T., 1992, Chlorites in reservoir sandstones of the Guadalupian Delaware Mountain Group: Bell Canyon and Cherry Canyon Formations, Waha field, West Texas: American Association of Petroleum Geologists Southwest Section, Publication SWS 92–90, p. 149–154.
- Williamson, C. R., 1978, Depositional processes, diagenesis and reservoir properties of Permian deep-sea sandstones, Bell Canyon Formation, Texas-New Mexico: The University of Texas at Austin, Ph.D. dissertation, 262 p.
- _____ 1979, Deep sea sedimentation and stratigraphic traps, Bell Canyon Formation (Permian), Delaware basin, *in* Sullivan, N. M., ed., Guadalupian Delaware Mountain Group of west Texas and southeast New Mexico, symposium and field trip conference guidebook: Society of Economic Paleontologists and Mineralogists (Permian Basin Section) Publication 79-18, p. 39–74.

APPENDIX 1: LIST OF PRESENTATIONS PRODUCED
BY BEG CLASS 3 PROJECT

1996

Dutton, S. P., Cole, A. G., and Hovorka, S. D., Application of advanced reservoir characterization, simulation, and production optimization strategies to maximize recovery in slope and basin clastic reservoirs, West Texas (Delaware Basin): poster presentation at DOE workshops on Class II and III Oil Projects at the Center for Energy and Economic Diversification (CEED), Midland, Texas, May 1996.

1997

Asquith, G. B., Petrophysics of the Ramsey Sandstone, Ford Geraldine Unit, Reeves and Culberson Counties, Texas: talk presented at the Permian Basin Well Log Society, Midland, Texas, February 1997.

Asquith, G. B., Petrophysics of submarine-fan sandstones of the Ramsey Sandstone reservoir, Ford Geraldine Unit, Delaware Basin, Texas: talk presented at the Society of Independent Professional Earth Scientists, Austin, Texas, March 1997.

Barton, M. D., Basin floor fan and channel-levee complexes, Permian Bell Canyon Formation: poster presentation at the 1997 Annual Meeting of the American Association of Petroleum Geologists, Dallas, Texas, April 1997.

Cole, A. G., Dutton, S. P., Barton, M. D., Hovorka, S. D., and Asquith, G. B., 1997, Geophysical characterization of Permian deep-water sandstones, Bell Canyon Formation and Cherry Canyon Formation, Ford Geraldine area, West Texas (Delaware Basin): poster presentation at the 1997 Annual Meeting of the American Association of Petroleum Geologists, Dallas, Texas, April 1997.

Dutton, S. P., Barton, M. D., Hovorka, S. D., Cole, A. G., and Asquith, G. B., 1997, Reservoir characterization of Permian deep-water Ramsey Sandstones, Bell Canyon Formation, Ford Geraldine Unit, West Texas (Delaware Basin): poster presentation at the 1997 Annual Meeting of the American Association of Petroleum Geologists, Dallas, Texas, April 1997.

Dutton, S. P., and Barton, M. D., Application of advanced reservoir characterization, simulation, and production optimization strategies to maximize recovery in slope and basin clastic reservoirs, West Texas (Delaware Basin), talk presented at the DOE Project Review Meeting, Houston, Texas, June 1997.

Malik, M. A., A practical approach to scaling-up permeability and relative permeabilities in heterogeneous permeable media: talk presented at the 1997 Society of Petroleum Engineers Western Regional Meeting, Long Beach, California, June 1997.

Asquith, G. B., Dutton, S. P., and Cole, A. G., Delaware effect and the Ramsey Sandstone, Ford Geraldine Unit, Reeves and Culberson Counties, Texas: presented at the 1997 Fall Symposium of the West Texas Geological Society, Midland, Texas, October 1997.

Asquith, G. B., Dutton, S. P., Cole, A. G., Razi, M., and Guzman, J. I., Petrophysics of the Ramsey Sandstone, Ford Geraldine Unit, Reeves and Culberson Counties, Texas: presented at the 1997 Fall Symposium of the West Texas Geological Society, Midland, Texas, October 1997. Dr. Asquith received the WTGS Best Paper Award for this presentation.

Dutton, S. P., Barton, M. D., Clift, S. J., Guzman, J. I., and Cole, A. G., Depositional history of Ramsey Sandstone channel-levee and lobe deposits, Bell Canyon Formation, Ford Geraldine Unit, West Texas (Delaware Basin): talk presented at the Fall Symposium of the West Texas Geological Society in Midland, Texas, October 1997.

Dutton, S. P., Barton, M. D., Clift, S. J., Guzman, J. I., Asquith, G. B., and Cole, A. G., Application of advanced reservoir characterization to Ramsey Sandstone reservoirs, Ford Geraldine Unit, West Texas (Delaware Basin): poster presented at the 1997 Fall Symposium of the West Texas Geological Society, Midland, Texas, October 1997.

Malik, M. A., Simulations for improved recovery by CO₂ flood in Ford Geraldine Unit, West Texas: presented at the 2d CO₂ Oil Recovery Forum PTTC Focused Technology Workshop, Socorro, New Mexico, October 1997.

Dutton, S. P., Reservoir characterization of a deep-water channel-levee and lobe system, Bell Canyon Formation, Geraldine Ford Field, West Texas (Delaware Basin): talk presented at the Texas Tech University Geoscience Colloquium, Lubbock, Texas, November 1997.

Asquith, G. B., Petrophysics of the Ramsey Sandstone, Ford Geraldine Unit, Reeves and Culberson Counties, Texas: talk presented at the Amarillo chapter of the Society of Professional Well Log Analysts, Amarillo, Texas, November 1997.

Asquith, G. B., Petrophysics of the Ramsey Sandstone, Ford Geraldine Unit, Reeves and Culberson Counties, Texas: talk presented at The University of Texas at El Paso, El Paso, Texas, December 1997.

Asquith, G. B., Petrophysics of the Ramsey Sandstone, Ford Geraldine Unit, Reeves and Culberson Counties, Texas: talk presented at New Mexico State University at Las Cruces, Las Cruces, New Mexico, December 1997.

1998

Dutton, S. P., Asquith, G. B., and Malik, M. A., Incorporation of core data into reservoir characterization of a deep-water channel-levee and lobe deposit, Ford Geraldine

Unit, Delaware Basin: poster and core display presented at the Sixth Archie Conference, Kerrville, Texas, February 1998.

Dutton, S. P., Barton, M. D., Clift, S. J., and Guzman, J. I., Ramsey sandstone deep-water channel-levee and lobe deposits, Ford Geraldine Unit, Reeves and Culberson Counties, Texas: core and poster display presented at the Permian Basin Section-SEPM meeting "Permian Basin Core Workshop—DOE Funded Reservoir Characterization Projects" in Midland, Texas, February 1998.

Malik, M. A., Compositional simulations of a CO₂ flood in Ford Geraldine Unit, Texas: talk presented at 1998 Society of Petroleum Engineers Permian Basin Oil and Gas Recovery Conference, Midland, Texas, March 1998.

Dutton, S. P., Barton, M. D., and Cole, A. G., 1998, Ramsey Sandstone channel-levee and lobe deposits: deep-marine clastic reservoirs in the Bell Canyon Formation, Delaware Basin, Texas: talk presented at the 1998 Annual Meeting of the American Association of Petroleum Geologists, Salt Lake City, Utah, May 1998.

1999

Dutton, S. P., Barton, M. D., Guzman, J. I., Asquith, G. B., and Cole, A. G., Controls on reservoir quality distribution in the Ramsey Sandstone deep-marine clastic reservoirs, Bell Canyon Formation, Delaware Basin, Texas: poster presented at the 1999 American Association of Petroleum Geologists Annual Meeting, San Antonio, Texas, April 1999.

Asquith, G. B., Petrophysics of the Ramsey Sandstone, Ford Geraldine Unit, Reeves and Culberson Counties, Texas: talk presented at the Roswell Geological Society, Roswell, New Mexico, April 1999.

Barton, M. D., and Dutton, S. P., 1999, Outcrop analysis of a sand-rich, basin-floor turbidite system, Permian Bell Canyon Formation, West Texas: talk and poster display presented at the 1999 Gulf Coast Section SEPM Foundation 19th Annual Research Conference on Advanced Reservoir Characterization, Houston, Texas, December 1999.

Dutton, S. P., and Barton, M. D., 1999, Application of outcrop analogs to reservoir characterization of Permian deep-water sandstones, Bell Canyon Formation, Ford Geraldine Unit, West Texas (Delaware Basin): poster display presented at the 1999 Gulf Coast Section SEPM Foundation Nineteenth Annual Research Conference on Advanced Reservoir Characterization, Houston, Texas, December 1999.

2000

Dutton, S. P., Barton, M. D., Zirczy, H. H., and Flanders, W. A., Characterization of reservoir heterogeneity in slope and basin clastic reservoirs, Bell Canyon

Formation, Delaware Basin, Texas: talk presented at the 2000 Annual Meeting of the Southwest Section of the American Association of Petroleum Geologists, Midland, Texas, February 2000. This paper received the A. I. Levorsen Memorial Award from AAPG for the best paper presented at the meeting.

Flanders, W. A., Ford Geraldine/East Ford: importance of reservoir deposition in CO₂ floods: talk presented at the Sixth Annual CO₂ Conference & Exhibition sponsored by PTTC and Society of Petroleum Engineers Permian Basin Section, Midland, Texas, December 2000.

2001

Dutton, S. P., and Flanders, W. A., Deposition and diagenesis of turbidite sandstones in East Ford Field, Bell Canyon Formation, Delaware Basin, Texas: talk presented at the 2001 annual meeting of the Southwest Section of the American Association of Petroleum Geologists, Dallas, Texas, March 2001.

Dutton, S. P., and Flanders, W. A., Field development of a Permian deep-water sandstone, East Texas field, Bell Canyon Formation, Delaware Basin, Texas: talk presented at the 2001 Annual Meeting of the American Association of Petroleum Geologists, Denver, Colorado, June 2001.

APPENDIX 2: LIST OF PUBLICATIONS PRODUCED BY BEG CLASS 3 PROJECT

Articles

- Asquith, G. B., Dutton, S. P., and Cole, A. G., 1997, "Delaware effect" and the Ramsey Sandstone, Ford Geraldine Unit, Reeves and Culberson Counties, Texas: West Texas Geological Society Publication No. 97-102, p. 71-74.
- Asquith, G. B., Dutton, S. P., Cole, A. G., Razi, M., and Guzman, J. I., 1997, Petrophysics of the Ramsey Sandstone, Ford Geraldine Unit, Reeves and Culberson Counties, Texas *in* DeMis, W. D., ed., Permian Basin oil and gas fields: turning ideas into production: West Texas Geological Society Publication No. 97-102, p. 61-69.
- Barton, M. D., and Dutton, S. P., 1999, Outcrop analysis of a sand-rich, basin-floor turbidite system, Permian Bell Canyon Formation, West Texas, *in* Transactions, Gulf Coast Section SEPM Nineteenth Annual Bob F. Perkins Research Conference, December 5-8, Houston, p. 53-64.
- Dutton, S. P., Asquith, G. B., Flanders, W. A., Guzman, J. I., and Zirczy, H. H., 1999, New techniques for using old geophysical logs in reservoir characterization: examples from Bell Canyon Sandstones, Ford Geraldine and East Ford units, Delaware Basin, Texas: Proceedings of the 1999 Oil & Gas Conference Technology Options for Producer Survival, Conference sponsored by the U.S. Department of Energy, Dallas, Publication DOE/FETC-99/1103, 25 p.
- Dutton, S. P., and Barton, M. D., 1999, Application of outcrop analogs to reservoir characterization of Permian deep-water sandstones, Bell Canyon Formation, Ford Geraldine Unit, West Texas (Delaware Basin), *in* Transactions, Gulf Coast Section SEPM 19th Annual Bob F. Perkins Research Conference, December 5-8, Houston, p. 65-76.
- Dutton, S. P., Barton, M. D., Asquith, G. B., Malik, M. A., Cole, A. G., Gogas, J., Guzman, J. I., and Clift, S. J., 1999, Geologic and engineering characterization of turbidite reservoirs, Ford Geraldine Unit, Bell Canyon Formation, West Texas: The University of Texas at Austin, Bureau of Economic Geology Report of Investigations No. 255, 88 p.
- Dutton, S. P., Barton, M. D., Clift, S. J., and Guzman, J. I., 1998, Ramsey sandstone deep-water channel-levee and lobe deposits, Ford Geraldine Unit, Reeves and Culberson Counties, Texas, *in* Stoudt, E. L., Dull, D. W., and Raines, M. R., eds., Permian Basin Core Workshop—DOE Funded Reservoir Characterization Projects: Permian Basin Section—SEPM Publication No. 98-40, 33 p.
- Dutton, S. P., Barton, M. D., Clift, S. J., Guzman, J. I., and Cole, A. G., 1997, Depositional history of Ramsey Sandstone channel-levee and lobe deposits, Bell

Canyon Formation, Ford Geraldine Unit, West Texas (Delaware Basin): West Texas Geological Society Publication No. 97-102, p. 53–60. Paper reprinted in the West Texas Geological Society Bulletin, v. 37, no. 4 (December 1997), p. 5–14.

Dutton, S. P., Barton, M. D., Zirczy, H. H., and Flanders, W. A., 2000, Characterization of reservoir heterogeneity in slope and basin clastic reservoirs, Bell Canyon Formation, Delaware Basin, Texas, *in* Reid, S. T., Southwest Section AAPG 2000 Convention transactions: West Texas Geological Society, Publication SWS 2000-107, p. 116–129.

Dutton, S. P., and Flanders, W. A., 1999, Application of advanced reservoir characterization, simulation, and production optimization strategies to maximize recovery in slope and basin clastic reservoirs, West Texas (Delaware Basin): The Class Act, v. 5, no. 2, p. 4–6.

Dutton, S. P., and Flanders, W. A., 2001, Deposition and diagenesis of turbidite sandstones in East Ford field, Bell Canyon Formation, Delaware Basin, Texas, *in* Southwest Section AAPG 2001 Convention transactions, 12 p.

Malik, M. A., 1998, Compositional simulations of a CO₂ flood in Ford Geraldine Unit, Texas: SPE Permian Basin Oil and Gas Recovery Conference, Midland, March 23–26, SPE paper 39794, p. 375–383.

Abstracts

Barton, M. D., 1997, Basin floor fan and channel-levee complexes, Permian Bell Canyon Formation (abs.): AAPG Annual Convention, Official Program, v. 6, Dallas, p. A9.

Cole, A. G., Dutton, S. P., Barton, M. D., Hovorka, S. D., and Asquith, G. B., 1997, Geophysical characterization of Permian deep-water sandstones, Bell Canyon Formation and Cherry Canyon Formation, Ford Geraldine area, West Texas (Delaware Basin) (abs.): AAPG Annual Convention, Official Program, v. 6, Dallas, p. A21.

Dutton, S. P., Asquith, G. B., Flanders, W. A., Guzman, J. I., and Zirczy, H. H., 1999, New techniques for using old geophysical logs in reservoir characterization: examples from Bell Canyon sandstones, Ford Geraldine and East Ford units, Delaware Basin, Texas (abs.): DOE Oil & Gas Conference, Agenda and Abstracts, p. 2B5.

Dutton, S. P., Asquith, G. B., and Malik, M. A., 1998, Incorporation of core data into reservoir characterization of a deep-water channel-levee and lobe deposit, Ford Geraldine Unit, Delaware Basin (abs.): Sixth Archie Conference, Kerrville .

Dutton, S. P., Barton, M. D., Clift, S. J., Guzman, J. I., Asquith, G. B., and Cole, A. G., 1997, Application of advanced reservoir characterization to Ramsey Sandstone

reservoirs, Ford Geraldine Unit, West Texas (Delaware Basin) (abs.): West Texas Geological Society Publication No. 97-102, p. 97.

Dutton, S. P., Barton, M. D., and Cole, A. G., 1998, Ramsey sandstone channel-levee and lobe deposits: deep-marine clastic reservoirs in the Bell Canyon Formation, Delaware Basin, Texas (abs.): AAPG Annual Convention, extended abstracts, v. 1, Salt Lake City, p. A173.

Dutton, S. P., Barton, M. D., Guzman, J. I., Asquith, G. B., and Cole, A. G., 1999, Controls on reservoir quality distribution in the Ramsey sandstone deep-marine clastic reservoirs, Bell Canyon Formation, Delaware Basin, Texas (abs.): AAPG Annual Convention, Official Program, v. 8, San Antonio, Texas, p. A35.

Dutton, S. P., Barton, M. D., Hovorka, S. D., Cole, A. G., Asquith, G. B., 1997, Reservoir characterization of Permian deep-water Ramsey Sandstones, Bell Canyon Formation, Ford Geraldine Unit, West Texas (Delaware Basin) (abs.): AAPG Annual Convention, Official Program, v. 6, Dallas, Texas, p. A31.

Dutton, S. P., Barton, M. D., Malik, M. A., Asquith, G. B., Cole, A. G., Pittaway, K. R., and Gogas, J., 1998, Characterization and development of turbidite reservoirs in a deepwater channel-levee and lobe system, Ford Geraldine Unit, Permian Bell Canyon Formation, Delaware Basin, USA (extended abstract): EAGE/AAPG Third Research Symposium on Developing and Managing Turbidite Reservoirs, extended abstracts book, Almeria, Spain, p. A009.

Dutton, S. P., Cole, A. G., and Hovorka, S. D., 1996, Application of advanced reservoir characterization, simulation, and production optimization strategies to maximize recovery in slope and basin clastic reservoirs, West Texas (Delaware Basin), *in* Improving production in shallow shelf carbonate (Class II) reservoirs, a workshop sponsored by the U.S. Department of Energy and BDM Oklahoma, Inc., at the Center for Energy and Economic Diversification, Midland, May 15–16, unpaginated.

Dutton, S. P., and Flanders, W. A., 2001, Field development of a Permian deep-water sandstone, East Texas field, Bell Canyon Formation, Delaware Basin, Texas (abs.): AAPG Annual Convention, Official Program, v. 10, Denver, Colorado, p. A54.

Dutton, S. P., and Flanders, W. A., 2001, Deposition and diagenesis of turbidite sandstones in East Ford field, Bell Canyon Formation, Delaware Basin, Texas (abs.): American Association of Petroleum Geologists Bulletin, v. 85, no. 2, p. 385–386.

Contract Reports

Dutton, S. P., Asquith, G. B., Barton, M. D., Cole, A. G., Gogas, J., Malik, M. A., Clift, S. J., and Guzman, J. I., 1997, Application of advanced reservoir characterization, simulation, and production optimization strategies to maximize recovery in slope

- and basin clastic reservoirs, West Texas (Delaware Basin): The University of Texas at Austin, Bureau of Economic Geology, annual report prepared for the U.S. Department of Energy, DOE/BC/14936-9, 187 p.
- Dutton, S. P., Barton, M. D., Malik, M. A., Asquith, G. B., Guzman, J. I., Clift, S. J., and Cole, A. G., 1998, Application of advanced reservoir characterization, simulation, and production optimization strategies to maximize recovery in slope and basin clastic reservoirs, West Texas (Delaware Basin): The University of Texas at Austin, Bureau of Economic Geology, annual report prepared for the U.S. Department of Energy, 88 p.
- Dutton, S. P., and Flanders, W. A., 2001, Application of advanced reservoir characterization, simulation, and production optimization strategies to maximize recovery in slope and basin clastic reservoirs, West Texas (Delaware Basin): The University of Texas at Austin, Bureau of Economic Geology, final report prepared for the U.S. Department of Energy, 170 p.
- Dutton, S. P., Flanders, W. A., Guzman, J. I., and Zirczy, H. H., 1999, Application of advanced reservoir characterization, simulation, and production optimization strategies to maximize recovery in slope and basin clastic reservoirs, West Texas (Delaware Basin): The University of Texas at Austin, Bureau of Economic Geology, annual report prepared for the U.S. Department of Energy, DOE/BC/14936-11, 106 p.
- Dutton, S. P., Flanders, W. A., and Mendez, D. L., 2001, Application of advanced reservoir characterization, simulation, and production optimization strategies to maximize recovery in slope and basin clastic reservoirs, West Texas (Delaware Basin): The University of Texas at Austin, Bureau of Economic Geology, annual report prepared for the U.S. Department of Energy, DOE/BC/14936-17, 72 p.
- Dutton, S. P., Flanders, W. A., and Zirczy, H. H., 2000, Application of advanced reservoir characterization, simulation, and production optimization strategies to maximize recovery in slope and basin clastic reservoirs, West Texas (Delaware Basin): The University of Texas at Austin, Bureau of Economic Geology, annual report prepared for the U.S. Department of Energy, DOE/BC/14936-15, 60 p.
- Dutton, S. P., Flanders, W. A., Zirczy, H. H., and Guzman, J. I., 1999, Geologic and engineering characterization of East Ford field, Reeves County, Texas: The University of Texas at Austin, Bureau of Economic Geology, topical report prepared for the U.S. Department of Energy, 113 p.
- Dutton, S. P., Hovorka, S. D., and Cole, A. G., 1996, Application of advanced reservoir characterization, simulation, and production optimization strategies to maximize recovery in slope and basin clastic reservoirs, West Texas (Delaware Basin): The University of Texas at Austin, Bureau of Economic Geology, annual report prepared for the U.S. Department of Energy, DOE/BC/14936-5, 81 p.

Dutton, S. P., Malik, M. A., Clift, S. J., Asquith, G. B., Barton, M. D., Cole, A. G., Gogas, J., and Guzman, J. I., 1997, Geological and engineering characterization of Geraldine Ford Field, Reeves and Culberson Counties, Texas: The University of Texas at Austin, Bureau of Economic Geology, topical report prepared for the U.S. Department of Energy, DOE/BC/14936-10, 115 p.

APPENDIX 3: CONTENT OF SHORT COURSES PRODUCED
BY BEG CLASS 3 PROJECT

**Reservoir Characterization of Permian Deep-Water Sandstones, Bell
Canyon Formation, Geraldine Ford Area, West Texas (Delaware Basin)**

A Technology Transfer Seminar

8:30-8:45	Introduction— <i>S. P. Dutton</i>
8:45-9:45	Description of architecture elements within a high-order cycle, Bell Canyon Formation, west Texas: a submarine channel-levee system with attached lobes— <i>M. D. Barton</i>
9:45-10:00	Coffee Break
10:00-11:00	Reservoir characterization of Geraldine Ford field— <i>S. P. Dutton</i>
11:00-12:00	Petrophysics of the Ramsey Sandstone, Ford Geraldine unit— <i>G. B. Asquith</i> Summary of core display of Ramsey sandstone cores, Geraldine Ford field— <i>S. J. Clift</i>
12:00-1:00	Lunch (core on display during lunch time)
1:00-1:30	Production history of Geraldine Ford field— <i>K. R. Pittaway</i>
1:30-2:30	Geophysical interpretation of a Bell Canyon reservoir with 3-D seismic data— <i>A. G. Cole and John Gogas</i>
2:30-3:00	Coffee break and core display of Ramsey sandstone cores, Geraldine Ford field— <i>S. J. Clift</i>
3:00-3:45	Stochastic permeability characterization and preliminary enhanced-recovery predictions of pilot area— <i>M. A. Malik</i>
3:45-4:00	Summary and conclusion of formal presentations— <i>S. P. Dutton</i>
4:00-5:00	Additional time for core viewing and discussion

Hosted by the West Texas Geological Society, Midland, Texas, March 25, 1997

Reservoir Characterization of Ford Geraldine Unit: Permian Bell Canyon Formation, Delaware Basin, West Texas

A Technology Transfer Seminar

Introduction—*S. P. Dutton*

Reservoir characterization of Geraldine Ford field—*S. P. Dutton*

Petrophysics of the Ramsey Sandstone, Ford Geraldine unit—
G. B. Asquith

Core display of Ramsey sandstone cores, Geraldine Ford
field—*S. J. Clift*

Production history of Geraldine Ford field—*K. R. Pittaway*

Geophysical interpretation of a Bell Canyon reservoir with
3-D seismic data—*A. G. Cole and John Gogas*

Simulations of a CO₂ flood, Ford Geraldine unit—*M. A. Malik*

Introduction to the field trip—*M. D. Barton*

Workshop held in Carlsbad, New Mexico, November 21, 1997.

Facies Architecture of Submarine Channel-Levee and Lobe Sandstones: Permian Bell Canyon Formation, Delaware Mountains, West Texas

A Technology Transfer Field Trip

Field Trip Leader: Mark D. Barton

Introduction

Regional Setting and Stratigraphic Framework

Study Area

Sedimentology

Field Stops

Day 1

Road Log

Stop 1.1: Lamar Limestone

Stop 1.2: Delaware Wash

Stop 1.3: Wild Horse Draw

Stop 1.4: Willow Draw

Day 2

Road Log

Stop 2.1: Willow Mountain

Stops 2.2–2.5: South Cowden Ranch; Cow Mountain; North Cow
Mountain: Buttes of Delaware Wash

Field trip based in Carlsbad, New Mexico, November 22–23, 1997.

CO₂ Flooding of Delaware Sandstones, Permian Basin:

Lessons Learned from East Ford Field

A Technology Transfer Workshop

8:30 - 8:45	Introduction— <i>S. P. Dutton</i>
8:45 - 9:00	Summary of Ramsey sandstone reservoirs— <i>S. P. Dutton</i>
9:00 - 9:50	Ramsey sandstone depositional model— <i>S. P. Dutton</i>
9:50 - 10:10	Break
10:10 - 10:25	Primary development of East Ford Field— <i>W. A. Flanders</i>
10:25 - 10:40	Results of CO ₂ flood of Twofreds Field and Ford Geraldine Unit— <i>W. A. Flanders</i>
10:40 - 11:30	CO ₂ flood of East Ford Field— <i>W. A. Flanders</i>

Hosted by Permian Basin Petroleum Association, Midland, Texas, May 2, 2000.